

Bowdoin College

## Bowdoin Digital Commons

---

Honors Projects

Student Scholarship and Creative Work

---

2020

### N,N'-Dimethyimidazolium-2-Carboxylate as a Ligand Precursor for the Accession of a Constrained Olefin Dimerization Catalyst

Michael Harris

Follow this and additional works at: <https://digitalcommons.bowdoin.edu/honorsprojects>

 Part of the [Organic Chemistry Commons](#)

---

#### Recommended Citation

Harris, Michael, "N,N'-Dimethyimidazolium-2-Carboxylate as a Ligand Precursor for the Accession of a Constrained Olefin Dimerization Catalyst" (2020). *Honors Projects*. 156.  
<https://digitalcommons.bowdoin.edu/honorsprojects/156>

This Open Access Thesis is brought to you for free and open access by the Student Scholarship and Creative Work at Bowdoin Digital Commons. It has been accepted for inclusion in Honors Projects by an authorized administrator of Bowdoin Digital Commons. For more information, please contact [mdoyle@bowdoin.edu](mailto:mdoyle@bowdoin.edu), [a.sauer@bowdoin.edu](mailto:a.sauer@bowdoin.edu).

**N,N'-Dimethylimidazolium-2-Carboxylate as a Ligand Precursor for  
the Accession of a Constrained Olefin Dimerization Catalyst**

**An Honors Project for the Department of Chemistry**

**Michael Russell Harris**

**Spring 2020**

Bowdoin College, 2020

© 2020 Michael Russell Harris

## Table of Contents

<b>Acknowledgements .....</b>	<b>iii</b>
<b>Abstract.....</b>	<b>iv</b>
<b>Introduction.....</b>	<b>1</b>
1. <i>Linear <math>\alpha</math>-Olefins</i> .....	1
1.1 <i>Applications and Limitations</i> .....	1
1.2 <i>Industrial Method of Production</i> .....	2
1.3 <i>Post-Synthesis Waste Processing</i> .....	3
2. <i>New Methods of Selective Production</i> .....	4
2.1 <i>Metallacycle Trimerization and Tetramerization</i> .....	4
2.2 <i>Selective Dimerization via Insertion</i> .....	5
2.3 <i>Controlling <math>\alpha</math>-Olefin Dimer Formation</i> .....	6
3. <i>Constrained Ligands</i> .....	7
3.1 <i>8-Quinoyl-Tetramethylcyclopentadiene</i> .....	7
3.2 <i>N-Heterocyclic Carbenes</i> .....	9
3.3 <i>N,N'-Dimethylimidazolium-2-Carboxylate</i> .....	10
3.4 <i>Research Objectives</i> .....	10
<b>Experimental .....</b>	<b>11</b>
1. <i>Synthesis of Cp*Co(ethene)<sub>2</sub> from dicobalt octacarbonyl</i> .....	11
1.1 <i>Formation of dicarbonyl-(<math>\eta^5</math>-pentamethylcyclopentadienyl)cobalt (1)</i> .....	11
1.2 <i>Synthesis of carbonyldiiodo-(<math>\eta^5</math>-pentamethylcyclopentadienyl)cobalt (2)</i> .....	12
1.3 <i>Synthesis of di-iodo-bis[iodo-(<math>\eta^5</math>-pentamethylcyclopentadienyl)cobalt] (3)</i> .....	13
1.4 <i>Synthesis of bis(<math>\eta^2</math>-ethene)(<math>\eta^5</math>-pentamethylcyclopentadienyl)cobalt (4)</i> .....	13
2. <i>Synthesis of N,N'-dimethylimidazolium iodide (5)</i> .....	14

3. Synthesis of <i>N,N'</i> -dimethylimidazolium-2-carboxylate (6).....	15
4. Coordination of <i>N,N'</i> -dimethylimidazolium-2-carboxylate to $[Cp^*Co(ethene)_2]$ .....	16
5. Catalyst Activation and Dimerization of 1-Hexene .....	19
6. Synthesis of bis[( <i>N,N'</i> -dimethylimidazolium-2-ylidene)( $\eta^5$ -pentamethylcyclopentadienyl) cobalt] .....	20
<b>Results and Discussion.....</b>	<b>22</b>
1. Synthesis of $Cp^*Co(ethene)_2$ (4) .....	22
2. Synthesis of <i>N,N'</i> -Dimethylimidazolium Iodide (5) .....	25
3. Synthesis of <i>N,N'</i> -Dimethylimidazolium-2-carboxylate (6).....	27
4. Coordination of <i>N,N'</i> -Dimethylimidazolium-2-carboxylate to $Cp^*Co(ethene)_2$ .....	29
5. Catalyst Activation and Dimerization of 1-Hexene .....	36
6. Synthesis of bis[( <i>N,N'</i> -dimethylimidazolium-2-ylidene)( $\eta^5$ -pentamethylcyclopentadienyl) cobalt] .....	39
<b>Conclusions.....</b>	<b>42</b>
<b>Future Work.....</b>	<b>43</b>
<b>References.....</b>	<b>44</b>
<b>Appendix: Color Images in Black and White.....</b>	<b>v</b>
<b>List of Figures.....</b>	<b>xvi</b>
<b>List of Tables .....</b>	<b>xix</b>

## Acknowledgements

I would like to express my sincerest gratitude to Professor Rick Broene, whose mentorship and wisdom has been integral to both this project, and my growth as a chemist. His expertise and advising have allowed me to sharpen my skill set and have shaped me into the chemist I am today. I would also like to thank Professor Jeff Nagle for his assistance with computational models, and Professor Benjamin Gorske for generously lending me chemicals at the beginning of this project. I would like to thank Professors Beth Stemmler and Dharni Vasudevan for their helpful comments on this work. I would like to additionally thank Professor Stemmler for helping me develop analytical methods and helping me retrieve important data when research was terminated. Additionally, I would like to thank Emily Murphy, Ren Bernier and Barbara Ames for keeping the department up and running. Furthermore, I would like to thank my officemates Rebecca Londoner and Kamyron Speller for lighting up the basement, and lab. I would like to especially thank my dear friend Katharine Toll for her invaluable support and friendship; without her this would not have been possible. Finally, I would like to thank the Littlefield Summer Research Fellowship and the Bowdoin College Department of Chemistry for funding this work, and providing me the opportunity to start my research journey.

## Abstract

A significant market share of modern plastics is held by long-chain hydrocarbon polymers, such as polyethylene and polypropylene, properties of which can be dramatically changed by addition of linear  $\alpha$ -olefins. Production of linear  $\alpha$ -olefins involves the creation of many unwanted byproducts, representing significant quantities of both economic and ecological waste. While catalysts have been designed to selectively produce industrially useful olefins, these catalysts often encounter challenges such as synthesis of other unwanted byproducts, slow reaction times, and difficulty of synthesis. Based on one such prior catalyst, we report here synthetic work towards a cobalt catalyst with a constrained N-heterocyclic carbene supporting ligand predicted to allow for more favorable product distributions. Synthesis of two precursors to a sterically unhindered N-heterocyclic carbene, as well as development of a synthetic protocol for the coordination of N,N'-dimethylimidazolium-2-carboxylate to  $\text{Cp}^*\text{Co}(\text{ethene})_2$  was completed. Activation of the precatalyst and preliminary catalytic experiments were performed, though abbreviated research periods made complete analysis impossible. Finally, we report evidence of the formation of a novel cobalt-NHC dimer as a temperature controlled byproduct of the desired catalyst synthesis.

# Introduction

## 1. Linear $\alpha$ -Olefins

### 1.1 Applications and Limitations

While it is well known that plastics are created from petroleum derivatives, the role of the linear  $\alpha$ -olefin is not common knowledge in the eyes of the consumer. Defined as a single chain alkene with a single, terminal double bond,<sup>1</sup> linear  $\alpha$ -olefins are useful property modifiers for polymers, additives for industrial lubricants and detergents, and are commonly used in the production of low density polyethylene (LDPE), high density polyethylene (HDPE), and polypropylene (Figure 1).<sup>2</sup> Consequently, a significant share of modern plastics are derivatives of linear  $\alpha$ -olefins and thus the details of production are important both industrially and ecologically.<sup>2</sup> Industrial importance of linear  $\alpha$ -olefins cannot be overstated, with production on the order of 10 billion pounds annually.<sup>3</sup> Problematically, only linear  $\alpha$ -olefins of medium length are industrially useful, with chain length between 12 and 18 carbons being the most desirable, and only 2% of longer (20+ carbons in length) linear  $\alpha$ -olefins having industrial uses.<sup>2</sup> Despite their widespread use, the production of linear  $\alpha$ -olefins contains many synthetic inefficiencies.<sup>4-5</sup>

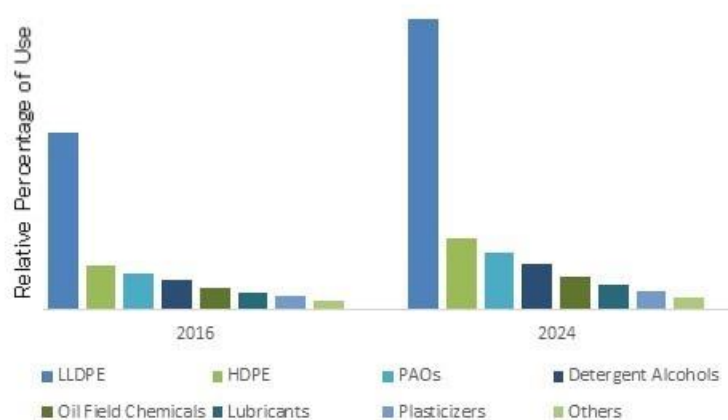


*Figure 1: A distribution of the common industrial uses of linear  $\alpha$ -olefins from 2016, and a projection for 2024. As seen, a vast majority are used for copolymer modification of LDPE. Figure adapted from Ahuja & Singh.<sup>3</sup>*

## 1.2 Industrial Method of Production

The Shell Higher Olefin Process (SHOP) is one current method of production, resulting in a ‘full range’ of products. Mechanistically, SHOP employs the similar rates of ethene insertion into nickel species, followed by  $\beta$ -elimination of alkyl ligands, to create a distribution of linear olefin products (Figure 2).<sup>4</sup> Beginning with a nickel-hydride catalyst **A**, ethene is inserted once to form ethyl complex **B**, and then again to form butyl complex **C**. At this point, the butyl ligand can either undergo  $\beta$ -elimination to form 1-butene and the original hydride catalyst or another ethene insertion to form hexyl complex **D**. The new complex **D** can then undergo the insertion of another ethene or elimination to form 1-hexene. This variable chain of insertions and eliminations results in a wide distribution of products, effectively from  $C_4$  to  $C_{50}$  (Figure 3).<sup>2</sup> This “full range” of products results in large quantities of long chain (20+ carbon) products, which are not industrially viable. These long chain olefin products present primarily as viscous oils and hard waxes, and must be further processed to yield useful material.<sup>2</sup>

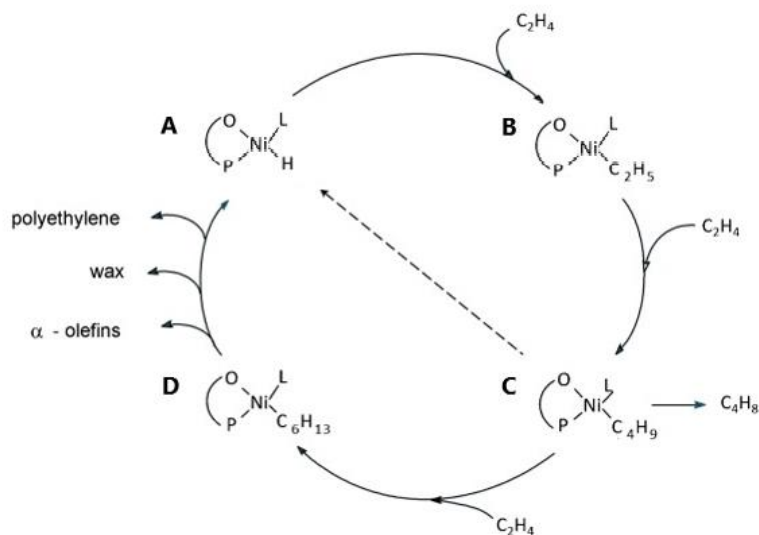


**Figure 2:** The catalytic cycle of the Shell Higher Olefin Process, complex A) undergoes repeated insertions of ethene to yield a distribution of alkyl complexes. These alkyl complexes then undergo  $\beta$ -elimination to give the desired olefin products. Figure adapted from Keim.<sup>4</sup>



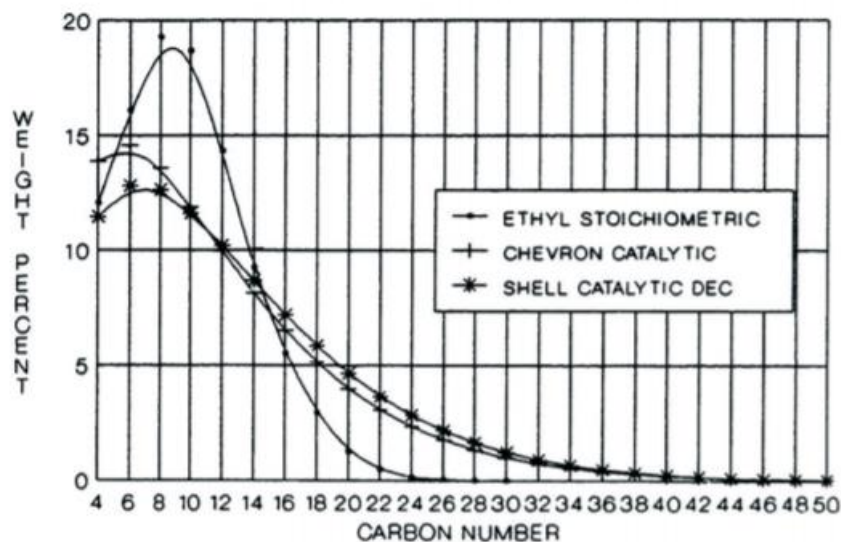


Figure 3: A measured distribution of linear  $\alpha$ -olefin production using three prevalent full range processes. As seen, a significant quantity is produced outside of the desired range (12-18 carbon number). Figure adapted from Lappin & Sauer.<sup>2</sup>

### 1.3 Post-Synthesis Waste Processing

One such method of processing allows for the formation of 2-tetradecene from a mixture of 1-octene and 1-eicosene (Figure 4).<sup>2,4</sup> Here, 1-octene and 1-eicosene are isomerized to form 4-octene and 10-tetradecene; these new internal olefins then undergo olefin metathesis, effectively breaking the chains and rearranging the alkene substituents, to yield 2 equivalents of 4-tetradecene. The newly formed internal olefins can undergo an additional isomerization to yield the linear olefin product, 2-tetradecene. This internal mono-olefin can be utilized in other industrial processes, but cannot be used as a linear  $\alpha$ -olefin.<sup>4</sup> While this provides some use for longer olefins, few other methods have been developed for the recycling waste products from ethene oligomerization. Thus,

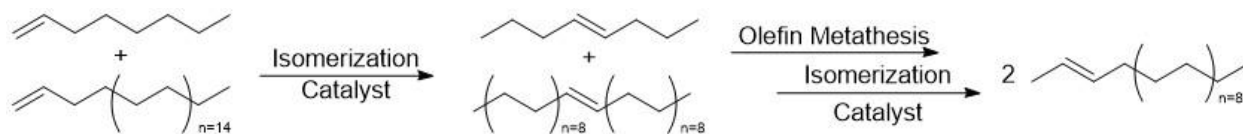


Figure 4: A reported pathway to recover some waste from linear  $\alpha$ -olefin production. 1 eq. 1-octene and 1 eq. 1-eicosene is isomerized and metathesized to form 2 eq. of 4-tetradecene, then isomerized again to form the linear olefin product, 2-tetradecene.

new synthetic processes are required to produce linear  $\alpha$ -olefins on an industrial scale, while reducing waste, an important goal both economically and ecologically.

## 2. New Methods of Selective Production

### 2.1 Metallacycle Trimerization and Tetramerization

Various groups report selective trimerization and tetramerization of ethene, however these methods only provide relatively short carbon chains.<sup>6-9</sup> Many ethene trimerization catalysts use a metallacyclic mechanism, which might be exploited to access medium length chains; the mechanism for the tetramerization of ethene is currently unknown (Figure 5A).<sup>9</sup> However, the tetramerization of ethene yields 1-octene, which is not as industrially important as other targets. Furthermore, this method of 1-octene production is plagued by many side products, including 1-hexene, methylcyclopentane, and methylene cyclopentane (Figure 5B).<sup>9</sup> As production of linear  $\alpha$ -olefins longer than 8 carbons is desired, new methods for selective production of industrially usable linear  $\alpha$ -olefins is necessary. Small and Brookhart showed the propensity of iron catalysts to oligomerize ethene to desirable linear  $\alpha$ -olefins, and the ability to tune the product distributions

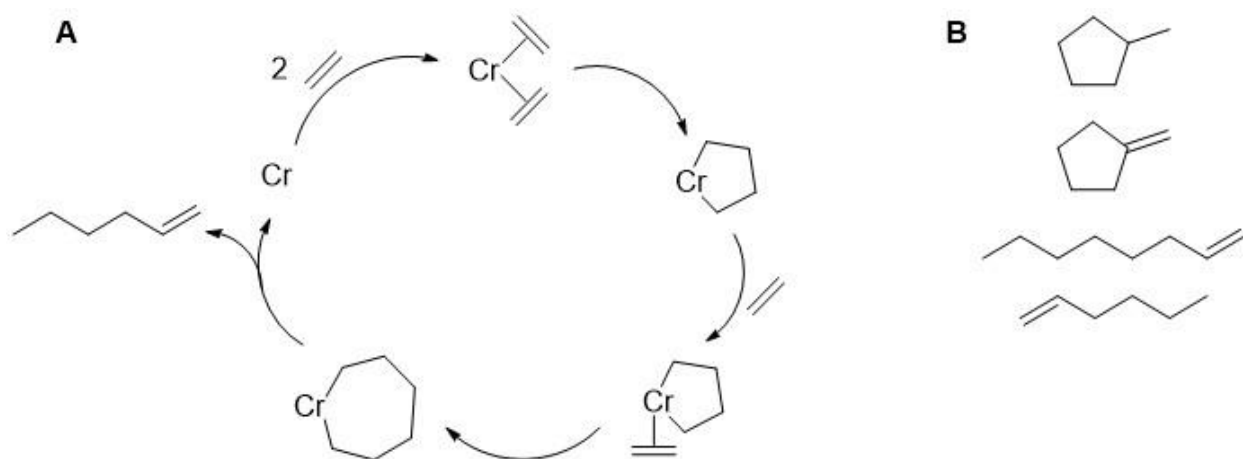


**Figure 5:** A) A trimerization catalytic cycle of ethene to 1-hexene showing metallacyclic addition of ethene and B) the products of Bollman et al. experiments on a tetramerization catalyst. The metallacyclic mechanism is suggested, but not confirmed due to doubt about the stability of a 9-membered ring.

by changing the steric demands of the ligand, though undesirable olefins (length <8 carbons) are still produced.<sup>10</sup>

## 2.2 Selective Dimerization via Insertion

A promising, alternative method is the selective dimerization of short chain linear  $\alpha$ -olefins to linear  $\alpha$ -olefins of medium length, for example the dimerization of 1-hexene to form 1-dodecene. Broene and Brookhart reported the dimerization of short chain  $\alpha$ -olefins to medium length, though this was still hindered by off-target product formation.<sup>11</sup> Specifically, a cationic cobalt-trimethylphosphite catalyst showed that 1-hexene was dimerized to 1-dodecene, among other products (Figure 6).<sup>11</sup> The 2,1-insertion of a second equivalent of a linear  $\alpha$ -olefin to **1** provides linear dimers. A series of  $\beta$ -elimination/1,2-insertions isomerizes the internal alkyl dimer **2** to the terminal alkyl complex **3**, which then generates a coordinated alpha olefin dimer via agostic hydrogen transfer. Similar to Small, reducing ligand bulk was key to formation of the

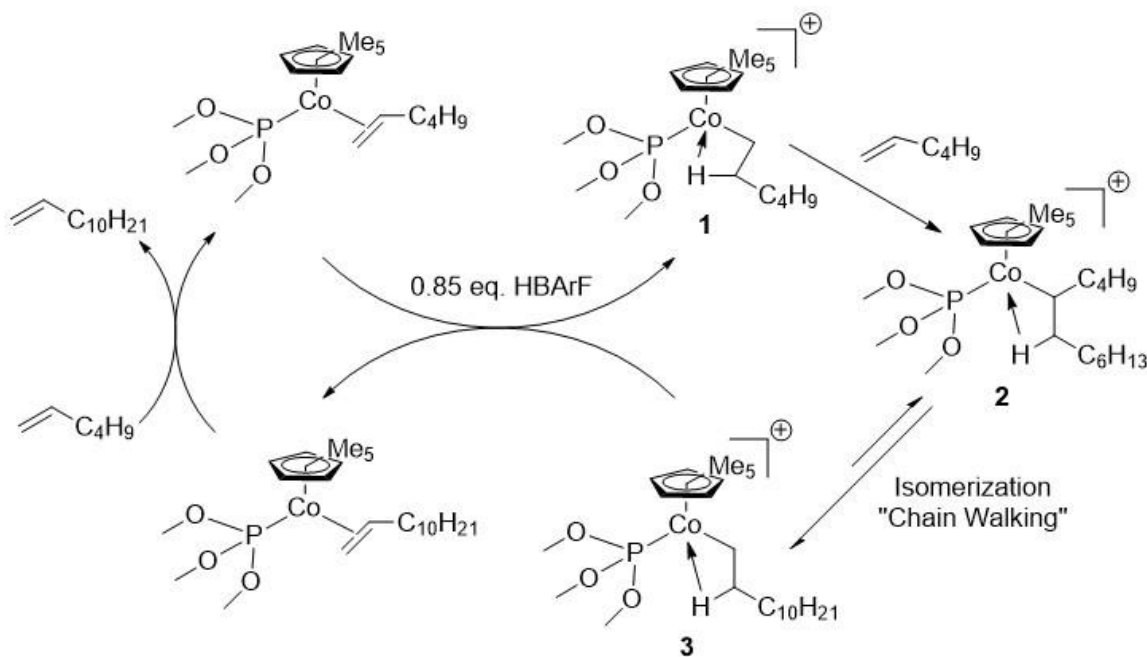


**Figure 6:** The catalytic cycle of the Broene-Brookhart catalyst, showing activation to a cationic species,  $\alpha$ -olefin insertion to form an internal species, isomerization to move the agostic interaction to a terminal  $\beta$ -hydrogen, and  $\beta$ -elimination to reform the olefin, coupled with charge transfer to a different cobalt species. As shown, only olefin dimers are created; the type of dimer is elaborated in detail in Fig. 7.

linear dimer and sterically larger ligands favor 1,2-insertion of the alkene, leading to formation of a non-linear  $\alpha$ -olefin (Figure 7).<sup>11</sup> More precisely, the geometry of ethene insertion into **1** was governed by an equilibrium between 1,2- and 2,1-insertions, where the linear olefin product was produced in greater yield when ligands of lower steric demand were used.

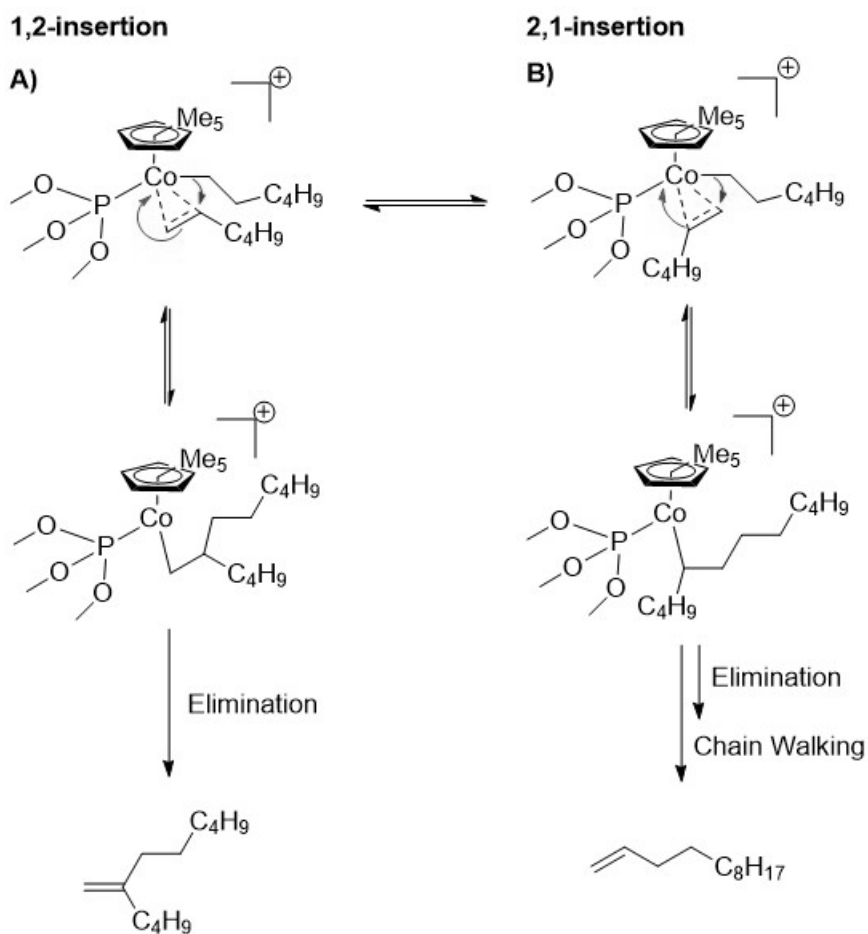


**Figure 7:** The insertion equilibrium of the  $\alpha$ -olefin to the cobalt catalyst, where it can be seen that the geometry of insertion is determined by the steric bulk of supporting ligands. Compounds A) and B) are in equilibrium, where insertion direction determines which isomer is created.

### 2.3 Controlling $\alpha$ -Olefin Dimer Formation

The steric demand of a ligand can be measured by the cone angle, which is the effective size of the cone formed by ligand-metal bond rotation. A variety of ligands with different cone

angles were tested on the Broene-type catalyst, and showed that smaller ligands did indeed correlate to better ratios of branched:linear product; electronic differences between ligands, as determined by the Tolman electronic parameter, were shown to have no correlation to product distribution (Table 1).<sup>11</sup> This confirmed the hypothesis that ligand bulk was the product determining factor, and thus reducing ligand bulk was necessary to achieve a favorable ratio of branched:linear  $\alpha$ -olefins.

*Table 1: A relationship between cone angle, electron donation, and the branched:linear product ratio. It can be seen that smaller cone angles corresponded to more favorable product ratios. Data from Broene.<sup>11</sup>*

Ligand	Cone Angle	Tolman Electronic Parameter (cm <sup>-1</sup> )	Branched:Linear Olefin Ratio
P(OMe) <sub>3</sub>	107°	2079.5	4.5:1
PMe <sub>3</sub>	118°	2064.1	20:1
PPh <sub>3</sub>	145°	2068.9	>100:1

### 3. Constrained Ligands

#### 3.1 8-Quinoyl-Tetramethylcyclopentadiene

Prior work in the Broene lab has focused on reducing the steric demand of supporting ligands, with a focus on chelating ligands (Figure 8).<sup>11-12</sup> In particular, 8-quinoyl-tetramethylcyclopentadiene was investigated, due to the quinoyl group being held perpendicular to the cyclopentadiene ring. It was believed that the chelating supporting ligand would not rotate, thus reducing the steric bulk of the ligand dramatically. However, the complex synthetic scheme involved in ligand preparation, as well as challenges in reducing the cobalt species were encountered (Figure 9),<sup>12</sup> and formation of the final precatalyst **C** presented large synthetic challenges. Primarily, no suitable reducing agent was found to reduce complex **B**

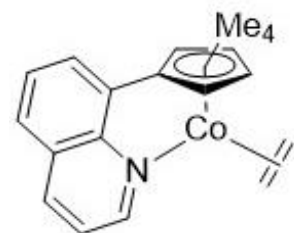


*Figure 8: The design of a targeted catalyst with a bidentate ligand. The chelating effect of this ligand was believed to prevent bond rotation, thus freeing space to allow for better ratios of linear to branched product.*

to complex **C**, and formation of the precatalyst was successful only in very low yield.<sup>12</sup> Additionally, photochemical methods for dissociating the carbonyl ligands from complex **A** were investigated, though such methods were deemed to be unsuccessful.<sup>12</sup> Failure to generate the

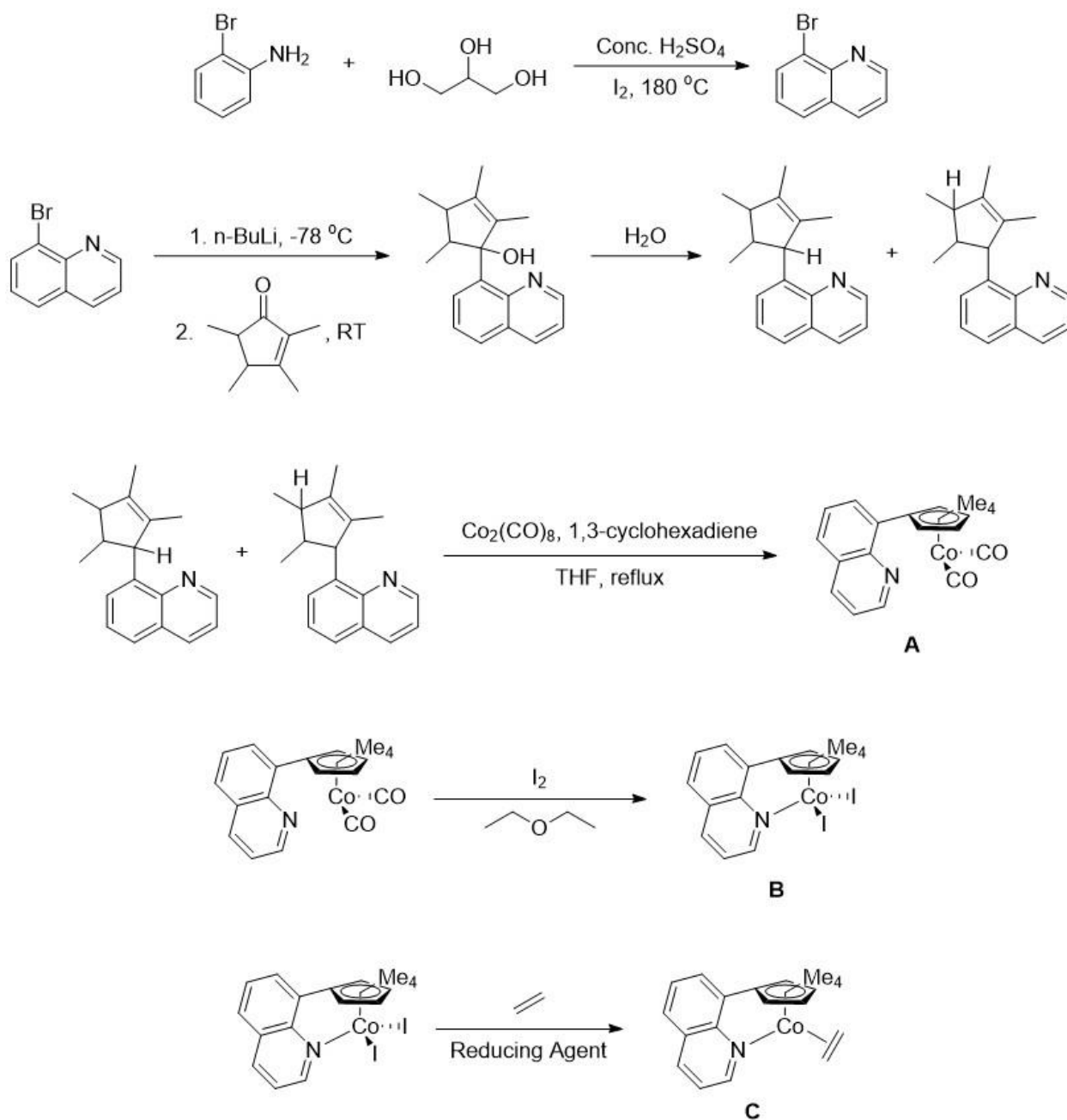


**Figure 9:** The complex synthetic scheme used by prior members of the Broene lab to attempt to synthesize the precatalyst ( $\eta^5$ -ethene)(1-(8-quinoyl)-2,3,4,5-tetramethylcyclopentadiene)cobalt. Complexes **A** and **B** are easily made, whereas methods of forming **C** have been unsuccessful to date. Figure adapted from Keefe.<sup>12</sup>

catalyst through both chemical and photochemical means led to investigations of other constrained ligands.

### 3.2 *N*-Heterocyclic Carbenes

*N*-heterocyclic carbenes (NHCs) present attractive candidates for constrained ligands, due to the strong  $\sigma$ -donation of the carbene lone pair.<sup>13-15</sup> As NHCs are commonly used as alternatives to phosphine ligands, they present an attractive candidate for reducing the steric demand of supporting ligands.<sup>16</sup> Additionally, complexes with NHC supporting ligands have been used for olefin polymerization, and NHCs could be a suitable replacement for previously investigated, sterically-constrained, supporting ligands for the Broene-type dimerization of linear  $\alpha$ -olefins described above.<sup>17-20</sup>

Problematically, large side chains attached to the nitrogen atoms within NHCs are commonplace to prevent dimerization or decomposition of the free carbene species and these large, stabilizing side chains are counterproductive to the goals of reducing steric bulk (Figure 10B and C).<sup>21-23</sup> While the use of small substituents, such as methyl groups (Figure 10A), is predicted to give better linear:branched olefin ratios, these small side chains may hinder olefin dimerization overall.<sup>17, 24-26</sup> For example, formation and coordination of the free carbene to the cobalt may be kinetically unattainable, due to competing, rapid dimerization of the carbene. However, the relatively easy syntheses of NHCs

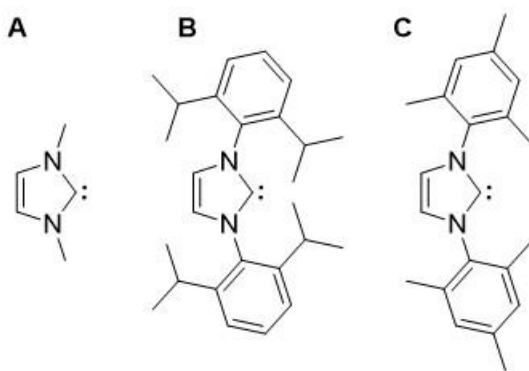


**Figure 10:** Examples of *N*-heterocyclic carbenes A) *N,N'*-dimethyl B) *N,N'*-di(2,6-diisopropyl) and C) *N,N'*-di(2,4,6-trimethylbenzene)-imidazolium-2-ylidene. Carbenes B and C are more commonplace due to ease of synthesis, whereas carbene A is kinetically unfavored to form.

makes them attractive candidates to replace ligands with complex synthetic pathways.<sup>22-23, 27-31</sup>

Classically, NHC formation results from the deprotonation of a halide salt, such as *N,N'*-

dimethylimidazolium iodide (Figure 11).<sup>13</sup> These halide salts require the use of strong reagents to form the NHC, such as NaH and KOtBu, and the resultant free carbene species requires large side chains or very dilute solutions to prevent dimerization.<sup>22, 31</sup> New methods of NHC formation utilize much milder reagents, and generation of a free carbene species might not be necessary.<sup>27, 29</sup>

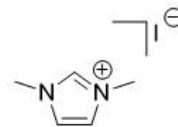


Figure 11: The structure of *N,N'*-dimethylimidazolium iodide.

### 3.3 *N,N'*-Dimethylimidazolium-2-Carboxylate

One such method of NHC formation is the use of carboxylate salts as precursors to the carbene itself. Specifically, the use of dimethylcarbonate has been explored to target the smallest synthetically viable NHC, *N,N'*-dimethylimidazolium-2-ylidene, using the carboxylate salt (Figure 12) to

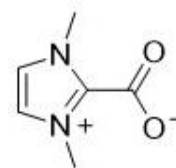


Figure 12: The structure of *N,N'*-dimethylimidazolium-2-carboxylate.

avoid the unstable free carbene species.<sup>29</sup> Previous literature studies have confirmed the use of NHC-carboxylate salts to form transition metal-NHC complexes, and the mild formation of carbene complexes presents a desirable target.

### 3.4 Research Objectives

This project investigates synthetic protocols for the formation of NHC precursor salts, both the traditional *N,N'*-dimethylimidazolium iodide salt, as well as the new *N,N'*-dimethylimidazolium-2-carboxylate salt. Additionally synthetic protocols have been developed for the formation of the precatalyst ( $\eta^5$ -pentamethylcyclopentadienyl)( $\eta^2$ -ethene)(*N,N'*-dimethylimidazolium-2-ylidene)cobalt (Figure 13) using mild reaction conditions. Catalyst activation via HBAR<sub>F</sub> and catalysis of 1-hexene was investigated, in addition to examining an unexpected cobalt dimer.

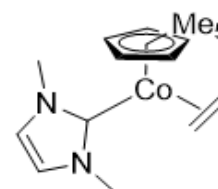


Figure 13: The structure of [*Cp*\*Co(ethene)(*N,N'*-dimethylimidazolium-2-ylidene)], the target molecule of this project.



## Experimental

All reactions were performed in oven dried glassware under nitrogen using standard Schlenk techniques, unless otherwise specified. All chemicals were stored and manipulated in a glovebox (Vacuum Atmospheres Company) under nitrogen, unless noted as air stable. Solvents denoted as “dry” were dried using a sodium benzophenone ketyl radical and distilled under nitrogen; “dry, degassed” solvents were dried, distilled and underwent at least two cycles of freeze-pump-thaw before use. NMR spectra were taken using a Bruker Avance 400 MHz NMR; NMR spectra of air-sensitive compounds were solvated in dry, degassed C<sub>6</sub>D<sub>6</sub>, while air-stable compounds were dissolved in CDCl<sub>3</sub> or D<sub>2</sub>O; all chemical shifts are reported in ppm using the residual protio-solvent peak as the reference. Gas chromatography was carried out on an Agilent 6890N GC with a flame ionization detector on a capillary column (Zebron ZB-5MS, 30m, 0.25 I.D., 0.25 μL film thickness; Phenomenex, Torrance, CA). Temperature program: held at 50 °C for 3 min, 10 °C/min ramp to 250 °C, and held at 250 °C 3 min. The injection port was maintained at 280 °C; Splitless injections of 1.0 μL were carried out with a helium flow rate of 1.6 mL/min. Data was analyzed using MSD ChemStation E.02.02.1431 (Agilent Technologies). Compound numbers are assigned as shown in Figure 14, Figure 19, Figure 22, and Figure 26.

### ***1. Synthesis of Cp\*Co(ethene)<sub>2</sub> from dicobalt octacarbonyl (Adapted from Frith et al.<sup>32</sup>)***

#### ***1.1 Formation of dicarbonyl-(η<sup>5</sup>-pentamethylcyclopentadienyl)cobalt (1)***

A 100 mL Schlenk flask was charged with dicobalt octacarbonyl (6 g, 17.5 mmol), and pentamethyl cyclopentadiene (Cp\*) (5.3 g, 39 mmol). The flask was transferred to a Schlenk line, and 1,3-cyclohexadiene (2.5 mL, 26.22 mmol) was added by syringe, along

with 50 mL dry dichloromethane. The Schlenk flask was capped with a reflux condenser and allowed to reflux for 2.75 hours. Then, solvent was removed *in vacuo* and the crude, dark red precipitate was used in the next step without purification.  $^1\text{H}$  NMR analysis showed the desired product as well as excess Cp\* (Shown in blue), as determined by the NMR integration ratios, the product is 93.8% pure.

Yield: 7.86 g (89.7%)

Yield (adjusted for purity): 7.372 (85.7%)

$^1\text{H}$  NMR (400 MHz, 20 °C,  $\text{C}_6\text{D}_6$ )  $\delta$ : 0.2 (s, 1H, CH), 1.0 (s, 6 H, CH<sub>3</sub>), 1.6 (s, 15 H, C<sub>5</sub>(CH<sub>3</sub>)<sub>5</sub>), 1.77 (s, 6 H, CH<sub>3</sub>), 2.41 (s, 3 H, CH<sub>3</sub>)

## 1.2 Synthesis of carbonyldiiodo-( $\eta^5$ -pentamethylcyclopentadienyl)cobalt (2)

A 250 mL Schlenk flask was charged with 150 mL of dry diethyl ether to which iodine (8.9 g, 35 mmol) was added. A second, 100 mL Schlenk flask was charged with all of the crude  $[(\text{CO})_2(\eta^5\text{Cp}^*)\text{Co}]$  was dissolved in 20 mL of dry ether. This latter solution was transferred over 5 minutes to the iodine solution by cannula. The solution was left to stir under nitrogen for 1 hour, then filtered in air, and washed with diethyl ether (3x20 mL). A dull black powder was obtained.

Yield: 13.473 g (90.15%)

$^1\text{H}$  NMR (400 MHz,  $\text{CDCl}_3$ , 20 °C)  $\delta$ : 2.2 (s, 15 H, C<sub>5</sub>(CH<sub>3</sub>)<sub>5</sub>)

### 1.3 Synthesis of di-iodo-bis[iodo-( $\eta^5$ -pentamethylcyclopentadienyl)cobalt] (**3**)

An oven dried 250 mL flask was charged with all of the crude  $[(\text{CO})(\text{I})_2(\eta^5\text{Cp}^*)\text{Co}]$  and 150 mL n-octane. The flask was fitted with a reflux condenser and allowed to reflux overnight. The suspension of black crystals was retrieved using a sintered glass funnel and washed thoroughly with hexane. The crude product was added to a paper thimble and placed in a Soxhlet extractor using a 250 mL round bottom flask charged 150 mL dry dichloromethane. This was fitted with a reflux condenser heated to reflux and the cobalt containing material was extracted overnight. The solution was then chilled to 0 °C for at least 3 hours, and the resulting black crystals were filtered in air.

Yield: 6.5628 g (81.7%)

$^1\text{H}$  NMR (400 MHz, 20 °C,  $\text{CDCl}_3$ )  $\delta$ : 1.8 (s, 15 H,  $\text{C}_5(\text{CH}_3)_5$ )

### 1.4 Synthesis of bis( $\eta^2$ -ethene)( $\eta^5$ -pentamethylcyclopentadienyl)cobalt (**4**)

In a 250 mL Schlenk flask, a zinc-mercury amalgam was prepared by adding zinc dust (20 g) and 25 mL 2M HCl. This was allowed to react for 5 minutes, while mercuric chloride (1.2 g) was added to an additional 25 mL 2M HCl. The HCl was decanted and the mercuric chloride mixture was added and allowed to react for an additional 5 minutes. Then, this was washed with water (2x20 mL), anhydrous ethanol (2x20 mL) and dry diethyl ether (3x20 mL), decanting the liquid after each addition. The amalgam was dried under vacuum at 100 mTorr for 3 hours. The flask was then flushed with ethene gas and a stir bar was added along with 100 mL dry tetrahydrofuran. All of the  $[(\text{Cp}^*)\text{Co}(\text{I})_2]_2$  from the prior step was added and the mixture was stirred vigorously for 1.5 hours under a gentle ethene flow. The dark red solution was decanted from the zinc amalgam to a dry 250 mL

Schlenk flask by cannula and residual solvent was evaporated to yield a dark solid. The flask was transferred to the glovebox under vacuum and the dark solid was dissolved in dry, degassed hexane. The hexane-soluble material was chromatographed (hexane, activity II alumina), and the resultant orange solution was evaporated to yield light orange crystals.

Yield: 1.133 g (19.35%)

$^1\text{H}$  NMR (400 MHz, 20 °C,  $\text{C}_6\text{D}_6$ )  $\delta$ : 1.0 (d, 4 H, alkene CH), 1.41 (s, 15 H,  $\text{C}_5(\text{CH}_3)_5$ ), 1.7 (d, 4 H, alkene CH)

## 2. *Synthesis of N,N'-dimethylimidazolium iodide (5)*

Trial 1) A 100 mL Schlenk flask was evacuated and flushed with nitrogen. Dry dichloromethane (5 mL) was added along with 1-methylimidazole (2 g, 25 mmol) and of iodomethane (4.2 g, 35 mmol); the Schlenk flask was capped with a stopper and allowed to stir for 1 hour at room temperature. After the reaction had completed, the solvent was removed *in vacuo* and the white precipitate was transferred into a glovebox freezer for storage. NMR analysis in MeOD did not show the desired product.

Yield: 3.24 g (mass of undesired product)

$^1\text{H}$  NMR (400 MHz, 20 °C, MeOD)  $\delta$ : 2.64 (s, 0.36 H), 4.06 (s, 4 H), 4.87 (s, 0.34 H), 6.96 (s, 4 H), 8.31 (s, 2 H)

Trial 2) A 100 mL Schlenk flask was evacuated and flushed with nitrogen. Toluene (20 mL) was dried over Na and distilled directly into the flask. Then 1-methylimidazole

(2 g, 25 mmol) and iodomethane (3.6 g, 25 mmol) were added; the Schlenk flask was capped with a reflux condenser and allowed to reflux at 110 °C for 1 hour. After the reaction had completed, the solvent was removed *in vacuo* and the off-white precipitate was transferred into a glovebox freezer for storage; a small sample was removed for NMR analysis in D<sub>2</sub>O showing high purity.

Yield: 5.517 g (98 %)

<sup>1</sup>H NMR (400 MHz, 20 °C, D<sub>2</sub>O) δ: 3.85 (s, 6 H, NCH<sub>3</sub>), 7.37 (s, 2 H, CH), 8.61 (s, 1 H, CH)

### 3. Synthesis of *N,N'*-dimethylimidazolium-2-carboxylate (6)

Trial 1) In a 25 mL sealable Schlenk flask, 1-methylimidazole (1 g, 12.5 mmol) and dimethyl carbonate (1.6 g, 17.8 mmol) were combined. The flask was sealed and refluxed at 120 °C for 24 hours. Note: As the reaction takes place in a sealed container above the boiling point of methanol, a byproduct of the reaction, the flask must be placed behind a blast shield in case of explosion. Flask pressure was calculated to be 6.35 atm.<sup>33</sup> The resulting off-white precipitate was separated from the methanol byproduct via filtration through a sintered glass funnel and washed thoroughly with diethyl ether. The white powder was dried for 5 minutes at 24 torr, then stored in a screw cap vial in air. An NMR taken in D<sub>2</sub>O showed a mixture the 2-carboxylate and 4-carboxylate products in a ratio of 3:1 (4-carboxylate shown in blue).

Yield: 0.9143 g (Mixture)

<sup>1</sup>H NMR (400 MHz, 20 °C, D<sub>2</sub>O) δ: 3.85 (s, 1.86 H, NCH<sub>3</sub>), 3.95 (s, 6 H, NCH<sub>3</sub>), 3.98 (s, 1.74 H, NCH<sub>3</sub>), 7.34 (s, 2 H, CH), 7.7 (s, 0.48 H, CH)

Trial 2) In a 25 mL sealable Schlenk flask, 1-methylimidazole (1 g, 12.5 mmol) and dimethyl carbonate (1.6 g, 17.8 mmol) were combined. The flask was sealed and refluxed at 90 °C for 4 days behind a blast shield; pressure was calculated at 2.5 atm.<sup>33</sup> The resulting white precipitate was retrieved from the methanol byproduct with a sintered glass funnel, and washed thoroughly with diethyl ether. The white powder was dried for 5 minutes at 24 torr, then stored in a screw cap vial in air. NMR analysis in D<sub>2</sub>O showed no 4-carboxylate product.

Yield: 0.701 g (28%)

<sup>1</sup>H NMR (400 MHz, 20 °C, D<sub>2</sub>O) δ: 1.0 (d, 4 H, CH), 1.41 (s, 15 H, C<sub>5</sub>(CH<sub>3</sub>)<sub>5</sub>), 1.7 (d, 4 H, CH)

#### 4. Coordination of *N,N'*-dimethylimidazolium-2-carboxylate to [Cp\*Co(ethene)<sub>2</sub>]

Trial 1) Cp\*Co(ethene)<sub>2</sub> (50 mg, 0.2 mmol) was added to a 25 mL sealable Schlenk flask, along with *N,N'*-dimethylimidazolium-2-carboxylate (40 mg, 0.2 mmol). Dry, degassed benzene (2 mL) was added and the flask was sealed and then placed in a 95 °C oil bath for 3 hours. Note: As the reaction takes place in a sealed container at temperatures greater than the boiling point of benzene, the flask must be placed behind a blast shield in case of explosion. Flask pressure was calculated to be 1.55 atm.<sup>33</sup> After 3 hours, a green solution was observed, along with an ashy brown precipitate. In the glovebox, the mixture was filtered through celite and glass wool, and solvent was removed *in vacuo* to yield a dark crystalline material. Proton NMR in C<sub>6</sub>D<sub>6</sub> showed a complex mixture.

$^1\text{H}$  NMR (400 MHz, 20 °C,  $\text{C}_6\text{D}_6$ )  $\delta$ : 0.245 (m, 0.755 H), 0.95 (m, 2 H), 1.4 (m, 2 H), 1.75 (s, 15 H), 1.88 (s, 2.9 H), 3.3 (m, 0.28 H), 3.48 (d, 1.2 H), 3.69 (s, 6.5 H), 5.2 (s, 0.33 H), 6.03 (s, 2.04 H), 6.09 (s, 0.32 H)

Trial 2)  $\text{Cp}^*\text{Co}(\text{ethene})_2$  (50 mg, 0.2 mmol) was added to a 25 mL sealable Schlenk flask, along with  $\text{N,N}'$ -dimethylimidazolium-2-carboxylate (60 mg, 0.3 mmol). Dry, degassed benzene (2 mL) was added. The flask was sealed then heated in a 95 °C oil bath for 3 hours, behind a blast shield. Flask pressure was calculated to be 1.55 atm.<sup>33</sup> After 3 hours, a green solution was observed, along with a significant quantity of brown precipitate. The solution was filtered through celite and glass wool in the glovebox, and solvent was removed *in vacuo* to yield a dark green solid. Proton NMR in  $\text{C}_6\text{D}_6$  showed a complex mixture.

$^1\text{H}$  NMR (400 MHz, 20 °C,  $\text{C}_6\text{D}_6$ )  $\delta$ : 0.29 (m, 3.14 H), 0.9 (m, 2.3 H), 1.4 (m, 1.9 H), 1.75 (s, 15 H), 1.88 (s, 1.81 H), 3.48 (d, 0.69 H), 3.69 (s, 6.25 H), 6.03 (s, 2.08 H), 6.09 (s, 0.248 H)

Trial 3)  $\text{N,N}'$ -dimethylimidazolium-2-carboxylate (40 mg, 0.2 mmol) was added to a 100 mL 3 necked flask along with dry degassed mesitylene (5 mL).  $\text{Cp}^*\text{Co}(\text{ethene})_2$  (50 mg, 0.2 mmol) was added to a solid addition tube, and placed on one of the flask necks. Another neck was capped with a reflux condenser on a Schlenk line, and the third neck was capped with a stopper. The carboxylate solution was refluxed under gentle nitrogen flow for 1 hour, then cooled. The  $\text{Cp}^*\text{Co}(\text{ethene})_2$  was added in one portion and left stirring at

90 °C for 3 hours. The mesitylene was removed *in vacuo* and the brown product was analyzed by NMR in C<sub>6</sub>D<sub>6</sub>, showing only paramagnetic material.

Trial 4) Cp\*Co(ethene)<sub>2</sub> (50 mg, 0.2 mmol) was placed in a 25 mL sealable Schlenk flask with N,N'-dimethylimidazolium-2-carboxylate (40 mg, 0.2 mmol). Dry, degassed benzene (2 mL) was added and the flask was sealed. The flask was then placed in a 95 °C oil bath for 24 hours behind a blast shield. Flask pressure calculated to be 1.55 atm.<sup>33</sup> After 24 hours had passed, a slightly cloudy, dark red solution was seen. The solution was filtered through glass wool and celite in the glovebox, and the clear red filtrate was evaporated *in vacuo* to yield dark red crystals. NMR analysis in C<sub>6</sub>D<sub>6</sub> showed a mixture of two products in a 3:1 ratio (major product shown in black, minor product shown in blue).

Yield: 21.5 mg (mixture)

<sup>1</sup>H NMR (400 MHz, 20 °C, C<sub>6</sub>D<sub>6</sub>) δ: 0.9 (d, 2 H, CH), 1.4 (d, 2 H, CH), 1.76 (s, 15 H, C<sub>5</sub>(CH<sub>3</sub>)<sub>5</sub>), 1.88 (s, 4.4 H), 3.47 (s, 1.5 H), 3.68 (s, 6 H, NCH<sub>3</sub>), 6.02 (s, 2 H, CH), 6.09 (s, 0.5 H)

Trial 5) Cp\*Co(ethene)<sub>2</sub> (50 mg, 0.2 mmol) was placed in a 25 mL sealable Schlenk flask with N,N'-dimethylimidazolium-2-carboxylate (40 mg, 0.2 mmol). Dry, degassed benzene (2 mL) was added and the flask was sealed. The flask was then placed in a 75 °C oil bath for 24 hours behind a blast shield. After time had elapsed, a slightly cloudy, dark red solution was seen. The solution was filtered through glass wool and celite in the glovebox, and the clear red filtrate was evaporated *in vacuo* to yield dark red crystals.



NMR analysis in C<sub>6</sub>D<sub>6</sub> showed a mixture of two products in a 10:1 ratio (major product shown in black, minor product shown in blue).

Yield: 38.2 mg (mixture)

<sup>1</sup>H NMR (400 MHz, 20 °C, C<sub>6</sub>D<sub>6</sub>) δ: 0.9 (d, 2 H, CH), 1.4 (d, 2 H, CH), 1.76 (s, 15 H, C<sub>5</sub>(CH<sub>3</sub>)<sub>5</sub>), 1.88 (s, 4.4 H), 3.47 (s, 1.5 H), 3.68 (s, 6 H, NCH<sub>3</sub>), 6.02 (s, 2 H, CH), 6.09 (s, 0.5 H)

Trial 6) Cp\*Co(ethene)<sub>2</sub> (50 mg, 0.2 mmol) was placed in a 25 mL sealable Schlenk flask with N,N'-dimethylimidazolium-2-carboxylate (40 mg, 0.2 mmol). Dry, degassed benzene (2 mL) was added and the flask was sealed. The flask was then placed in a 60 °C oil bath for 24 hours behind a blast shield. After time had elapsed, a slightly cloudy, dark red solution was seen. The solution was filtered through glass wool and celite in the glovebox and the clear red filtrate was evaporated *in vacuo* to yield dark red crystals. NMR analysis in C<sub>6</sub>D<sub>6</sub> showed a mixture of two products in a 20:1 ratio (major product shown in black, minor product shown in blue).

Yield: 46.9 mg (mixture)

<sup>1</sup>H NMR (400 MHz, 20 °C, C<sub>6</sub>D<sub>6</sub>) δ: 0.9 (d, 2 H, CH), 1.4 (d, 2 H, CH), 1.76 (s, 15 H, C<sub>5</sub>(CH<sub>3</sub>)<sub>5</sub>), 1.88 (s, 4.4 H), 3.47 (s, 1.5 H), 3.68 (s, 6 H, NCH<sub>3</sub>), 6.02 (s, 2 H, CH), 6.09 (s, 0.5 H)

##### 5. Catalyst Activation and Dimerization of 1-Hexene

In a 20 mL vial, Cp\*Co(ethene)(N,N'-dimethylimidazolium-2-ylidene) (4.5 mg, 0.014 mmol) was dissolved in dry, degassed 1,2-difluorobenzene (0.5 mL). In a separate

20 mL vial, 0.7 eq. HBA<sub>rF</sub> (10 mg, 0.01 mmol) was dissolved in dry, degassed 1,2-difluorobenzene (0.5 mL). The two solutions were combined and a mesitylene internal standard was added (2.5 μL), along with dry, degassed 1-hexene (1 mL, 8 mmol); the vial was capped and left stirring in the glovebox. At 24 hours, 1 drop was removed and placed in a 4 mL vial. This vial was removed from the drybox and distilled water (1 mL) was added, along with dichloromethane (1 mL). The organic products were extracted into the dichloromethane and diluted to an appropriate concentration for GC analysis. Aliquots were planned to be taken every day for 11 days, though only the 24 and 48 hour aliquots were taken before the termination of research.

**6. Synthesis of bis[(N,N'-dimethylimidazolium-2-ylidene)(η<sup>5</sup>-pentamethylcyclopentadienyl)cobalt]**

Trial 1) A 25 mL sealable Schlenk flask was charged with Cp\*Co(ethene)<sub>2</sub> (50 mg, 0.2 mmol) and N,N'-dimethylimidazolium-2-carboxylate (40 mg, 0.2 mmol). Dry, degassed benzene (2 mL) was added and the flask was sealed under nitrogen. The flask was placed into a 110 °C oil bath, behind a blast shield, and allowed to stir for 24 hours. Flask pressure calculated at 2.31 atm.<sup>33</sup> After time, the flask was moved into the glovebox and a dark brown precipitate was filtered out using glass wool and celite, yielding a dark red solution. The solvent was evaporated *in vacuo* to give dark red crystals. <sup>1</sup>H NMR analysis in C<sub>6</sub>D<sub>6</sub> showed the two products present in a 1:1 ratio (cobalt monomer shown in black, cobalt dimer in blue).

<sup>1</sup>H NMR (400 MHz, 20 °C, C<sub>6</sub>D<sub>6</sub>) δ: 0.9 (d, 2 H, CH), 1.4 (d, 2 H, CH), 1.76 (s, 15 H, C<sub>5</sub>(CH<sub>3</sub>)<sub>5</sub>), 1.88 (s, 15 H, Cp\*), 3.47 (s, 6 H, NCH<sub>3</sub>), 3.68 (s, 6 H, NCH<sub>3</sub>), 6.02 (s, 2 H, alkene CH), 6.09 (s, 2 alkene CH)

Trial 2) A 25 mL sealable Schlenk flask was charged with Cp\*Co(ethene)<sub>2</sub> (50 mg, 0.2 mmol) and N,N'-dimethylimidazolium-2-carboxylate (40 mg, 0.2 mmol). Dry, degassed mesitylene (2 mL) was added and the flask was sealed under nitrogen. The flask was placed in a 130 °C oil bath, behind a blast shield, for 24 hours. After the time had elapsed the flask was removed from the heat and cooled, a dark red solution was observed. The solution was filtered through celite and glass wool, and an NMR sample was prepared in C<sub>6</sub>D<sub>6</sub>; NMR analysis showed only one product present. The product was taken up in a minimal amount of benzene, and layered with hexane in an NMR tube, in an attempt to form crystals. Additionally, an additional <sup>1</sup>H NMR spectrum was taken after one week of attempted crystal formation, showing decomposition of the compound, as evidenced by new resonances in the <sup>1</sup>H NMR. However, crystal formation proved difficult and no crystals were obtained before experiments ended.

<sup>1</sup>H NMR (400 MHz, 20 °C, C<sub>6</sub>D<sub>6</sub>) δ: 1.87 (s, 15 H, Cp\*), 3.5 (s, 6 H, NCH<sub>3</sub>), 6.1 (s, 2 H, alkene CH)

<sup>1</sup>H NMR (400 MHz, 20 °C, C<sub>6</sub>D<sub>6</sub>, 7 days) δ: -2.72 (s, 1.3 H), 1.87 (s, 15 H, Cp\*), 3.5 (s, 6 H, NCH<sub>3</sub>), 6.1 (s, 2 H, alkene CH), 10.2 (s, 2.5 H)

## Results and Discussion

The synthesis of **4** (Figure 14) as well as the formation of ligands **5** and **6** (Figure 19 and Figure 22) are discussed. The development of the synthetic procedure for the coordination of **6** to **4** is also shown (Figure 26). Additionally, preliminary catalytic experiments for the dimerization of 1-hexene are shown, as is the proposed catalytic cycle of **7** (Figure 37).

### 1. Synthesis of $Cp^*Co(ethene)_2$ (**4**)

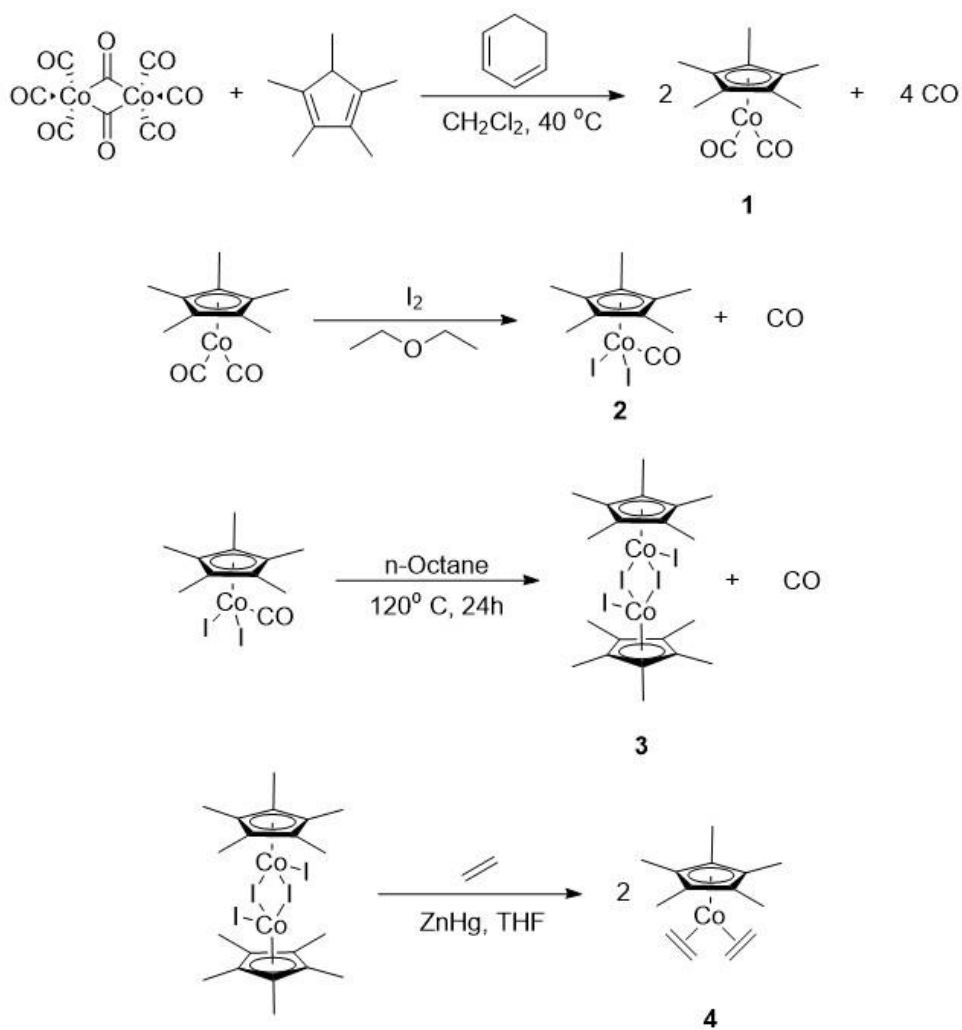
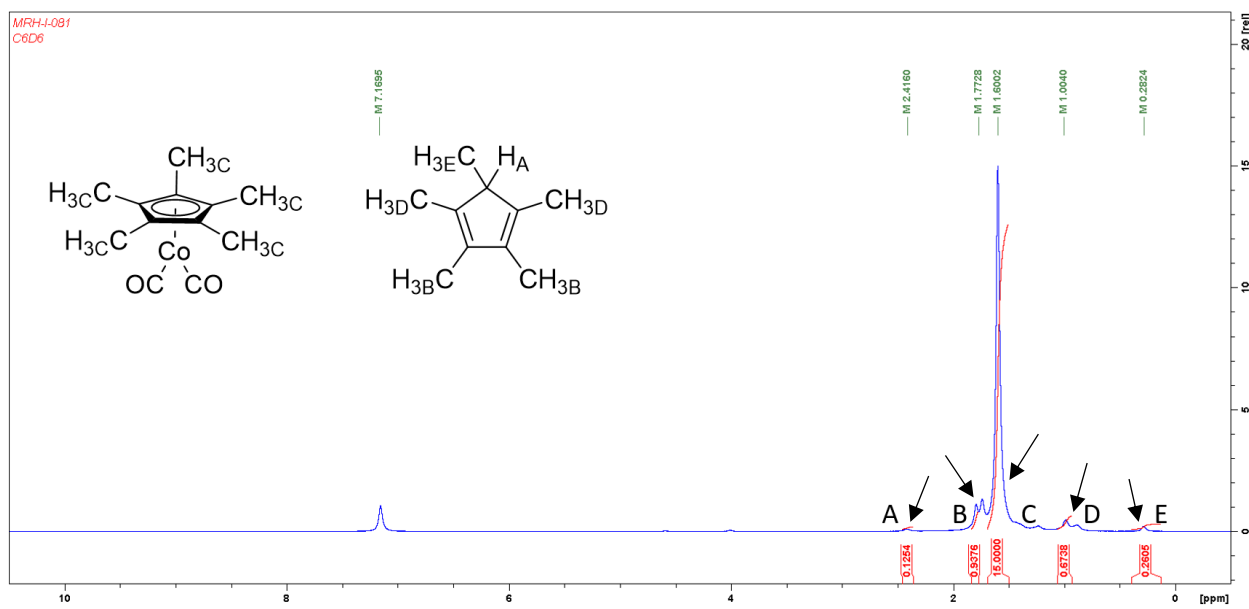
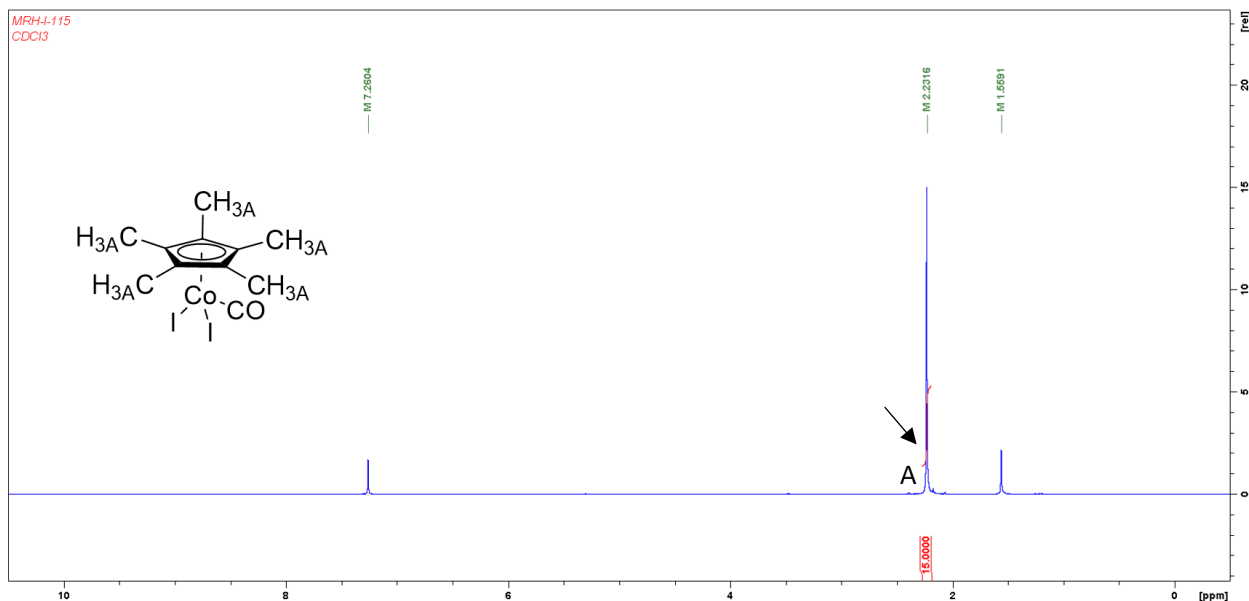


Figure 14: The synthetic scheme detailing formation of  $[Cp^*Co(ethene)_2]$  from  $[Co_2(CO)_8]$ .



**Figure 15:** The NMR spectra of Cp\*Co(CO)<sub>2</sub> (**1**) in C<sub>6</sub>D<sub>6</sub> ( $\delta=7.16$ ). As shown, two components are present, the desired cobalt complex and excess Cp\*. Paramagnetic material is also present, as seen by the line broadening of the resonances.

Cp\*Co(ethene)<sub>2</sub> was synthesized in high purity through a well characterized synthetic pathway, detailed in Figure 14.<sup>32</sup> Beginning from readily available cobalt carbonyl, Co<sub>2</sub>(CO)<sub>8</sub>, dicarbonyl species **1** was synthesized in high yield and purity (85.7% yield, adjusted for impurity, 93.8% pure) (Experimental: 1.1). The NMR spectrum of the resulting material shows excess Cp\* used in the reaction (Figure 15 Peaks A, B, D, E), as well as some paramagnetic material, determined by the significant line broadening of the resonances (Figure 15). As per the literature procedure, this material was used in the next synthetic step without purification.<sup>32</sup> This material was then oxidized with I<sub>2</sub> in ether, resulting in the dissociation of one carbonyl ligand, and the formation of **2** (Experimental: 1.2). This step was also completed in high yield (90.15%) and purity was assessed by <sup>1</sup>H NMR (Figure 16). The minor resonance at  $\delta=1.6$  is due to water in the deuteriochloroform. Additionally, the downfield shift of the Cp\* peak from **1** to **2** is consistent with the reduced electron density at cobalt, due to the oxidation from cobalt (I) to cobalt (III). Next, the dissociation of the remaining carbonyl ligand was achieved under thermal conditions (Experimental: 1.3). This process gave **3** in high yield (81.7%) and purity determined by <sup>1</sup>H NMR



**Figure 16:** The NMR spectra of  $\text{Cp}^*\text{Co}(\text{CO})(\text{I})_2$  (**2**) in  $\text{CDCl}_3$  ( $\delta=7.26$ ). It can be seen that the material is pure, with the minor peak at  $\delta=1.6$  being water.

(Figure 17). The upfield shifting of the  $\text{Cp}^*$  peak is consistent with the loss of the electron withdrawing carbonyl ligand. As before, the peak at  $\delta=1.6$  indicates the presence of water in the NMR solvent. Finally, this cobalt dimer was reduced under an ethene atmosphere using a zinc-mercury amalgam to yield **4** (Experimental: 1.4). While isolated in poor overall yield (19.35%), this loss of material is believed to have come from exposure of the reaction solution to atmospheric

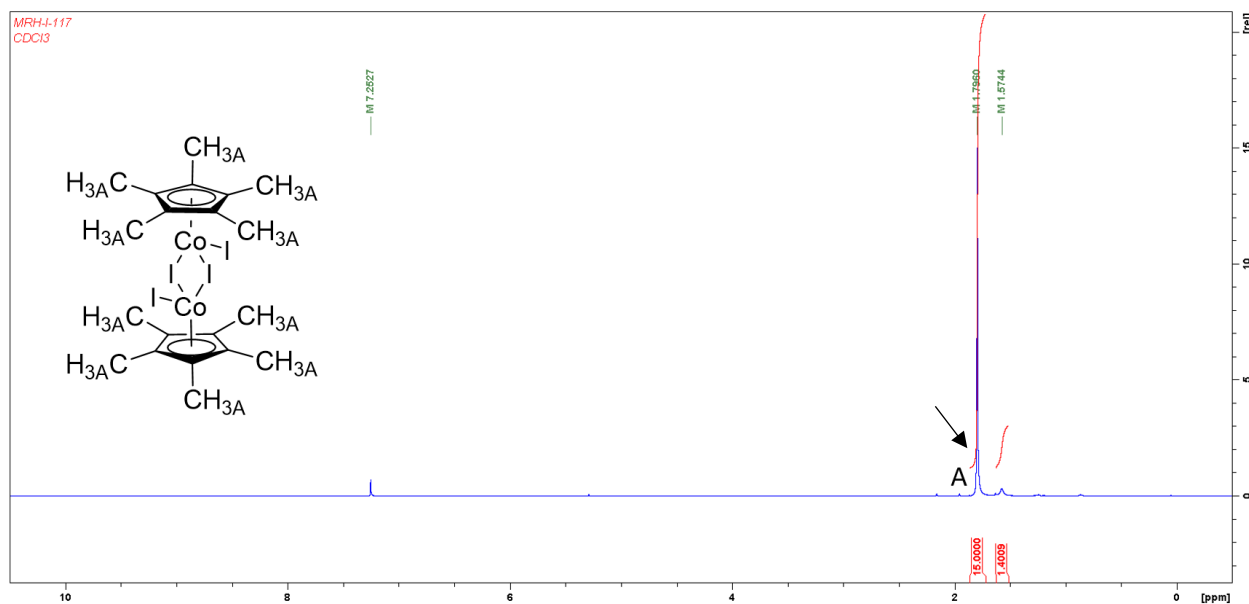


**Figure 17:** The NMR spectra of  $[\text{Cp}^*\text{Co}(\text{I})_2]_2$  (**3**) in  $\text{CDCl}_3$  ( $\delta=7.26$ ). As shown, the material is pure, the minor peak at  $\delta=1.6$  is determined to be water.

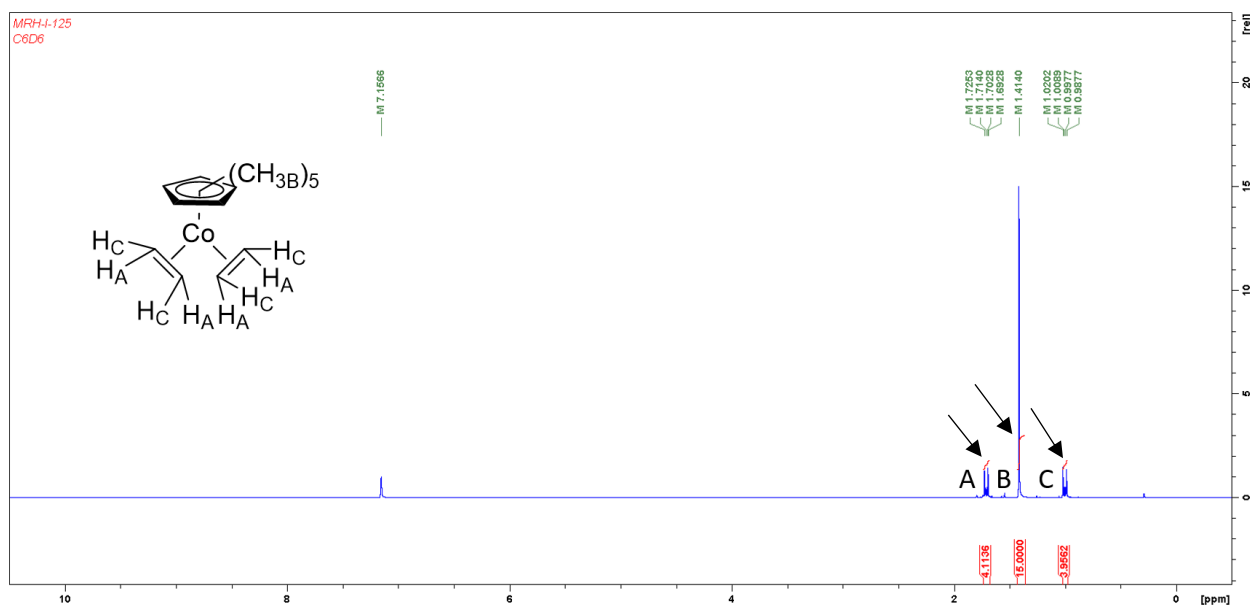


**Figure 18:** The NMR spectra of  $\text{Cp}^*\text{Co}(\text{ethene})_2$  (**4**) in  $\text{C}_6\text{D}_6$  ( $\delta=7.16$ ). Three narrow resonances are assigned structurally, and indicate high purity of the compound.

oxygen at some point during the reaction. The material was purified via column chromatography over activity II alumina, resulting in light orange crystals (as described in literature), and  $^1\text{H}$  NMR showed three narrow resonances, indicating one diamagnetic compound in solution (Figure 18).

## 2. Synthesis of $N,N'$ -Dimethylimidazolium Iodide (**5**)

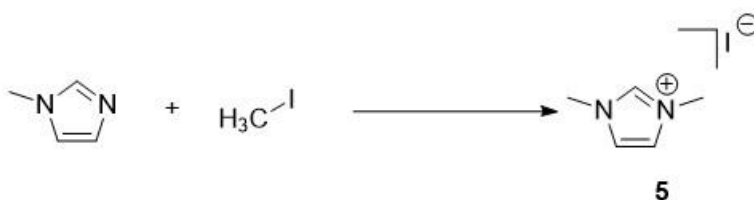


**Figure 19:** The synthetic scheme of  $N,N'$ -dimethylimidazolium iodide.

The synthesis of  $N,N'$ -dimethylimidazolium iodide by methylation of 1-methylimidazole with iodomethane was investigated as a method of forming the NHC precursor **5** (Figure 19). With room temperature, dry dichloromethane as the solvent, this synthesis was unsuccessful, and none of the desired **5** was seen in the  $^1\text{H}$  NMR (Figure 20). This was determined by analyzing combinations of the integration ratios of the peaks in the spectra. Based on the molecular structure, a set of resonances would be expected to have the integration ratio 1:2:6, however this is not seen

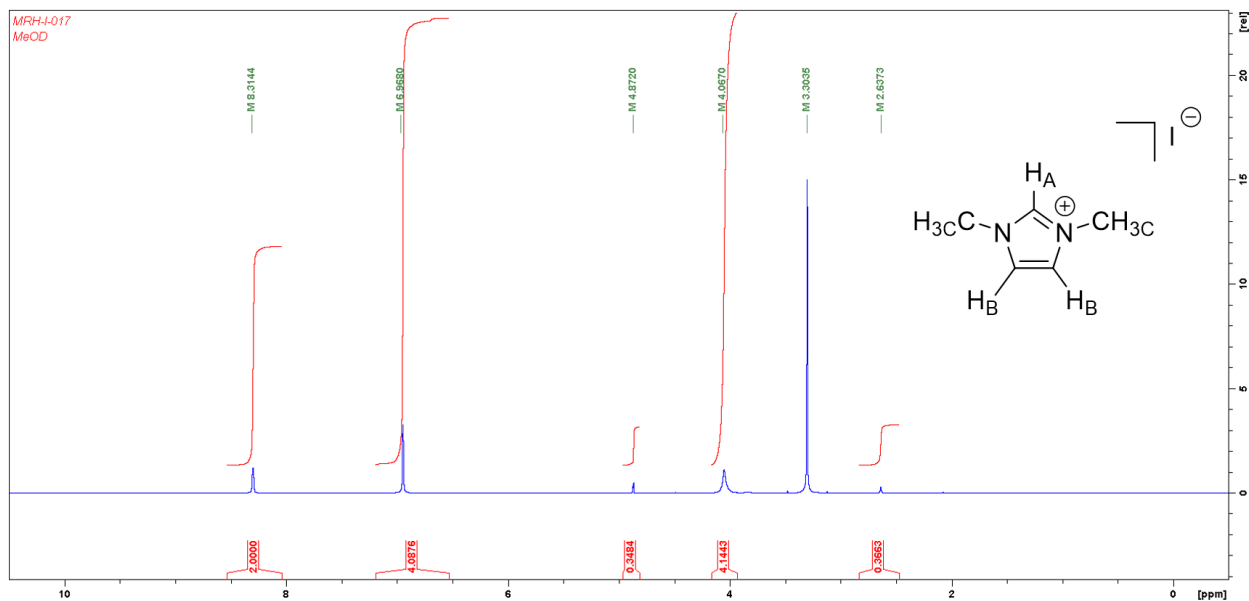


**Figure 20:** The NMR spectrum of the unsuccessful synthesis of *N,N'*-dimethylimidazolium iodide Trial 1 in MeOD ( $\delta=3.31$ ). The structure of the compound is provided for reference, though the material is unidentified.

in the spectrum. The major peaks have an integration ratio of 1:2:2, which is not consistent with

5. Upon reaction in refluxing toluene (Experimental: 2 Trial 2), the methylation of 1-methylimidazole went to completion, with significantly improved yield (98% yield) and no undesired peaks seen in the  $^1\text{H}$  NMR; the peak around  $\delta=0$  denotes silicon grease (Figure 21). This *N,N'*-dimethylimidazolium iodide salt is the traditional precursor to access the dimethyl-NHC

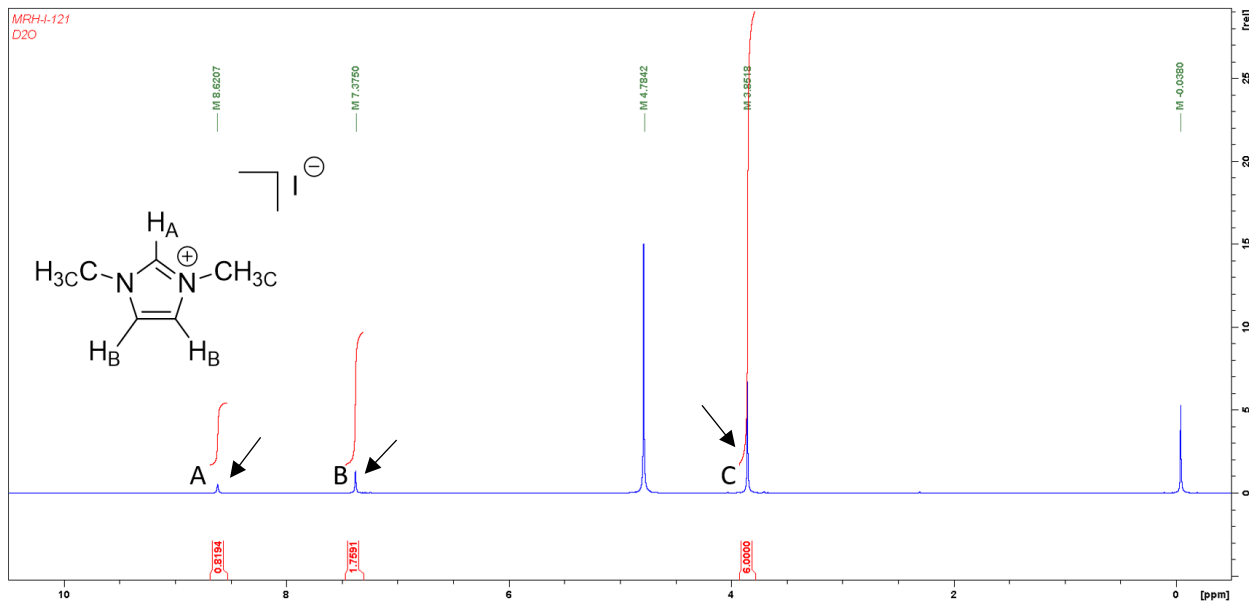


**Figure 21:** The synthesis of *N,N'*-dimethylimidazolium iodide (5) Trial 2 in  $\text{D}_2\text{O}$  ( $\delta=4.79$ ).



species, and through deprotonation by NaH, the free carbene can be generated.<sup>22</sup> Ultimately this material was not used given the more favorable reaction conditions afforded by N,N'-dimethylimidazolium-2-carboxylate.

### 3. *Synthesis of N,N'-Dimethylimidazolium-2-carboxylate (6)*

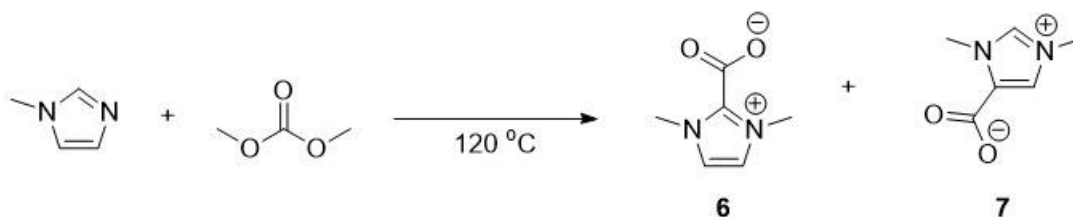


*Figure 22: The synthetic scheme for the synthesis of N,N'-dimethylimidazolium-2-carboxylate Trial 1. Though only 6 is desired, 7 was formed as an unwanted byproduct.*

Dimethylcarbonate presents a unique candidate for the methylation of 1-methylimidazole, by directly attaching the counter ion to the NHC precursor and allowing for the formation of the carbene species without the use of strongly basic reagents, as would be required for **5**. Previous studies suggested that synthesis of **6** from dimethylcarbonate and 1-methylimidazole at 120 °C in the absence of solvent was optimal,<sup>27,30</sup> however it was found that this elevated temperature led to a mixture of isomeric **6** and **7**, the 2-carboxylated-NHC and 4-carboxylated-NHC products, respectively (Experimental: 3 Trial 1) (Figure 22). This was determined by NMR analysis where **7** appears as 25% of the mixture (Figure 23). Purification attempts using both activity II alumina and silica, as well as recrystallization, failed to separate **6** from **7**. As purification proved difficult, due to the similar structure and properties of the two isomers, reaction conditions were investigated to produce pure **6**.

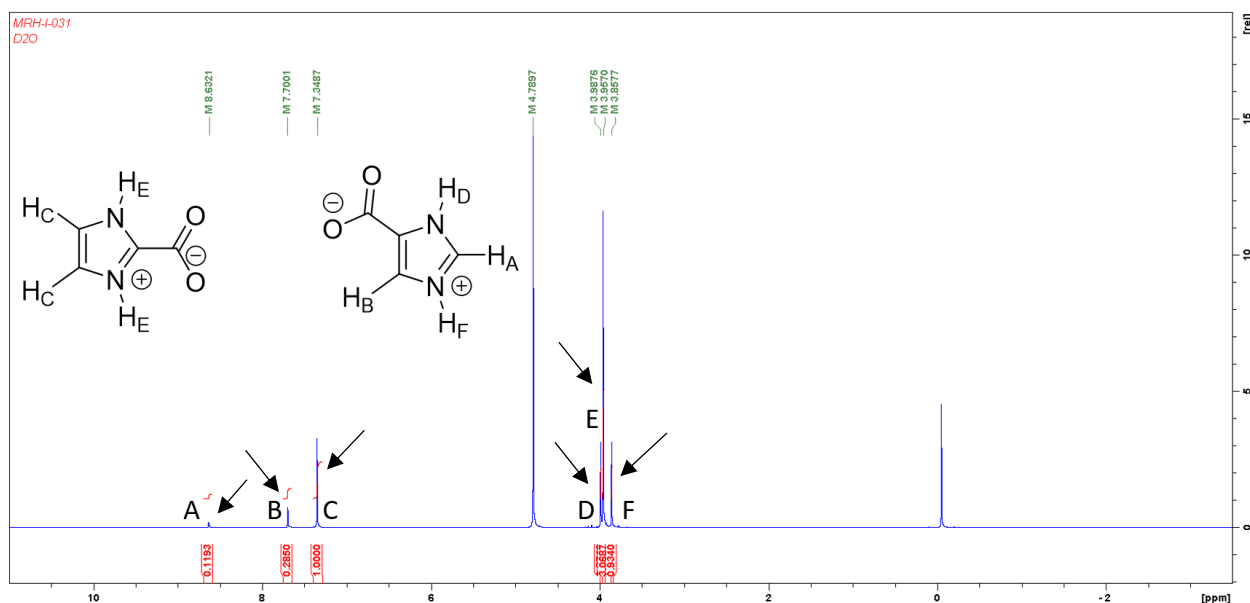


**Figure 23:** The NMR spectra of the synthesis of *N,N'*-dimethylimidazolium-2-carboxylate (**6**) Trial 1 in  $D_2O$  ( $\delta=4.79$ ). Here the mixture of products can be seen, with their peaks assigned to their respective structures.

Temperature modulation presented itself as a promising method to eliminate the formation of multiple isomers. As the most electron poor hydrogen is located between the two nitrogen atoms, this is the most probable site for hydrogen abstraction by the methyl carbonate counter ion, and would likely be the kinetically formed anion (Figure 24).<sup>29</sup> Higher temperatures allow for abstraction of other hydrogen atoms, and would lead to thermodynamically more stable, less sterically hindered **7**. Therefore, lower reaction temperatures were predicted to give a higher ratio of **6** to **7**. The neat reaction of 1-methylimidazole and dimethylcarbonate at 90 °C for 4 days

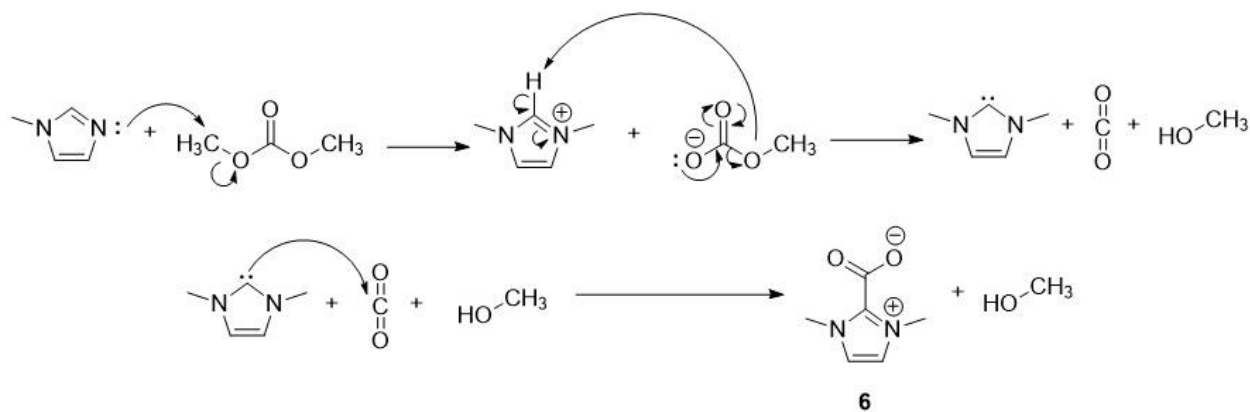


**Figure 24:** A proposed literature mechanism for the formation of *N,N'*-dimethylimidazolium-2-carboxylate from 1-methylimidazole and dimethylcarbonate. Mechanism adapted from Voutchkova.<sup>29</sup>

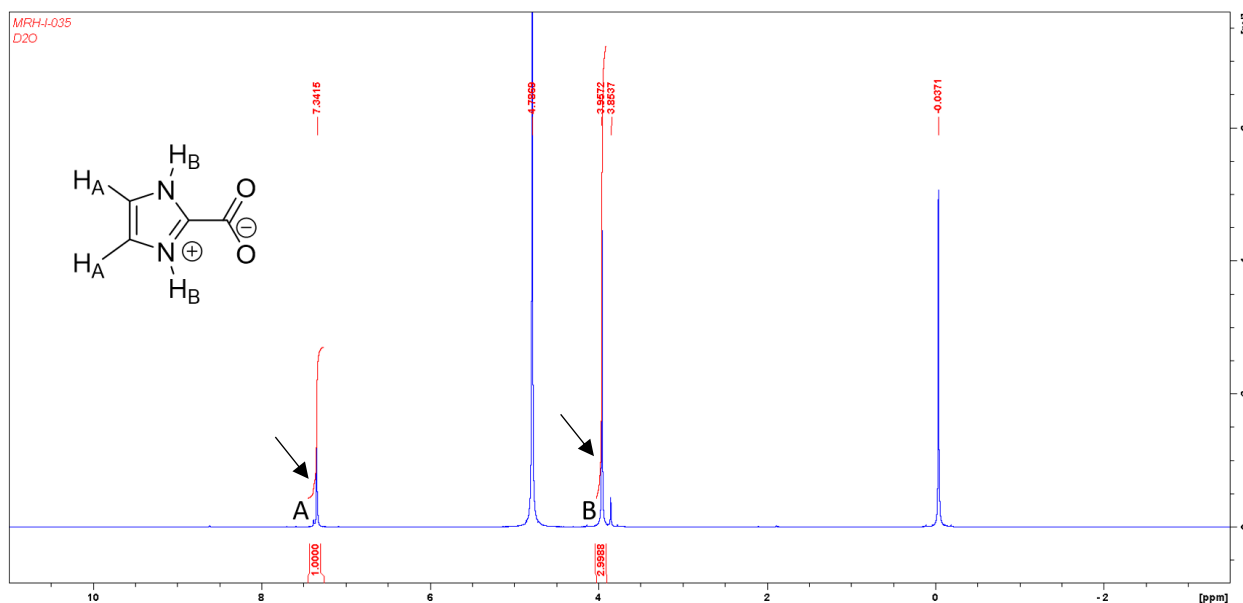


**Figure 25:** The NMR spectra of *N,N'*-dimethylimidazole-2-carboxylate Trial 2 in  $D_2O$  ( $\delta=4.79$ ). Impurities consist of methanol;  $\delta=0$  indicates TMS.

formed pure *N,N'*-dimethylimidazolium-2-carboxylate, at the cost of a dramatically increased reaction time. This resulted in high yield (98%), as determined by  $^1H$  NMR; the peak at  $\delta=0$  indicates a TMS standard (Figure 25).

#### 4. Coordination of *N,N'*-Dimethylimidazolium-2-carboxylate to $Cp^*Co(ethene)_2$

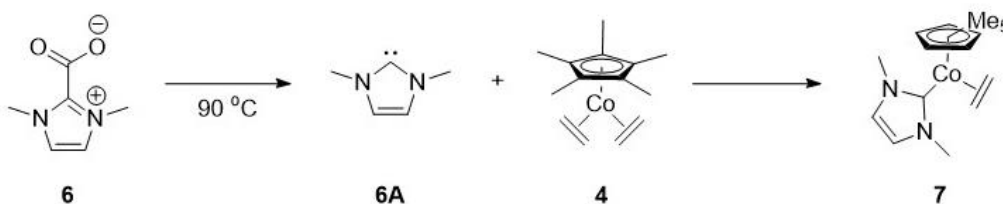


**Figure 26:** The initial reaction conditions for the coordination of *N,N'*-dimethylimidazolium-2-carboxylate to  $Cp^*Co(ethene)_2$ . Here the free NHC **6A** is formed by thermal dissociation of  $CO_2$  from **6**, this carbene species readily coordinates to cobalt, forming  $Cp^*Co(ethene)(N,N'$ -dimethylimidazolium-2-ylidene).

The coordination of *N,N'*-dimethylimidazolium-2-carboxylate (**6**) to  $Cp^*Co(ethene)_2$  (**4**) is unreported in literature, and many different conditions were explored. Initial coordination attempts consisted of heating **4** and **6** at elevated temperature in benzene for a short time (Experimental: 4 Trial 1). Benzene was chosen due to the high solubility of **4**, as well as its availability in deuterated form for NMR experiments. Additionally, 95 °C was initially chosen as

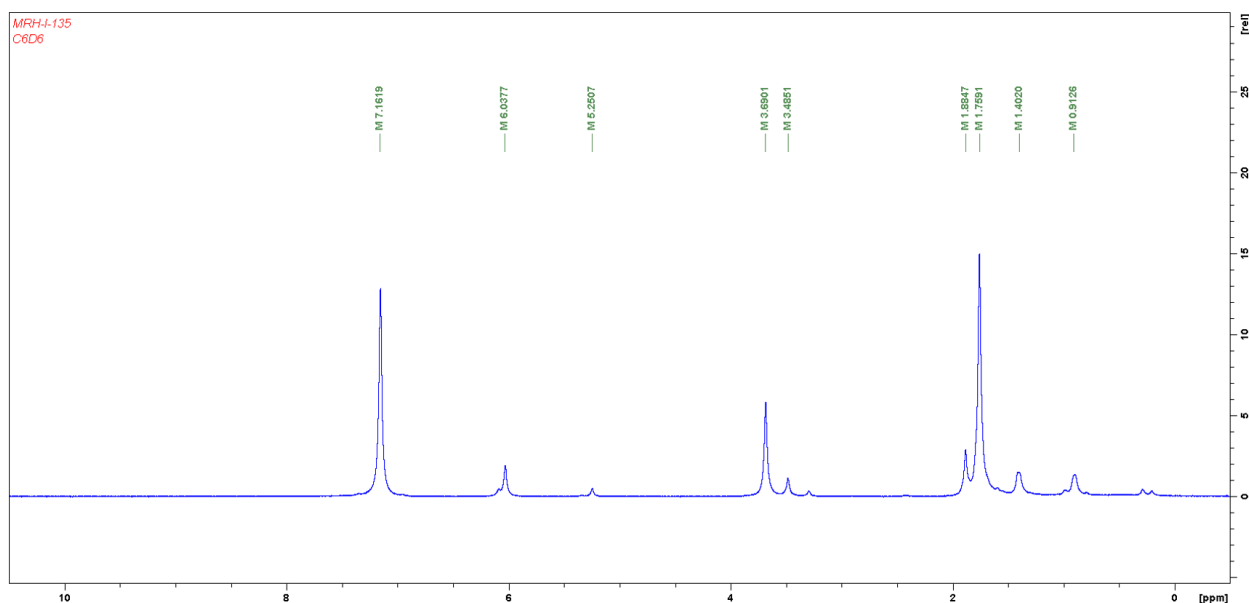


**Figure 27:** The NMR spectra of the coordination of *N,N'*-dimethylimidazolium-2-carboxylate to  $Cp^*Co(ethene)_2$  Trial 1 in  $C_6D_6$  ( $\delta=7.16$ ). As shown, a large quantity of paramagnetic material is present, preventing accurate analysis.

it was reported that the carboxyl group on **6** would quickly dissociate at this temperature, forming the free NHC species **6A** *in situ*, thus avoiding formation of **6A** in an independent step, such as would be required with formation of **6A** from **5** (Figure 26).<sup>29</sup> This is advantageous, as the *in situ* formation of **6A** allows the carbene to be used instantaneously, avoiding the rapid kinetic dimerization predicted for sterically unhindered **5**.<sup>22</sup> As the rate of coordination of free NHCs, such as **6A**, to transition metals is fast,<sup>14</sup> *in situ* generation of **6A** would avoid dimerization as a major reaction pathway. Due to reaction temperature above the boiling point of benzene, a sealed reaction vessel behind a blast shield was required.<sup>a</sup> After the initial reaction time of 3 hours, <sup>1</sup>H NMR analysis on the isolated material showed a significant amount of paramagnetic material, determined by a significant line broadening (Figure 27). After filtration through celite, the NMR spectra showed a complex mixture of products, including a set of resonances believed to correlate to the desired complex **7** (Peaks: A, B, C, D, E) (Figure 28). Furthermore, other resonances were

<sup>a</sup> Pressure was calculated at 1.55 atm using a spreadsheet prepared by Professor Thomas Hoye at the University of Minnesota<sup>33</sup>

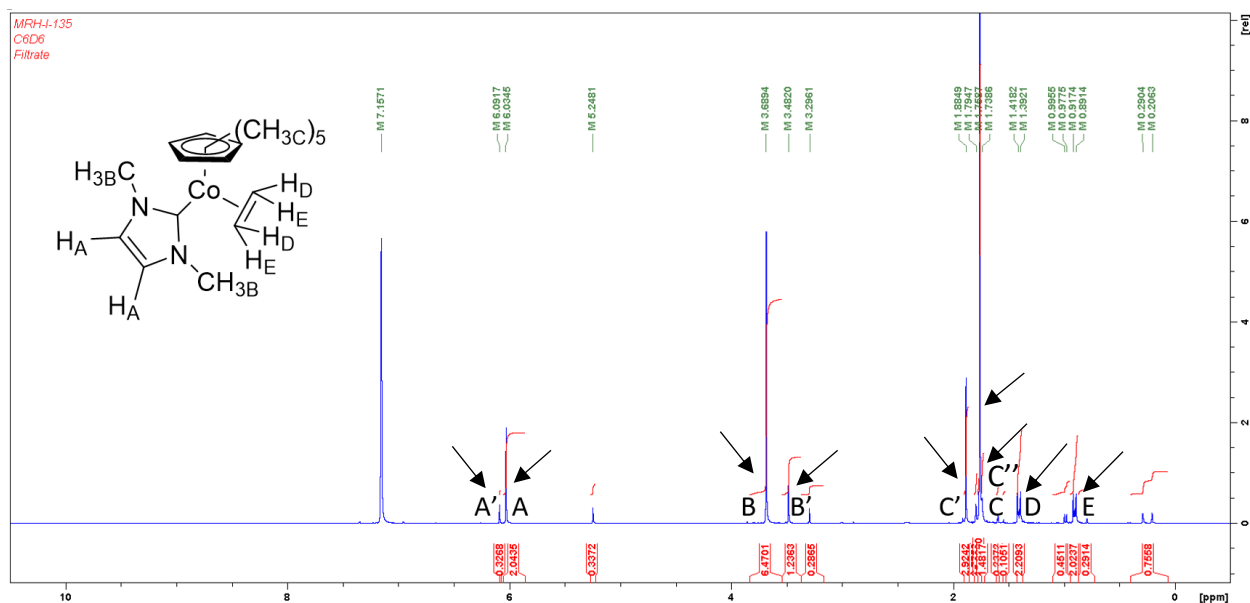


**Figure 28:** The NMR spectra of the coordination of *N,N'*-dimethylimidazolium-2-carboxylate to  $\text{Cp}^*\text{Co}(\text{ethene})_2$  Trial 1 in  $\text{C}_6\text{D}_6$  ( $\delta=7.16$ ) after filtration. The structure of the desired complex is shown, and the relevant peaks are labeled. *C'* and *C''* refer to minor peaks in the vicinity of *C* that may represent  $\text{Cp}^*$  in a minor product.

ascribed to the coordination of a second equivalent of **6A**. The major and minor resonances in the spectrum, A, B, C, and A', B', and C', have the same integration ratio 2:6:15, though the minor resonance C'', seen directly adjacent to major resonance C, has a ratio of 4:12:15 with A' and B'. This is consistent with coordination of two equivalents of **6A** to **4** to give **7A** (Figure 29).

To investigate the possibility of forming **7A**, 1.5 equivalents of the **6** were added to **4** for a reaction at 95 °C for 3 hours (Experimental: 4 Trial 2) (Figure 29). If a reaction pathway to **7A** occurred, increasing the molar equivalents of **6** in the reaction should lead to an increase in the amount of **7A** formed. This trial showed a similarly complex spectrum, as well as a significant amount of paramagnetic precipitate that was filtered out of the solution (Figure 30). The A:A'

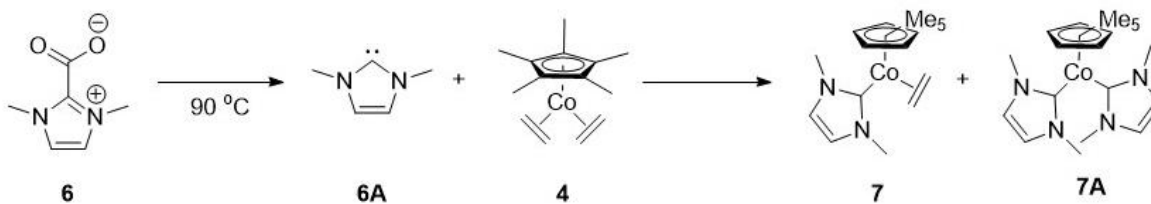


**Figure 29:** An updated reaction scheme of the coordination of *N,N'*-dimethylimidazolium-2-carboxylate to  $\text{Cp}^*\text{Co}(\text{ethene})_2$  showing the possible formation of a bis-NHC complex.

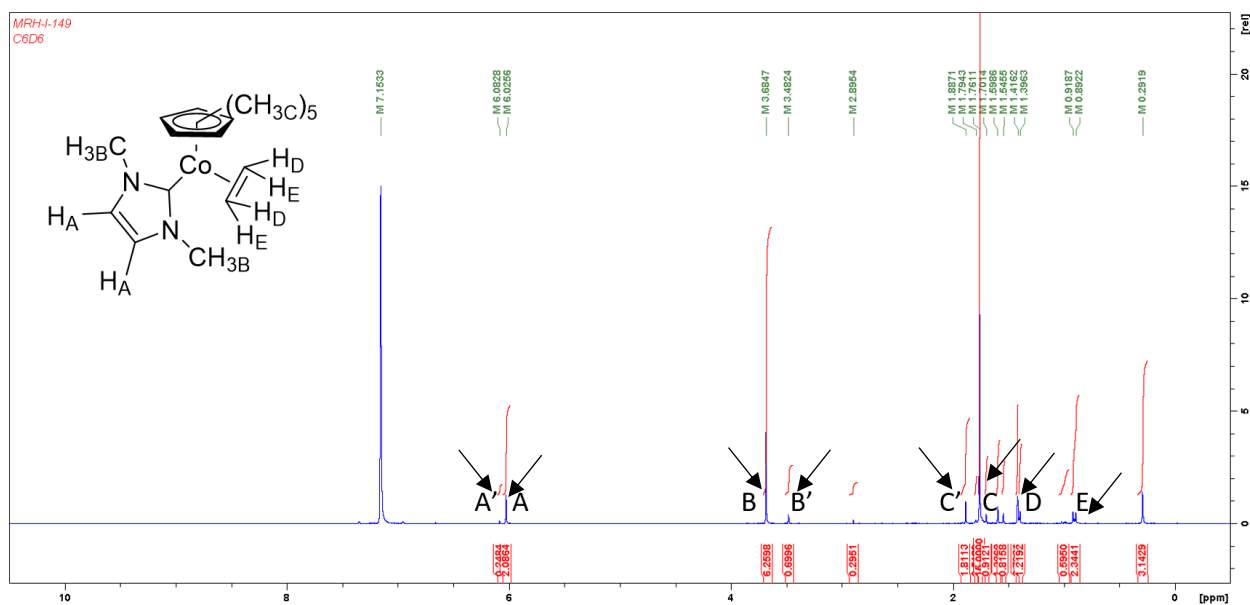


**Figure 30:** The NMR spectra of the coordination of *N,N'*-dimethylimidazolium-2-carboxylate to  $\text{Cp}^*\text{Co}(\text{ethene})_2$  Trial 2 in  $\text{C}_6\text{D}_6$  ( $\delta=7.16$ ). The structure is provided for the desired product, and peaks are labeled. The use of ' refers to peaks from the same ligands on a different product, i.e. A and A' refer to the alkene hydrogens on the NHC, where A' is in the minor product

NMR integration ratio, which is used as a reference to the relative concentration of **7** to **7A** increased from 6.6:1 in trial 1 to 10:1 in trial 2, which is not consistent with increased formation of **7A** resulting from an excess of **6A**.

The cobalt bis-ethene complex **4** is known to be thermally unstable<sup>23</sup> and could be decomposing at 95 °C. However, high temperature was required for the decarboxylation of the NHC-carboxylate and to prevent the dimerization of NHCs.<sup>21, 29</sup> The possibility of a stepwise reaction was explored (Experimental: 4 Trial 3), in which the decarboxylation of the **6** was carried out at high temperature (165 °C) for several hours, followed by the addition of **4** at lower temperatures. Under these conditions, the free carbene generated at high temperature might quickly coordinate to the cobalt center via displacement of an ethene, without requiring **4** to be subjected to high temperatures. In the reaction, an inseparable mixture was formed that, as evidenced by the broad linewidths in the NMR spectrum, contained paramagnetic and diamagnetic

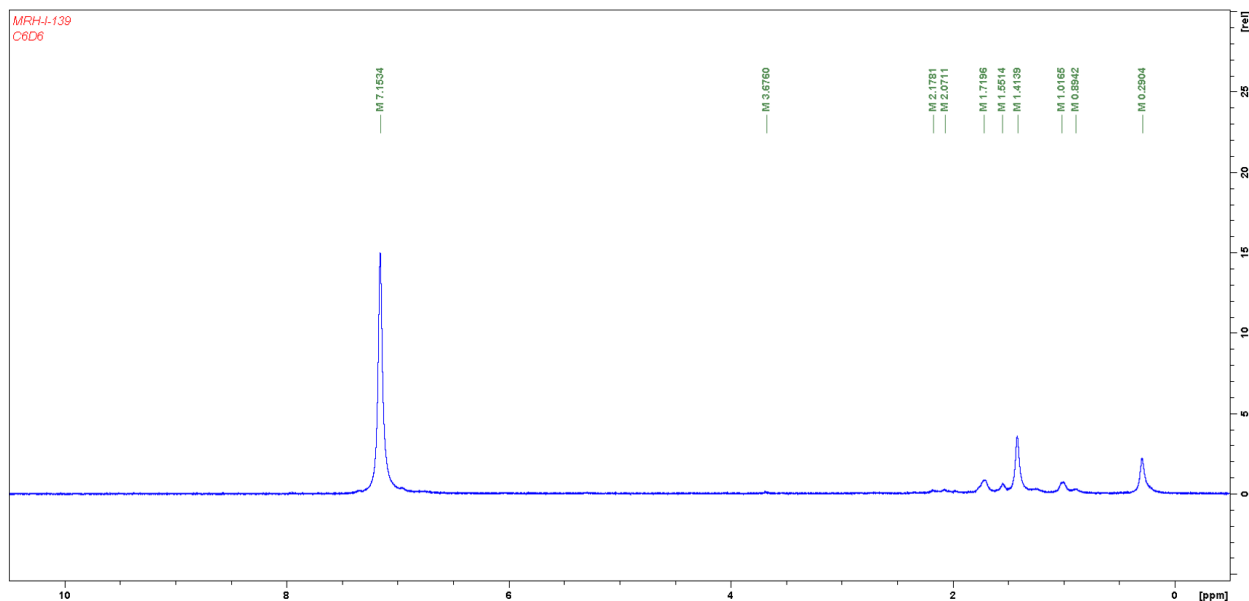


**Figure 31:** The NMR spectra of the stepwise decarboxylation of *N,N'*-dimethylimidazolium-2-carboxylate and coordination to *Cp*\*Co(ethene)<sub>2</sub> Trial 3 in C<sub>6</sub>D<sub>6</sub> ( $\delta=7.16$ ). The separation of the paramagnetic material formed was not possible, and thus characterization of the reaction products was not possible.

material (Figure 31). However, the lack of very broad downfield peaks in the <sup>1</sup>H NMR suggest that none of the desired complex **7** was formed.

It was possible that the paramagnetic precipitate seen in the trials done at 95 °C could potentially be a reaction intermediate, and that the reaction may not have completed under those

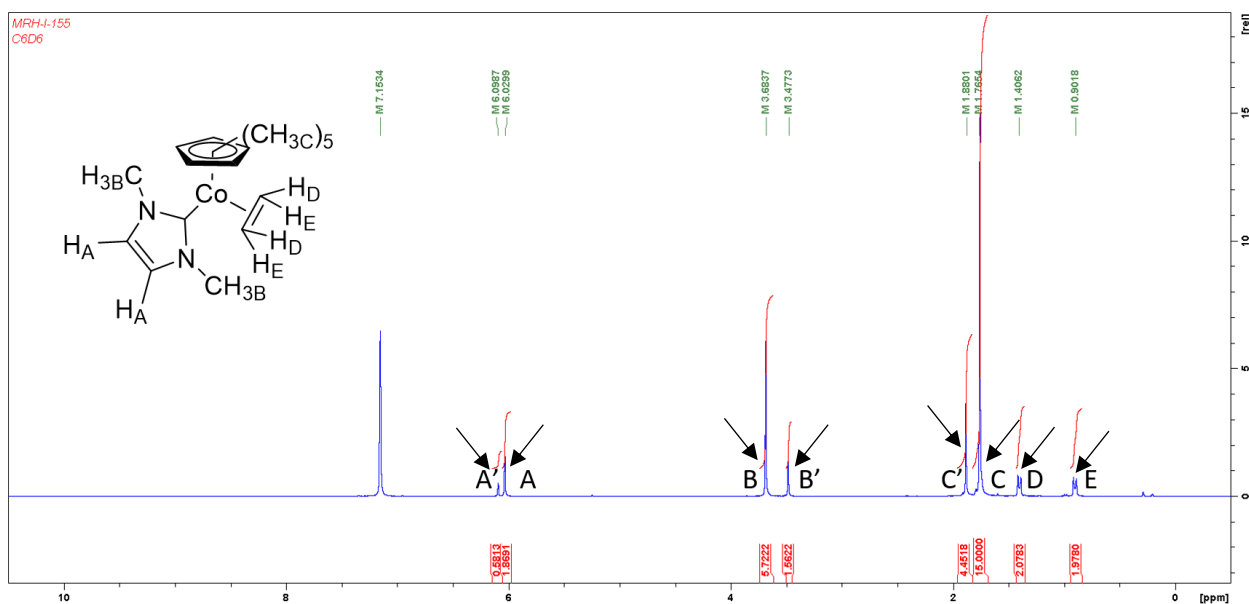


**Figure 32:** The NMR spectra of the coordination of *N,N'*-dimethylimidazolium-2-carboxylate to *Cp*\*Co(ethene)<sub>2</sub> Trial 4 in C<sub>6</sub>D<sub>6</sub> ( $\delta=7.16$ ). The desired complex is shown, and peaks were assigned as shown.

conditions. To test this hypothesis, an identical reaction to Trials 1 and 2 was prepared, and heated at 95 °C for 24 hours (Experimental: 4 Trial 4). The longer reaction time was successful in avoiding many of the minor products seen in the crude NMR spectrum, and substantially reducing the amount of paramagnetic material formed (Figure 32). However, under the longer reaction time conditions, the  $^1\text{H}$  NMR spectrum showed that two different compounds were formed, as determined by the proton NMR integration ratios. The integration ratio as a series of integers 2:6:15:2:2 observed for resonances A, B, C, D, and E is consistent with the proposed structure of **7**, and indicates a single species. The integration ratio of A':B':C' is nearly identical to that of A:B:C at 2:6:15, but do not correlate with any coordinated ethene ligand. The integer ratio similarly suggests a single species for the minor resonances, and is consistent with a cobalt-NHC dimer with the formula  $[\text{Cp}^*\text{Co}(\mathbf{6})]_2$ , previously unreported in the literature. Investigations into this novel dimer are discussed below. As the integration ratios of A:A', B:B', and C:C' are roughly 3:1, **7** represents approximately 75% of the NMR detectable material formed.

Analysis of the 2D COSY NMR of the product mixture provided further information about the structure and identity of the materials (Figure 33). The major product of the reaction exhibits cross peaks between hydrogens A, B, and C, as well as a strong correlation between D and E, consistent with the assignment of the major product as **7**. Cross peaks are present between A', B', and C', consistent with the implication of the integration values that these resonances refer to hydrogen atoms within a single molecule; there is no evidence that an ethene ligand is present in the minor product, due to the lack of cross peaks to other resonances. The cross peak for the unlabeled doublet at 1.2 ppm (between those labelled D and E in Figure 33) indicates coupling to



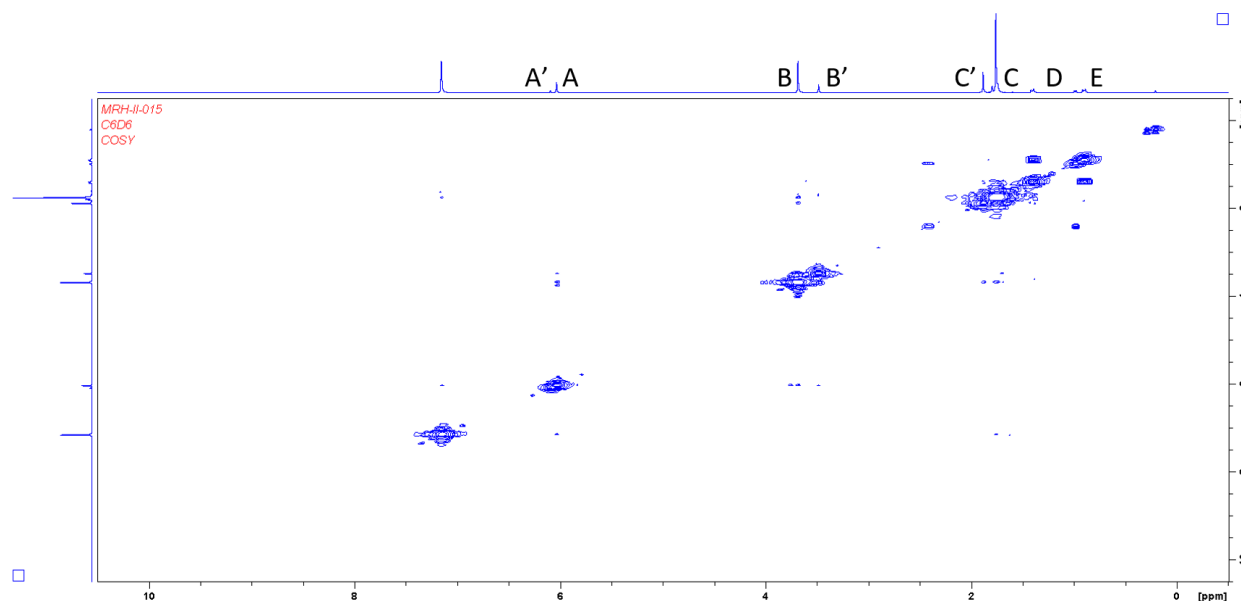


**Figure 33:** The COSY NMR spectra of the coordination of *N,N'*-dimethylimidazolium-2-carboxylate to  $Cp^*Co(ethene)_2$  Trial 4 in  $C_6D_6$ . As can be seen, no cross peaks are present for the minor peaks A', B', and C'.

a resonance at  $\delta=2.1$ , however, the absence of these resonances in other 1D spectra suggest that these are due to contaminants.

As ethene is a thermally labile ligand, a lower reaction temperatures might prevent the dissociation of the second ethene, thus preventing formation of the purported cobalt dimer

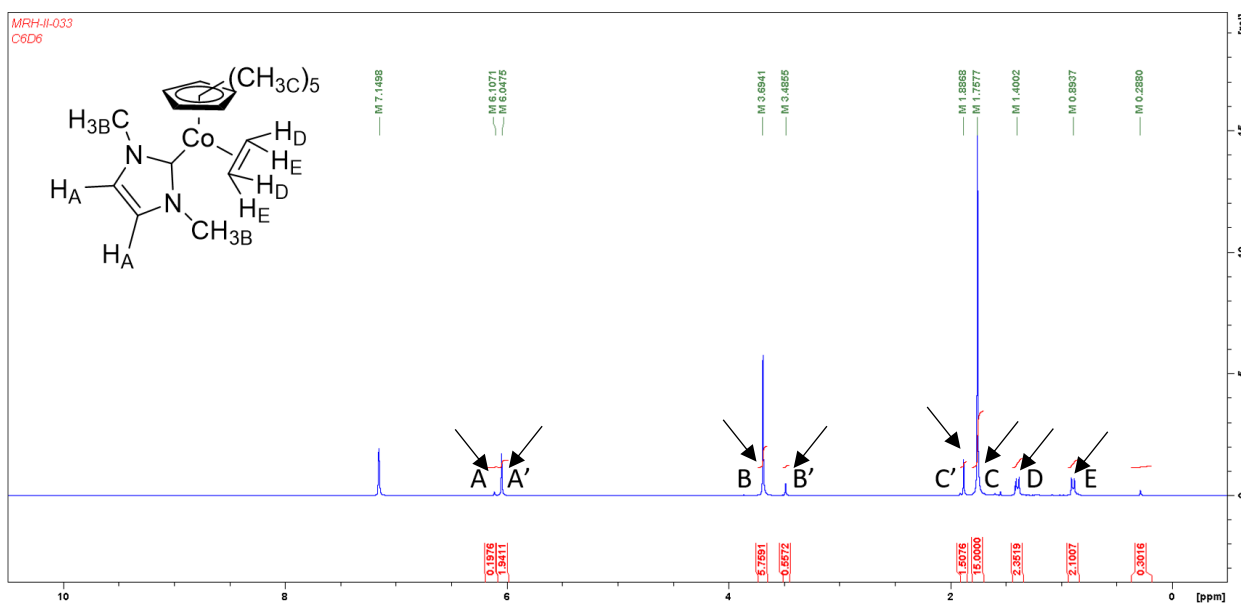


**Figure 34:** The NMR spectra of the coordination of *N,N'*-dimethylimidazole-2-carboxylate to  $Cp^*Co(ethene)_2$  Trial 5 in  $C_6D_6$  ( $\delta=7.16$ ).

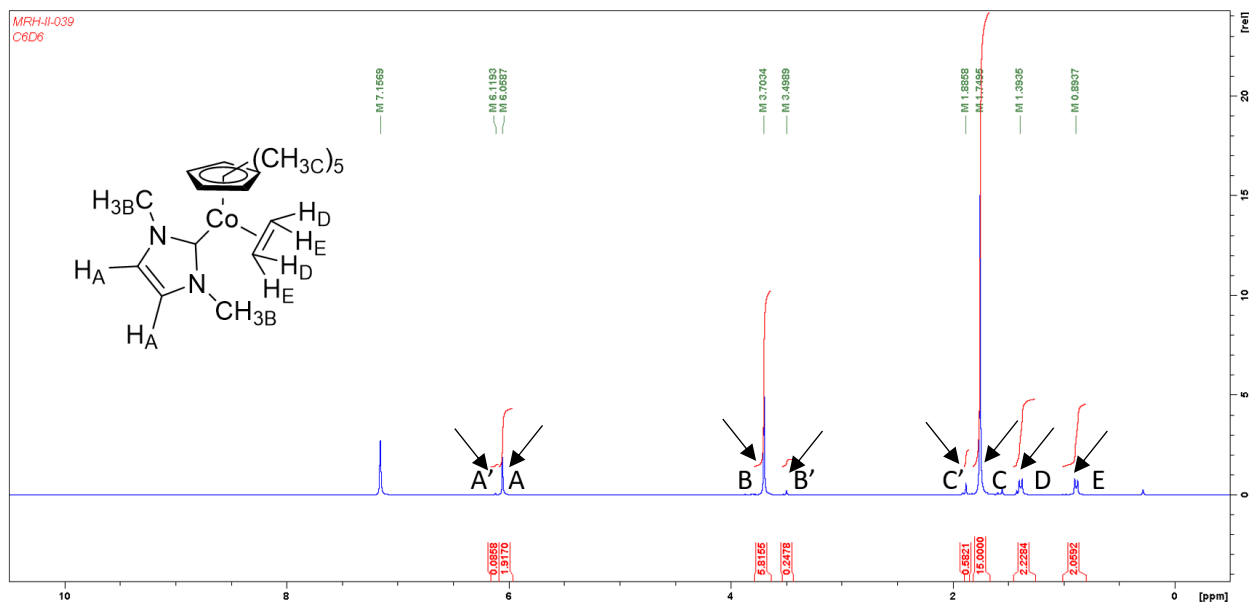


**Figure 35:** The NMR spectra of the coordination of *N,N'*-dimethylimidazolium-2-carboxylate to  $\text{Cp}^*\text{Co}(\text{ethene})_2$  Trial 6 in  $\text{C}_6\text{D}_6$  ( $\delta=7.16$ ).

$[\text{Cp}^*\text{Co}(\mathbf{6A})]_2$ . To test this, under otherwise identical conditions, the reactions were attempted at both 75 °C (Experimental: 4 Trial 5) and 65 °C (Experimental: 4 Trial 6) for 24 hours.  $^1\text{H}$  NMR analysis of both resulting products showed a significant reduction of the minor peaks, correlating to decreased reaction temperature. At 75 °C, the  $^1\text{H}$  NMR spectrum showed a sharp decrease in the amount of minor product formed from 25% to 9% (Figure 34). Further lowering the temperature to 60 °C correlated to the decrease in yield of the minor product to 5% (Figure 35) (Table 2).

**Table 2:** The correlation of reaction temperature to the ratio of products formed. It can be seen that lower reaction temperatures give significantly improved purity of the desired coordination complex.

Reaction Temperature	Coordination Product Ratio
95 °C	3:1
75 °C	10:1
60 °C	20:1

## 5. Catalyst Activation and Dimerization of 1-Hexene

As the desired precatalyst was isolated in high enough purity (95%), experiments moved on to the catalytic dimerization of 1-hexene (Experimental: 5). Following the catalytic procedure

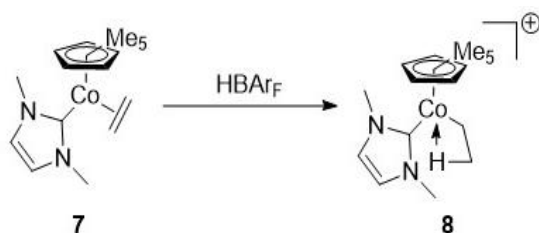


**Figure 36:** A scheme showing the activation of the desired precatalyst  $\text{Cp}^*\text{Co}(\text{ethene})(\text{Me}_2\text{Im})$  by Brookhart's Acid. This forms the agostic hydrogen complex **8**.

from Broene *et al.*<sup>11</sup>, the catalyst was activated by the addition of Brookhart's acid, a strong, non-coordinating acid. Activation entailed the protonation of the olefin ligand, forming the cationic cobalt (I) species **8** (Figure 36). As the catalytic reaction is contingent upon a bi-molecular agostic hydrogen transfer between a cobalt cation and a neutral cobalt species, 0.7 eq. of HBArF was used. This partial activation of the catalyst increases the speed of the catalytic cycle, believed to be due to hydrogen transfer between catalyst molecules (Figure 37).

Reaction aliquots were taken at 24 hour intervals, and samples were prepared via aqueous workup and extraction into dichloromethane. These were analyzed by GC-FID to detect the changing quantities of 1-hexene, 1-dodecene, and potentially 5-methyleneundecane (the branched

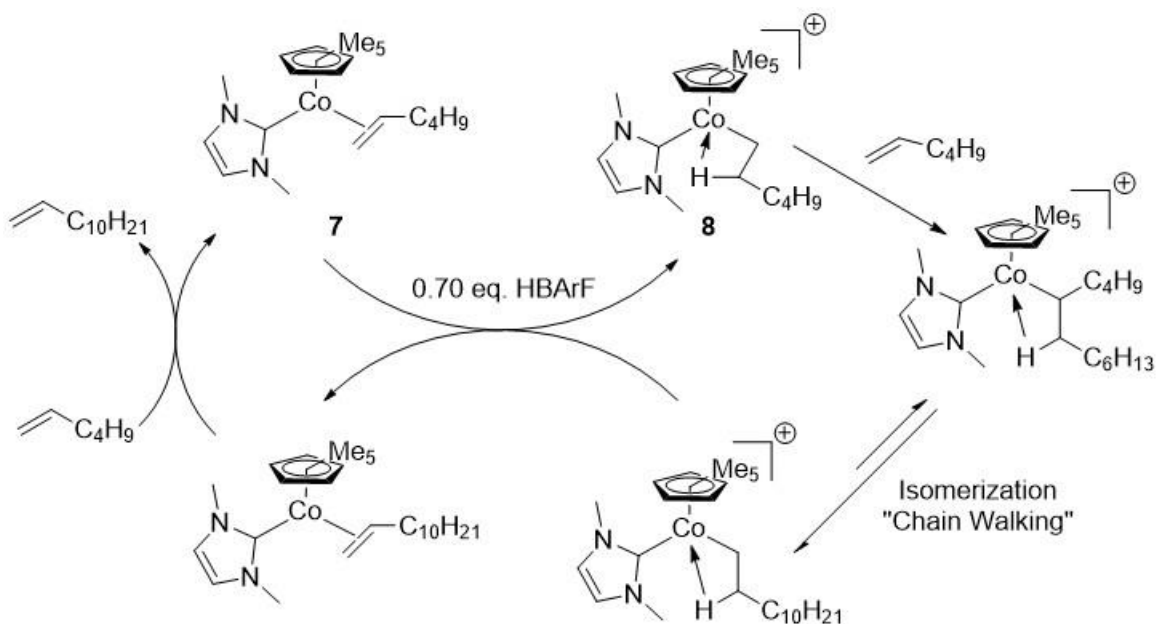


**Figure 37:** The proposed catalytic cycle of complex **7**, showing activation to complex **8**, and catalysis as described by Broene *et al.*<sup>11</sup>

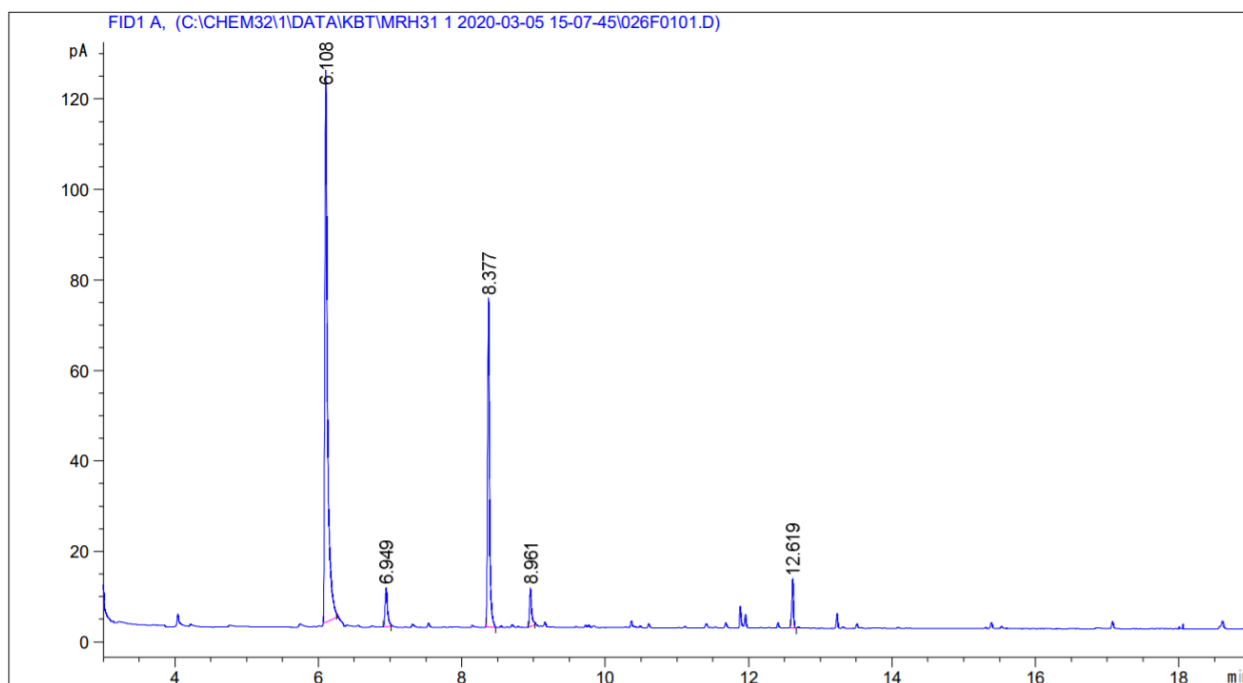


Figure 38: The GC-FID chromatogram for the 24 hour reaction aliquot.

product). The sample taken at 24 hours shows 5 main components in solution (Figure 38), peaks are expected to correlate to 1,2-difluorobenzene, mesitylene, 1-hexene; after time, peaks for 1-dodecene and 5-methyleneundecane are expected to grow in. Unfortunately, characterization of

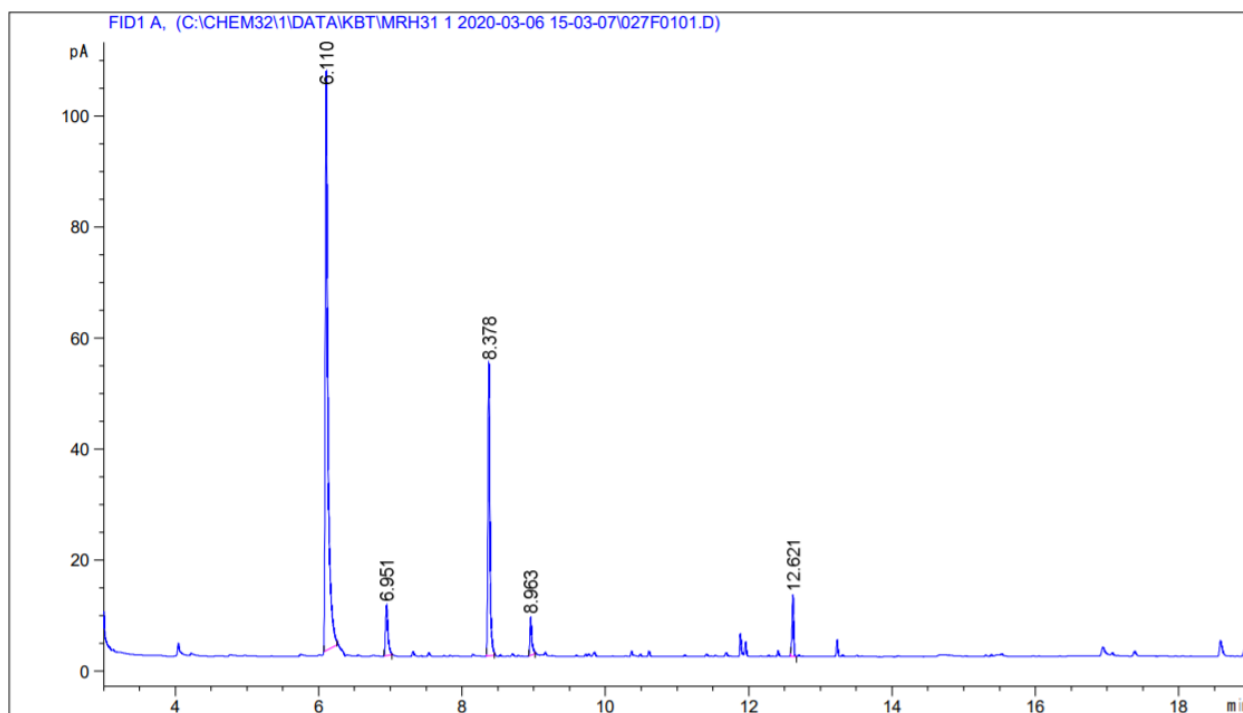


Figure 39: The GC-FID chromatogram for the 48 hour reaction aliquot.

the chromatograms using standards was not completed before the termination of research. In the 48 hour reaction aliquot, the peak integrations were very similar, with small differences that may be attributed to different sample concentrations (Figure 39). Neither chromatogram showed the growth of peaks that could correlate to 1-dodecene or 5-methylundecane, the linear and branched products of catalysis, which is consistent with the reaction time described by Broene *et al.* (11 days);<sup>11</sup> data from later reaction aliquots is necessary to determine the extent of olefin catalysis.

### 6. Synthesis of bis[(*N,N'*-dimethylimidazolium-2-ylidene)( $\eta^5$ -pentamethylcyclopentadienyl)cobalt]

To investigate the byproduct of the coordination of NHC-carboxylate **6** to Cp\*Co(ethene)<sub>2</sub>, a series of reactions were set up. Identification of the byproduct would provide insights into the coordination mechanism of **6** to **4**, as well as potentially increasing the efficiency of the synthetic process; if the purported dimer could reform **7** under catalytic conditions, extended reaction times to form **7** could be avoided. Because the ratio of A:A' was temperature dependent and favored A as temperature decreased, the reactions were set up with increasing temperature. Indeed, when

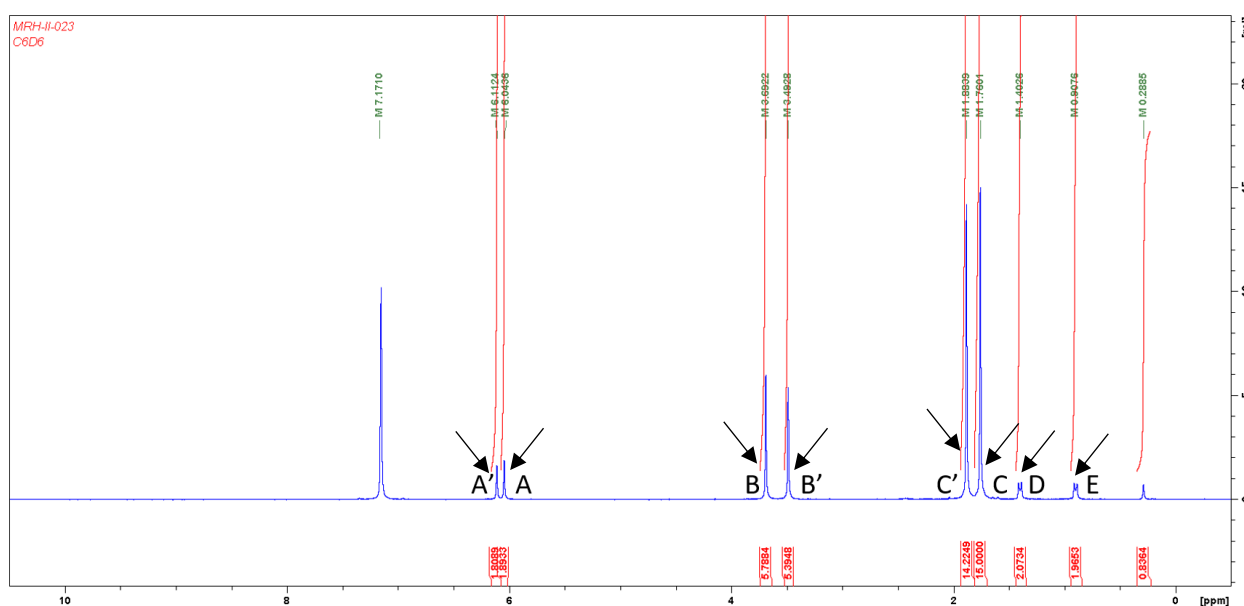
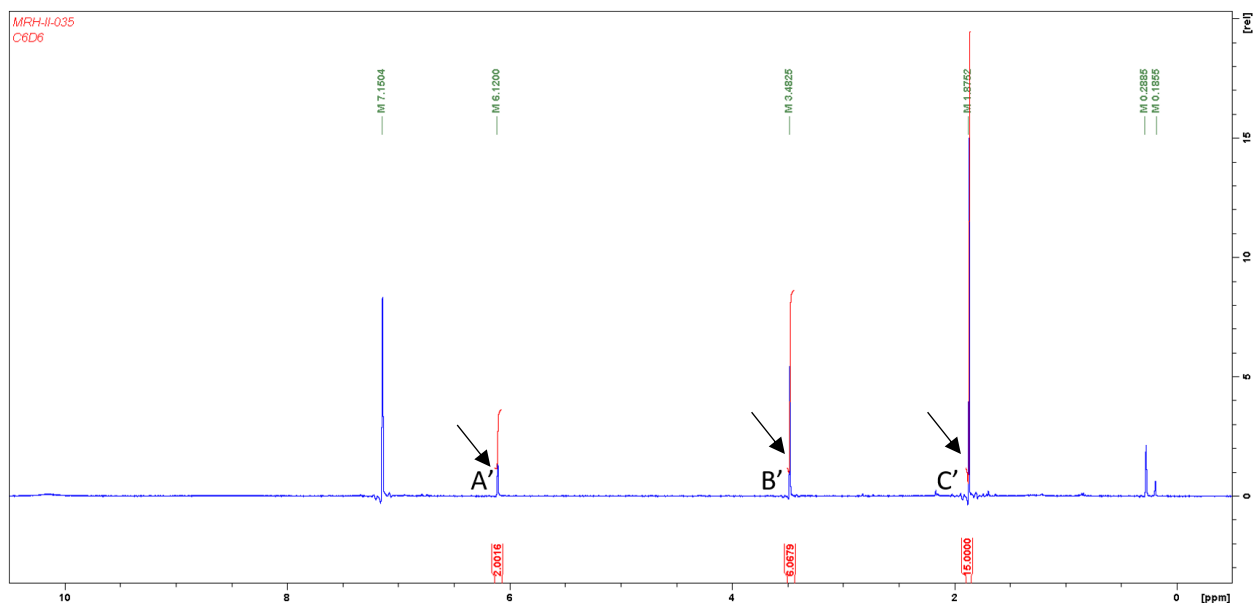
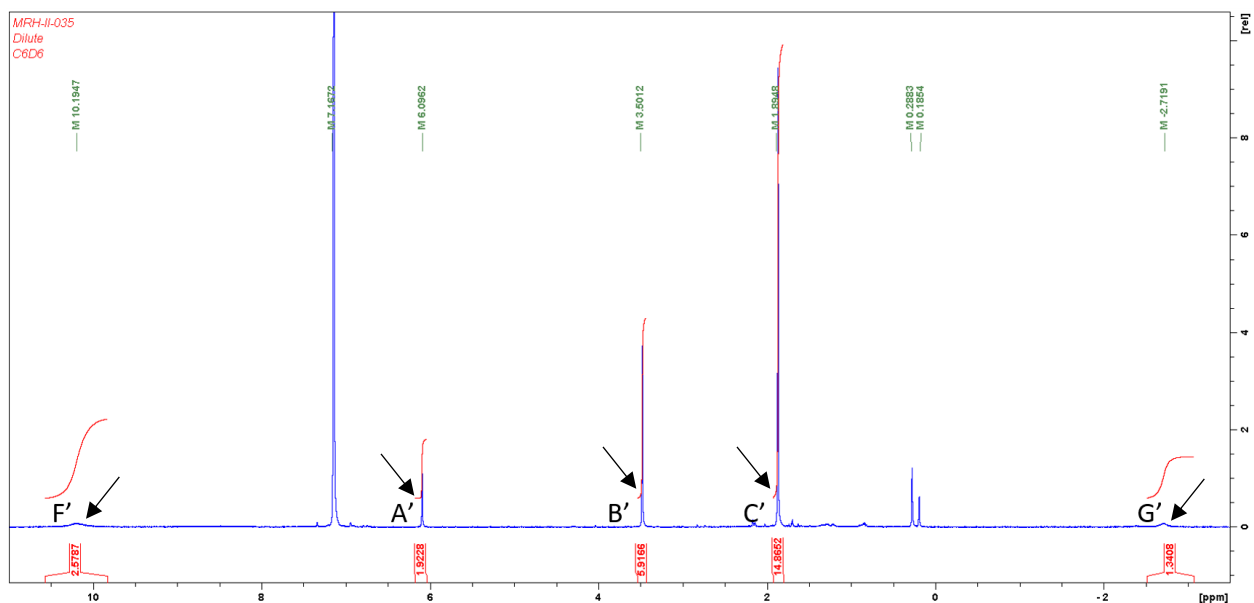


Figure 40: The NMR spectra of the synthesis of [Cp\*Co(Me<sub>2</sub>Im)]<sub>2</sub> Trial 1 in C<sub>6</sub>D<sub>6</sub> ( $\delta=7.16$ ). It can be seen that the major and minor peaks are at equal proportions



**Figure 41:** The NMR spectra of the synthesis of  $[\text{Cp}^*\text{Co}(\text{Me}_2\text{Im})_2]$  Trial 2 in  $\text{C}_6\text{D}_6$  ( $\delta=7.16$ ). It can be seen that the monomeric material has been driven off, leaving only the dimer product.

reacted at  $110^\circ\text{C}$  (Experimental: 6 Trial 1), the two products were present in equal proportions (Figure 40). Increasing the temperature to  $135^\circ\text{C}$  (Experimental: 6 Trial 2), gave a product in which **7** was not detectable by  $^1\text{H}$  NMR (Figure 41). Peaks A', B', and C' remain in the spectra, as does a peak representing grease. As before, the coordination product of **6A** with  $\text{Cp}^*\text{Co}(\text{ethene})_2$  is shown to be temperature dependent, forming what appears to be pure



**Figure 42:** The NMR spectra of the synthesis of  $[\text{Cp}^*\text{Co}(\text{Me}_2\text{Im})_2]$  Trial 2 in  $\text{C}_6\text{D}_6$  ( $\delta=7.16$ ) after one week. Peaks F' and G' are new, and are labeled as so to not imply their identity is ethene.

[Cp\*Co(**6A**)]<sub>2</sub> at high temperature. This is consistent with thermal loss of ethene from **7** and dimerization of the resulting coordinatively unsaturated complex. However, more data is required to propose a structure of the cobalt dimer.

After one week, the <sup>1</sup>H NMR spectrum of this material was reacquired, showing the decomposition of the purported dimer (Figure 42). Interestingly this NMR spectrum shows new resonances, specifically one at δ=-2.7 (G'), which may imply the decomposition product is a hydride complex. Attempts to crystallize the product were unsuccessful, and efforts were not continued.

## Conclusions

Overall, a synthetic procedure for the coordination of an NHC-carboxylate salt **6** to the cobalt half-sandwich complex **4** was developed using mild reagents and conditions. Though the exact mechanism is unknown, we propose a stepwise ligand coordination, as longer reaction times gave more pure product. Additionally, the coordination product of the NHC-carboxylate salt has been shown to be temperature dependent, with lower temperatures favoring a monomeric cobalt complex with the formula  $\text{Cp}^*\text{Co}(\text{ethene})(\text{N},\text{N}'\text{-dimethylimidazolium-2-ylidene})$ , and higher temperatures favoring a cobalt dimer with the formula  $[\text{Cp}^*\text{Co}(\text{N},\text{N}'\text{-dimethylimidazolium-2-ylidene})]_2$ .

The complex  $\text{Cp}^*\text{Co}(\text{ethene})(\text{N},\text{N}'\text{-dimethylimidazolium-2-ylidene})$  has been activated and used in preliminary catalytic trials, though data collection was terminated in the early stages of the reaction due to the closure of research facilities. This catalytic data would not only provide the linear:branched olefin ratio of the synthesized precatalyst, but would also inform the use of NHCs as supporting ligands for the dimerization of linear  $\alpha$ -olefins, and would provide insights into future ligand design. Work into elucidating the structure of the cobalt dimer  $[\text{Cp}^*\text{Co}(\text{N},\text{N}'\text{-dimethylimidazolium-2-ylidene})]_2$  has begun, though NMR analysis only allows us to determine ligand identity; crystallographic data is required to determine the exact structure of the complex.



## Future Work

Though a project is never quite complete, this project has a wealth of avenues for future work. Continuing catalytic experiments are necessary to determine the efficacy of **6A** as a supporting ligand for the dimerization of linear  $\alpha$ -olefins. Analysis of the catalytic product ratio and speed of the reaction would inform the future use of NHCs, as well as providing insight into limiting steric bulk to produce better ratios. Additionally, structure confirmation of the precatalyst is necessary by x-ray crystallography, and x-ray quality crystals must be grown. Structure determination of the alleged cobalt dimer must be completed via x-ray crystallography; crystal formation has been unsuccessful to date, and further efforts must be made to obtain x-ray quality crystals. Obtaining a crystallographic structure for this material may improve understanding of the coordination mechanism of **6** to **4**, as well as the structure elucidation of a novel cobalt-NHC dimer.

Additionally, further constraining the supporting ligand may prove to be a rich area of investigation. For example, combining previous work in the Broene lab to tether the Cp\* to the NHC may further reduce the steric demand of the supporting ligand. A chelating NHC would lock the conformation of the ligand, and may give more favorable ratios of linear:branched olefin dimers. Furthermore, investigating NHCs based on benzimidazole may serve to constrain the ligand more, due to different electronic properties and effects on the carbene.

## References

1. Moss, G. P.; Smith, P. A. S.; Tavernier, D., Glossary of Class Names of Organic Compounds and Reactivity Intermediates Based on Structure. *Pure and Applied Chemistry* **1995**, *67* (8-9), 1307-1375.
2. Lappin, G. R.; Sauer, J. D., *Alpha Olefins Applications Handbook*. Marcel Dekker Inc.: New York, NY, 1989.
3. Ahuja, K.; Singh, S. *Linear Alpha Olefins Market Size By Product, By Application, Regional Outlook Competitive Market Share & Forecast 2017-2024*; Global Market Insights: 2017.
4. Keim, W., Oligomerization of ethylene to alpha-olefins: discovery and development of the shell higher olefin process (SHOP). *Angewandte Chemie* **2013**, *52* (48), 12492-6.
5. Chemical, I., Alpha Olefin Supply Chain. Study, L. L. A. O. M., Ed. IHS Chemical: 2016.
6. Carter, A.; Cohen, S. A.; Cooley, N. A.; Murphy, A.; Scutt, J.; Wass, D. F., High Activity Ethylene Trimerisation Catalysts Based on Diphosphine Ligands. *Chem. Comm.* **2002**, (8), 858-859.
7. McGuinness, D. S.; Wasserschied, P.; Morgan, D. H.; Dixon, J. T., Ethylene Trimerization with Mixed-Donor Ligand (N,P,S) Chromium Complexes: Effect of Ligand Structure on Activity and Selectivity. *Organometallics* **2005**, *24* (4), 552-556.
8. Deckers, P. J. W.; B, H.; H., T. J., Switching a Catalyst System from Ethene Polymerization to Ethene Trimerization with a Hemilabile Ancillary Ligand. *Angewandte Chemie* **2001**, *40* (13), 2516-2519.
9. Bollmann, A.; Blann, K.; Dixon, J. T.; Hess, F. M.; Killian, E.; Maumela, H.; McGuinness, D. S.; Morgan, D. H.; Neveling, A.; Otto, S.; Overett, M.; Slawin, A. M. Z.; Wasserschied, P.; Kuhlmann, S., Ethylene Tetramerization: A New Route to Produce 1-Octene in Exceptionally High Selectivities. *J. Am. Chem. Soc.* **2004**, *126* (45), 14712-14713.
10. Small, B. L.; Brookhart, M., Iron-Based Catalysts with Exceptionally High Activities and Selectivities for Oligomerization of Ethylene to Linear  $\alpha$ -Olefins. *J. Am. Chem. Soc.* **1998**, *120* (28), 7143-7144.
11. Broene, R. D.; Brookhart, M.; Lamanna, W. M.; Volpe, A. F., Jr., Cobalt-Catalyzed Dimerization of  $\alpha$ -Olefins to Give Linear  $\alpha$ -Olefin Products. *J. Am. Chem. Soc.* **2005**, *127* (49), 17194-17195.
12. Keefe, R. C. 8-Quinoyl-Tetramethylcyclopentadiene: A Supporting Ligand for the Cobalt Catalyzed Dimerization of Linear Alpha-Olefins. Bowdoin College, 2018.

13. Herrmann, W. A., N-Heterocyclic Carbenes: A New Concept in Organometallic Catalysis. *Angewandte Chemie* **2002**, *41*, 1290-1309.
14. Herrmann, W. A.; Elison, M.; Fisher, J.; Kocher, C.; Artus, G. R. J., Metal Complexes of N-Heterocyclic Carbenes: A New Structural Principle for Catalysis in Homogeneous Catalysis. *Angewandte Chemie* **1995**, *34* (21), 2371-2374.
15. Hopkinson, M. N.; Richter, C.; Schedler, M.; Glorius, F., An overview of N-heterocyclic carbenes. *Nature* **2014**, *510* (7506), 485-96.
16. Enachi, A.; Baabe, D.; Zaretske, M. K.; Schweyen, P.; Freytag, M.; Raeder, J.; Walter, M. D., [(NHC)CoR<sub>2</sub>]: pre-catalysts for homogeneous olefin and alkyne hydrogenation. *Chemical communications* **2018**, *54* (98), 13798-13801.
17. Wang, X.; Liu, S.; Jin, G.-X., Preparation, Structure, and Olefin Polymerization Behavior of Functionalized Nickel(II) N-Heterocyclic Carbene Complexes. *Organometallics* **2004**, *23* (6002-6007).
18. Bianchini, C.; Mantovani, G.; Meli, A.; Migliacci, F.; Laschi, F., Selective Oligomerization of Ethylene to Linear  $\alpha$ -Olefins by Tetrahedral Cobalt(II) Complexes with 6-(Organyl)-2-(imino)pyridyl Ligands: Influence of the Heteroatom in the Organyl Group on the Catalytic Activity. *Organometallics* **2003**, *22* (13), 2545-2547.
19. Jin, Z.; Gu, X.-P.; Qiu, L.-L.; Wu, G.-P.; Song, H.-B.; Fang, J.-X., Air-stable CpPd(NHC)Cl (NHC = N-heterocyclic carbene) complexes as highly active precatalysts for Kumada–Tamao–Corriu coupling of aryl and heteroaryl chlorides. *Journal of Organometallic Chemistry* **2011**, *696* (4), 859-863.
20. McGuinness, D. S.; Sutil, J. A.; Gardiner, M. G.; Davies, N. W., Ethylene Oligomerization with Cr-NHC Catalysts: Further Insights into the Extended Metallacycle Mechanism of Chain Growth. *Organometallics* **2008**, *27*, 4238-4247.
21. Böhm, V. P. W.; Herrmann, W. A., The "Wanzlick Equilibrium". *Angewandte Chemie* **2000**, *39* (22), 4036-4038.
22. Arduengo, A. J., 3rd; Dias, H. V. R.; Harlow, R. L.; Kline, M., Electronic Stabilization of Nucleophilic Carbenes. *J. Am. Chem. Soc.* **1992**, *114* (14), 5530-5534.
23. Dürr, S.; Zarzycki, B.; Ertler, D.; Ivanovic-Burmazovic, I.; Radius, U., Aerobic CO Oxidation of a Metal-Bound Carbonyl in a NHC-Stabilized Cobalt Half-Sandwich Complex. *Organometallics* **2012**, *31*, 1730-1742.
24. Weskamp, T.; Böhm, V. P. W.; Herrmann, W. A., N-Heterocyclic Carbenes: State of the Art in Transition-Metal-Complex Synthesis. *Journal of Organometallic Chemistry* **1999**, *600* (1-2), 12-22.

25. Rodriguez-Castillo, M.; Laurencin, D.; Tielens, F.; van der Lee, A.; Clement, S.; Guari, Y.; Richeter, S., Reactivity of gold nanoparticles towards N-heterocyclic carbenes. *Dalton transactions* **2014**, 43 (16), 5978-82.
26. Danopoulos, A. A.; Simler, T.; Braunstein, P., N-Heterocyclic Carbene Complexes of Copper, Nickel, and Cobalt. *Chemical reviews* **2019**.
27. Holbrey, J. D.; Reichert, W. M.; Tkatchenko, I.; Bouajila, E.; Walter, O.; Tommasi, I.; Rogers, R. D., 1,3-Dimethylimidazolium-2-carboxylate: the unexpected synthesis of an ionic liquid precursor and carbene-CO<sub>2</sub> adduct. *Chem. Comm.* **2003**, (1), 28-29.
28. Wakita, F., 1,3-Dimethylimidazolyl-2-ylidene borane. *Organic Syntheses* **2015**, 92, 342-355.
29. Voutchkova, A. M.; Feliz, M.; Clot, E.; Eisenstein, O.; Crabtree, R. H., Imidazolium carboxylates as versatile and selective N-heterocyclic carbene transfer agents: synthesis, mechanism, and applications. *J. Am. Chem. Soc.* **2007**, 129 (42), 12834-46.
30. Smiglak, M.; Holbrey, J. D.; Griffin, S. T.; Reichert, W. M.; Swatloski, R. P.; Katritzky, A. R.; Yang, H.; Zhang, D.; Kirichenko, K.; Rogers, R. D., Ionic liquids via reaction of the zwitterionic 1,3-dimethylimidazolium-2-carboxylate with protic acids. Overcoming synthetic limitations and establishing new halide free protocols for the formation of ILs. *Green Chem.* **2007**, 9 (1), 90-98.
31. Herrmann, W. A.; Elison, M.; Fischer, J.; Kocher, C.; Artus, G. R. J., N Heterocyclic Carbenes: Generation under Mild Conditions and Formation of Group 8-10 Transition Metal Complexes Relevant to Catalysis. *Chem. Eur. J.* **1996**, 2 (7), 772-780.
32. Frith, S. A.; Spencer, J. L.; Edwin, J., ( $\eta^5$ -pentamethylcyclopentadienyl) Cobalt Complexes. In *Inorganic Syntheses*, 1990; Vol. 23, pp 15-21.
33. Hoye, T. R. Antoine Equation and Coefficients (A/B/C) for estimating Vapor Pressure.

## Appendix: Color Images in Black and White

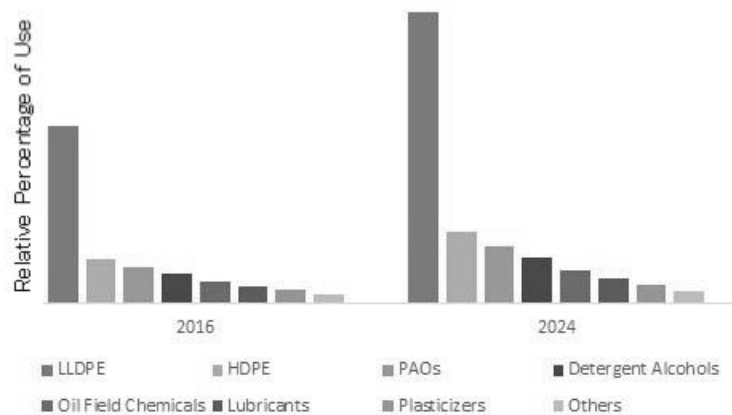


**Figure 1:** A distribution of the common industrial uses of linear  $\alpha$ -olefins from 2016, and a projection for 2024. As seen, a vast majority are used for copolymer modification of LDPE. Figure adapted from Ahuja & Singh.<sup>3</sup>

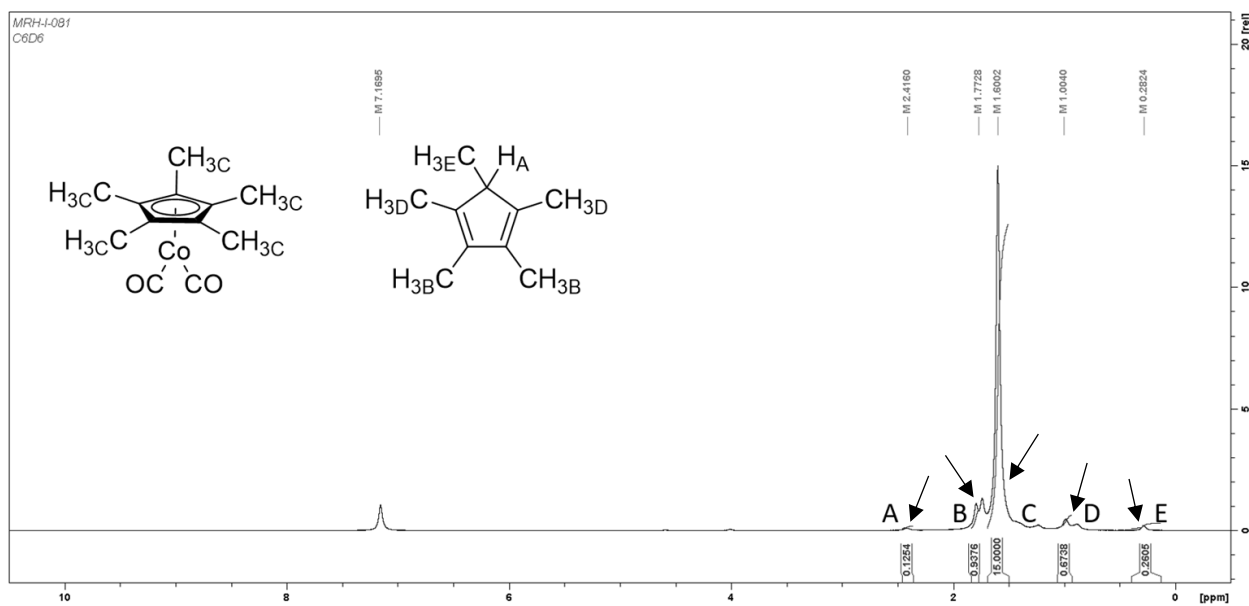


**Figure 15:** The NMR spectra of  $\text{Cp}^*\text{Co}(\text{CO})_2$  (1) in  $\text{C}_6\text{D}_6$  ( $\delta=7.16$ ). As shown, two components are present, the desired cobalt complex and excess  $\text{Cp}^*$ . Paramagnetic material is also present, as seen by the line broadening of the resonances.

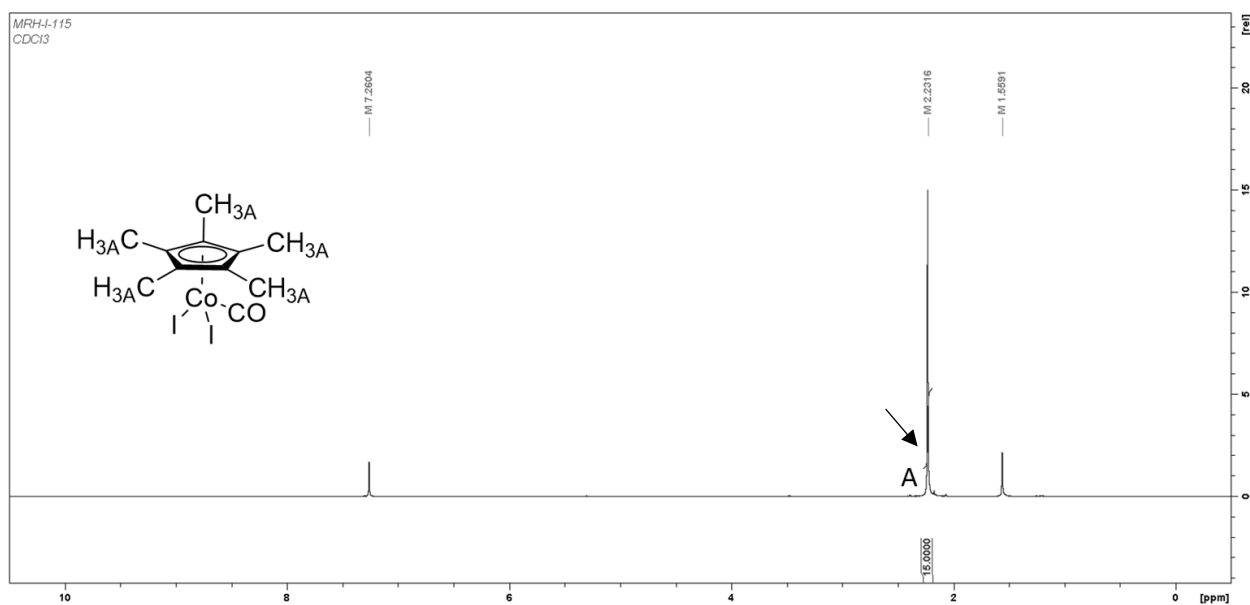


**Figure 16:** The NMR spectra of  $\text{Cp}^*\text{Co}(\text{CO})(\text{I})_2$  (2) in  $\text{CDCl}_3$  ( $\delta=7.26$ ). It can be seen that the material is pure, with the minor peak at  $\delta=1.6$  being water.

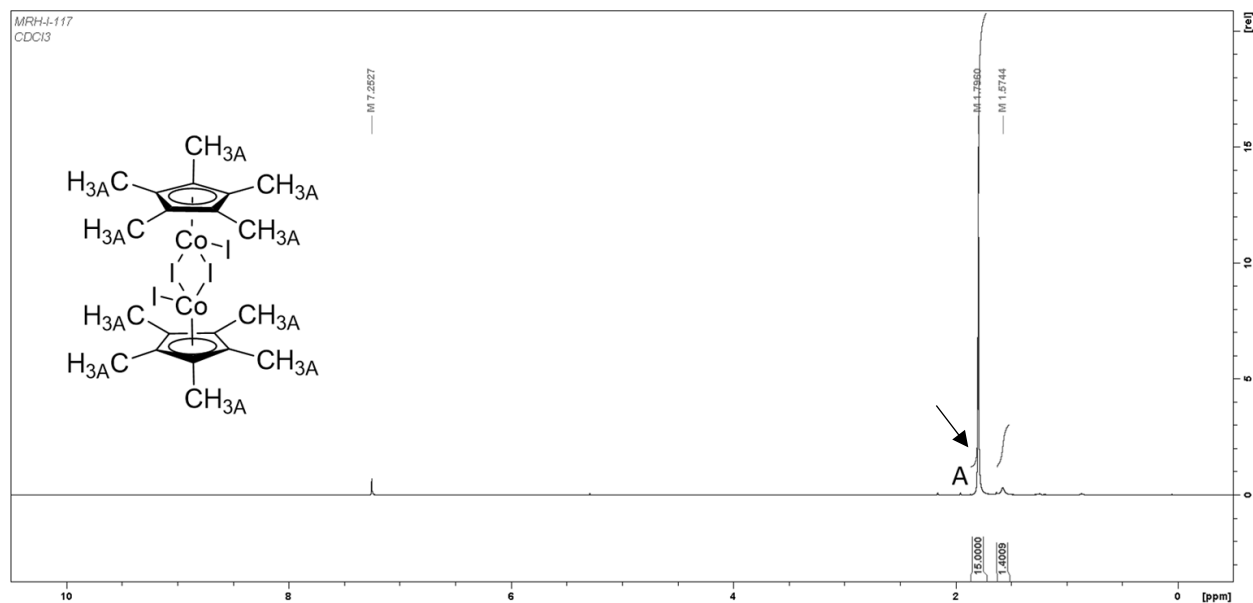


**Figure 17:** The NMR spectra of  $[\text{Cp}^*\text{Co}(\text{I})_2]_2$  (3) in  $\text{CDCl}_3$  ( $\delta=7.26$ ). As shown, the material is pure, the minor peak at  $\delta=1.6$  is determined to be water.

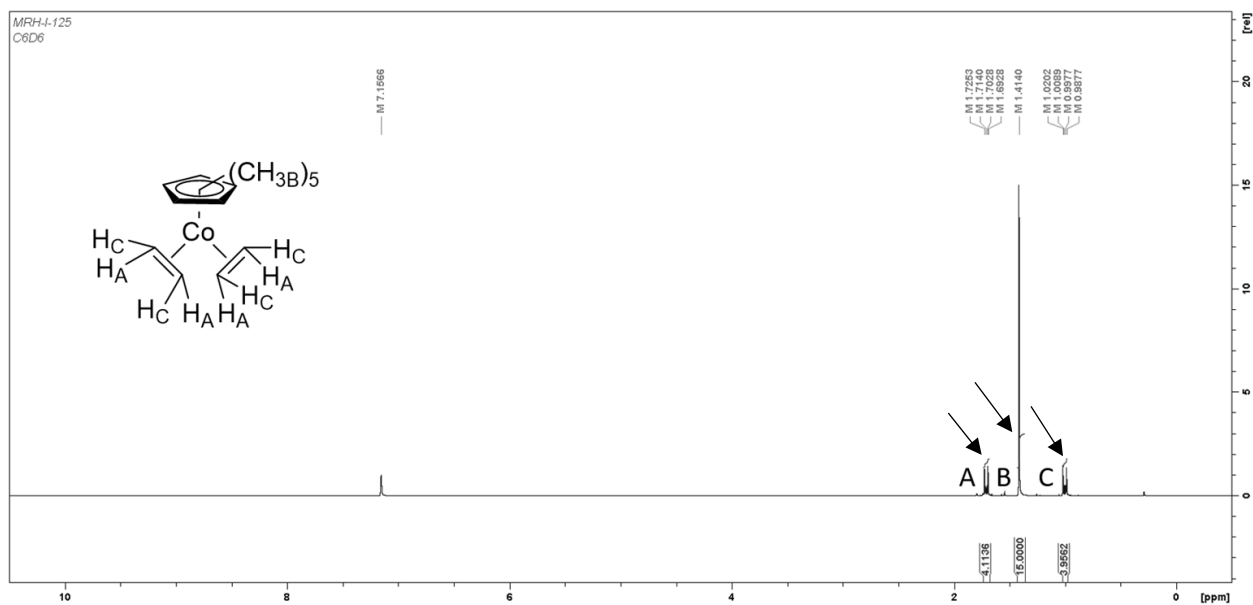


**Figure 18:** The NMR spectra of Cp\*Co(ethene)<sub>2</sub> (4) in C<sub>6</sub>D<sub>6</sub> ( $\delta=7.16$ ). Three narrow resonances are assigned structurally, and indicate high purity of the compound.

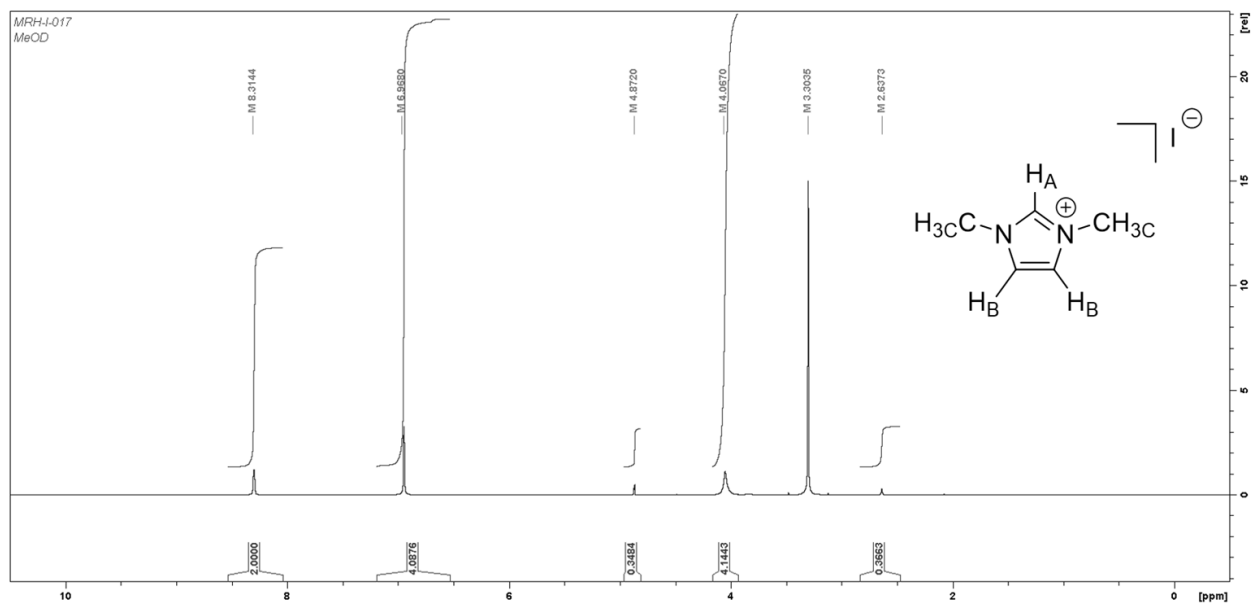


**Figure 20:** The NMR spectrum of the unsuccessful synthesis of N,N'-dimethylimidazolium iodide Trial 1 in MeOD ( $\delta=3.31$ ). The structure of the compound is provided for reference

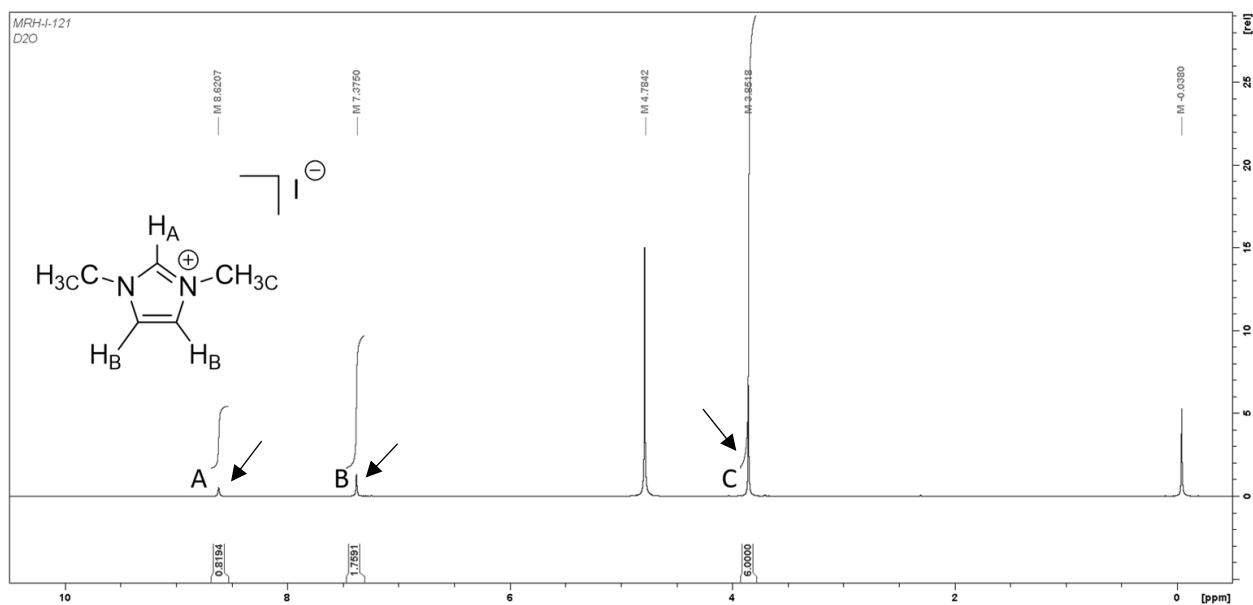


**Figure 21:** The synthesis of N,N'-dimethylimidazolium iodide (5) Trial 2 in D<sub>2</sub>O ( $\delta=4.79$ ).

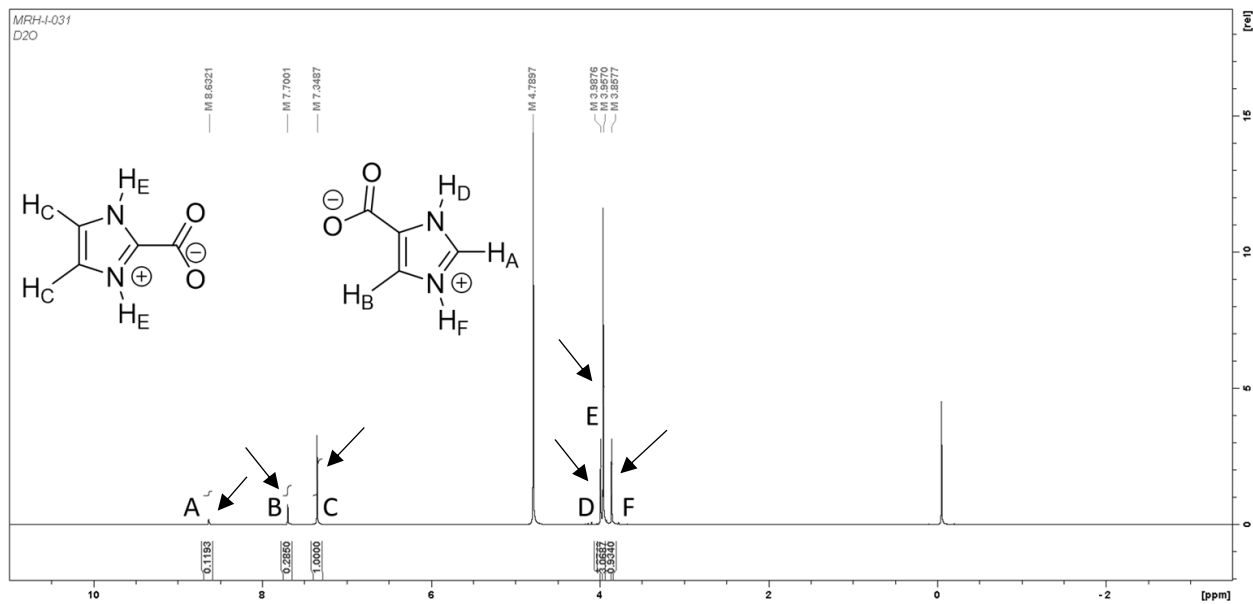


**Figure 23:** The NMR spectra of the synthesis of N,N'-dimethylimidazolium-2-carboxylate (6) Trial 1 in D<sub>2</sub>O ( $\delta=4.79$ ). Here the mixture of products can be seen, with their peaks assigned to their respective structures.



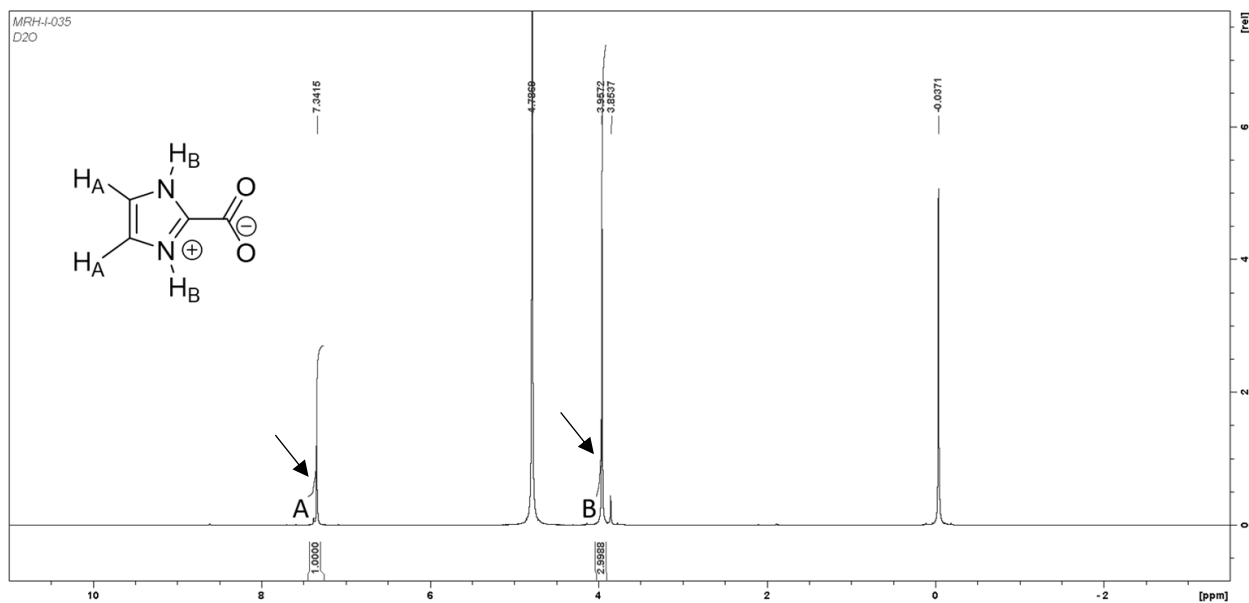


**Figure 25:** The NMR spectra of N,N'-dimethylimidazole-2-carboxylate Trial 2 in D<sub>2</sub>O ( $\delta=4.79$ ). Impurities consist of methanol;  $\delta=0$  indicates TMS.

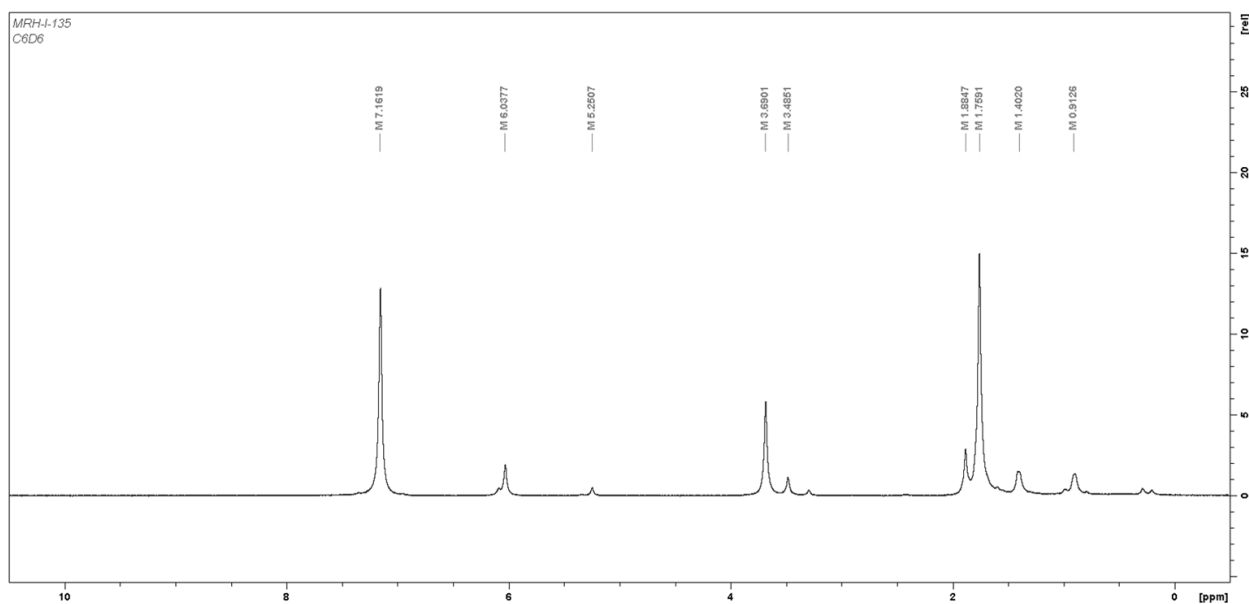


**Figure 27:** The NMR spectra of the coordination of N,N'-dimethylimidazolium-2-carboxylate to Cp\*Co(ethene)<sub>2</sub> Trial 1 in C<sub>6</sub>D<sub>6</sub> ( $\delta=7.16$ ). As shown, a large quantity of paramagnetic material is present, preventing accurate analysis

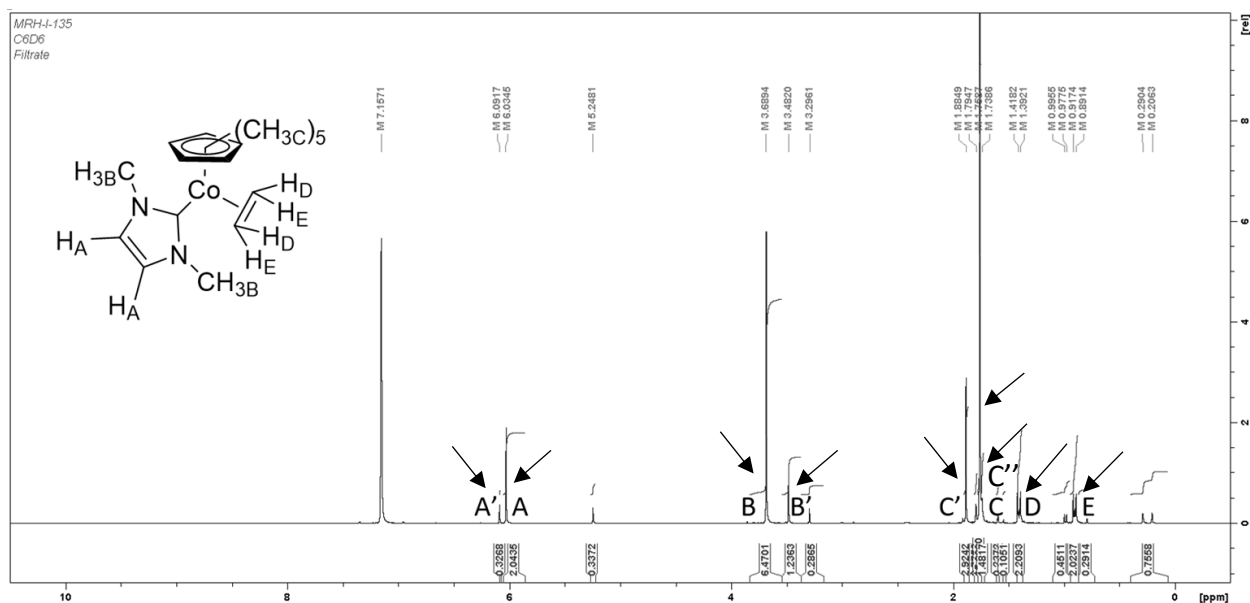


**Figure 28:** The NMR spectra of the coordination of N,N'-dimethylimidazolium-2-carboxylate to Cp\*Co(ethene)<sub>2</sub> Trial 1 in C<sub>6</sub>D<sub>6</sub> ( $\delta=7.16$ ) after filtration. The structure of the desired complex is shown, and the relevant peaks are labeled.

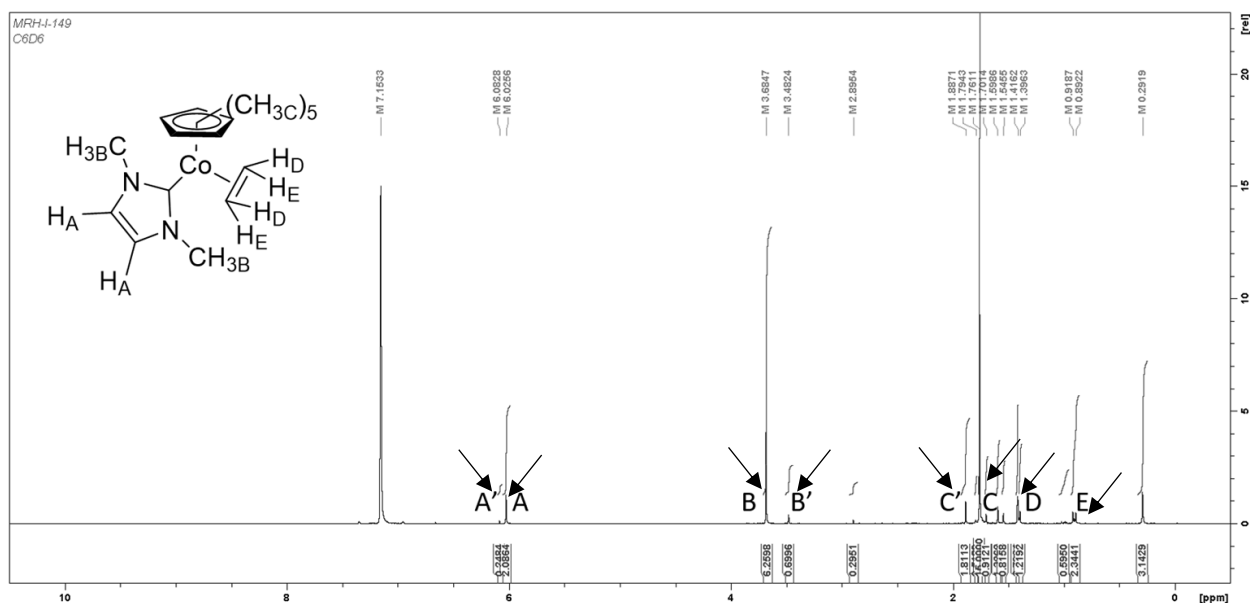


**Figure 30:** The NMR spectra of the coordination of N,N'-dimethylimidazolium-2-carboxylate to Cp\*Co(ethene)<sub>2</sub> Trial 2 in C<sub>6</sub>D<sub>6</sub> ( $\delta=7.16$ ). The structure is provided for the desired product, and peaks are labeled.

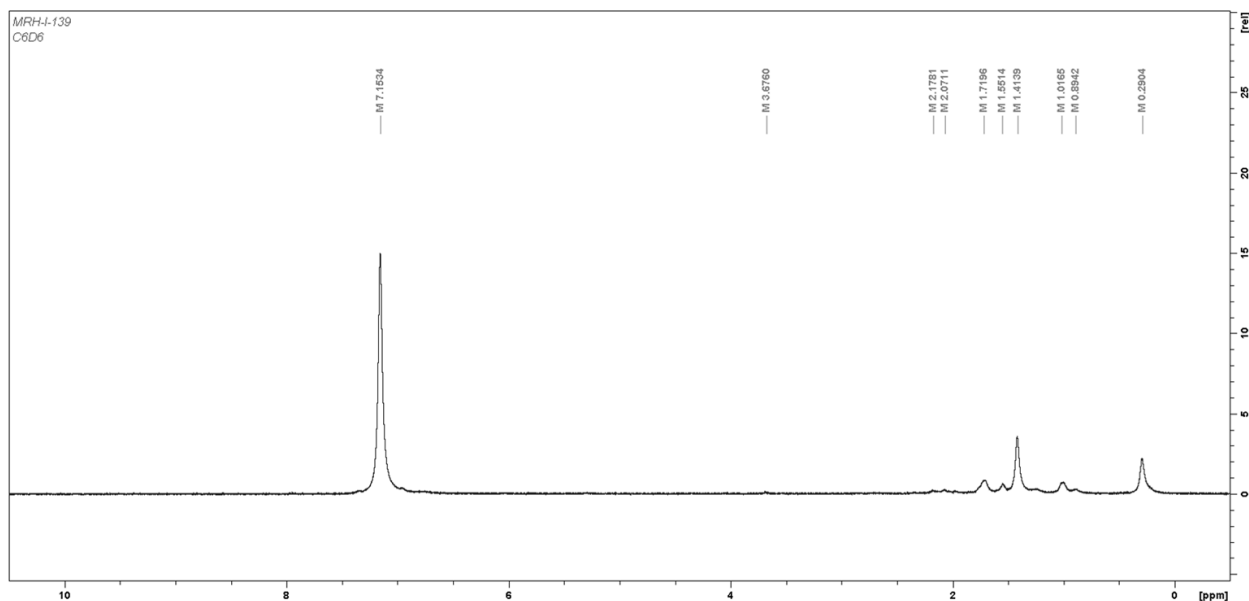


**Figure 31:** The NMR spectra of the stepwise decarboxylation of N,N'-dimethylimidazolium-2-carboxylate and coordination to Cp\*Co(ethene)<sub>2</sub> Trial 3 in C<sub>6</sub>D<sub>6</sub> ( $\delta=7.16$ ). The separation of the paramagnetic material formed was not possible, and thus characterization of the reaction products was not possible.

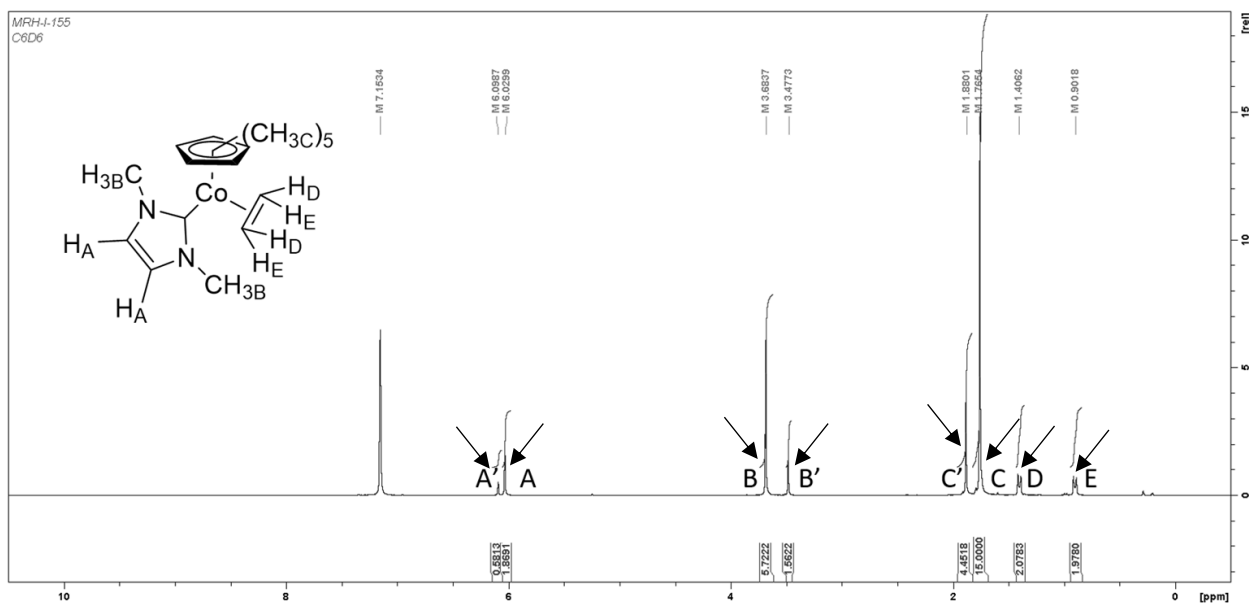


**Figure 32:** The NMR spectra of the coordination of N,N'-dimethylimidazolium-2-carboxylate to Cp\*Co(ethene)<sub>2</sub> Trial 4 in C<sub>6</sub>D<sub>6</sub> ( $\delta=7.16$ ). The desired complex is shown, and peaks were assigned as shown.

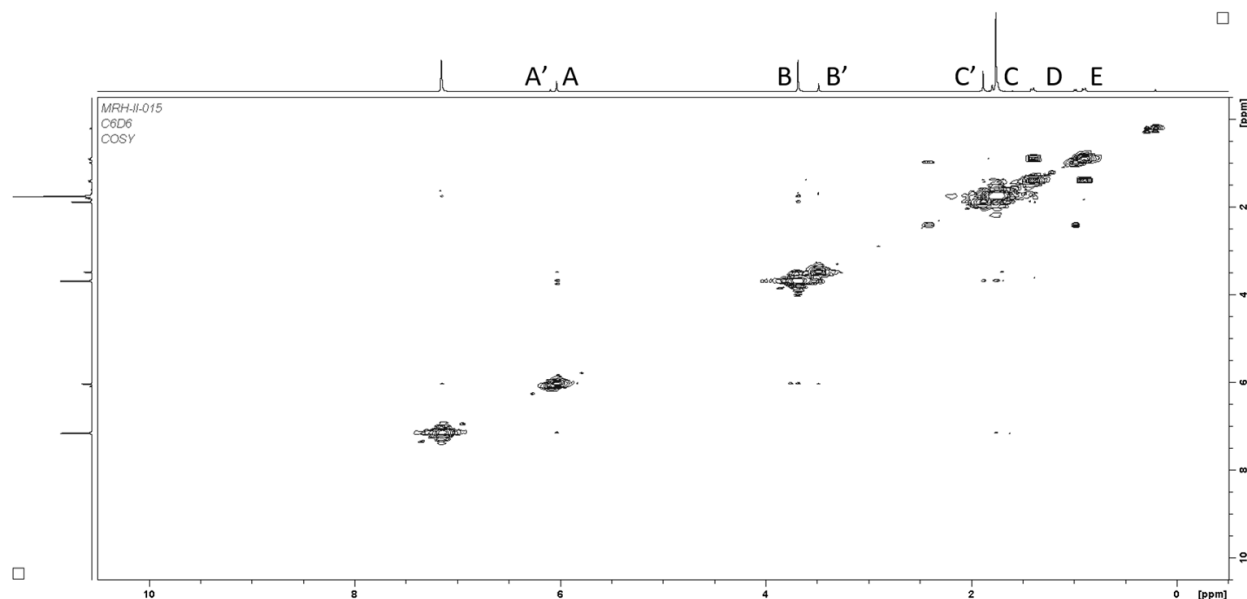


**Figure 33:** The COSY NMR spectra of the coordination of N,N'-dimethylimidazolium-2-carboxylate to Cp\*Co(ethene)<sub>2</sub> Trial 4 in C<sub>6</sub>D<sub>6</sub>. As can be seen, no cross peaks are present for the minor peaks A', B', and C'.

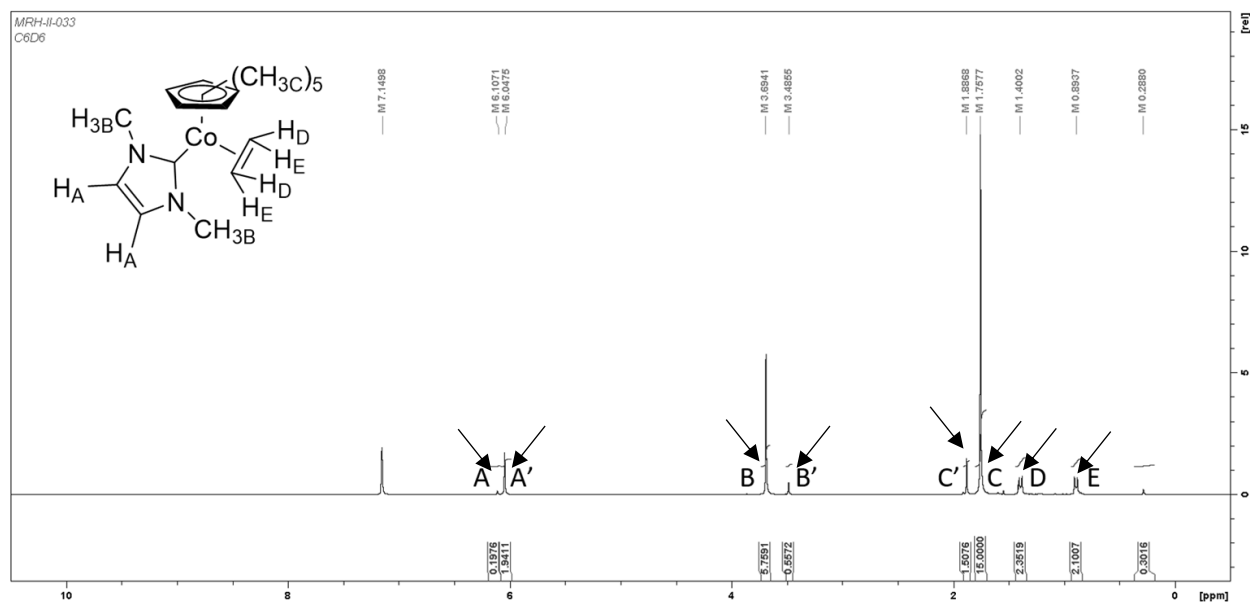


**Figure 34:** The NMR spectra of the coordination of N,N'-dimethylimidazole-2-carboxylate to Cp\*Co(ethene)<sub>2</sub> Trial 5 in C<sub>6</sub>D<sub>6</sub> ( $\delta=7.16$ ).

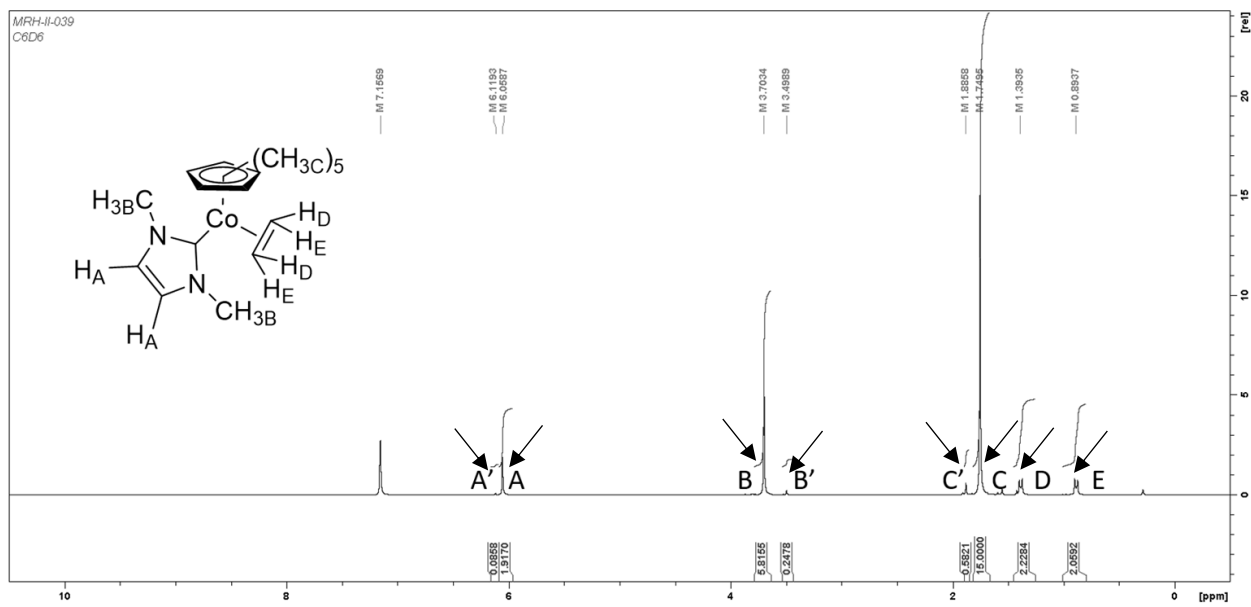


**Figure 35:** The NMR spectra of the coordination of N,N'-dimethylimidazolium-2-carboxylate to Cp\*Co(ethene)<sub>2</sub> Trial 6 in C<sub>6</sub>D<sub>6</sub> ( $\delta=7.16$ ).

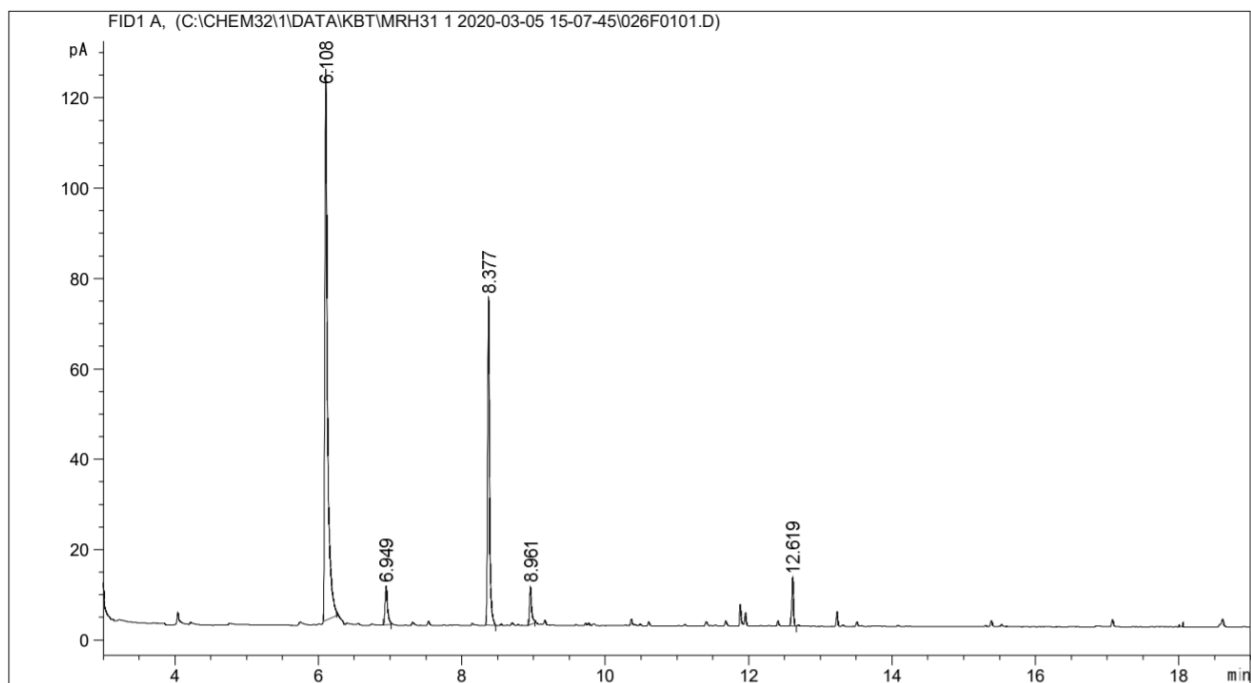


**Figure 38:** The GC-FID chromatogram for the 24 hour reaction aliquot.

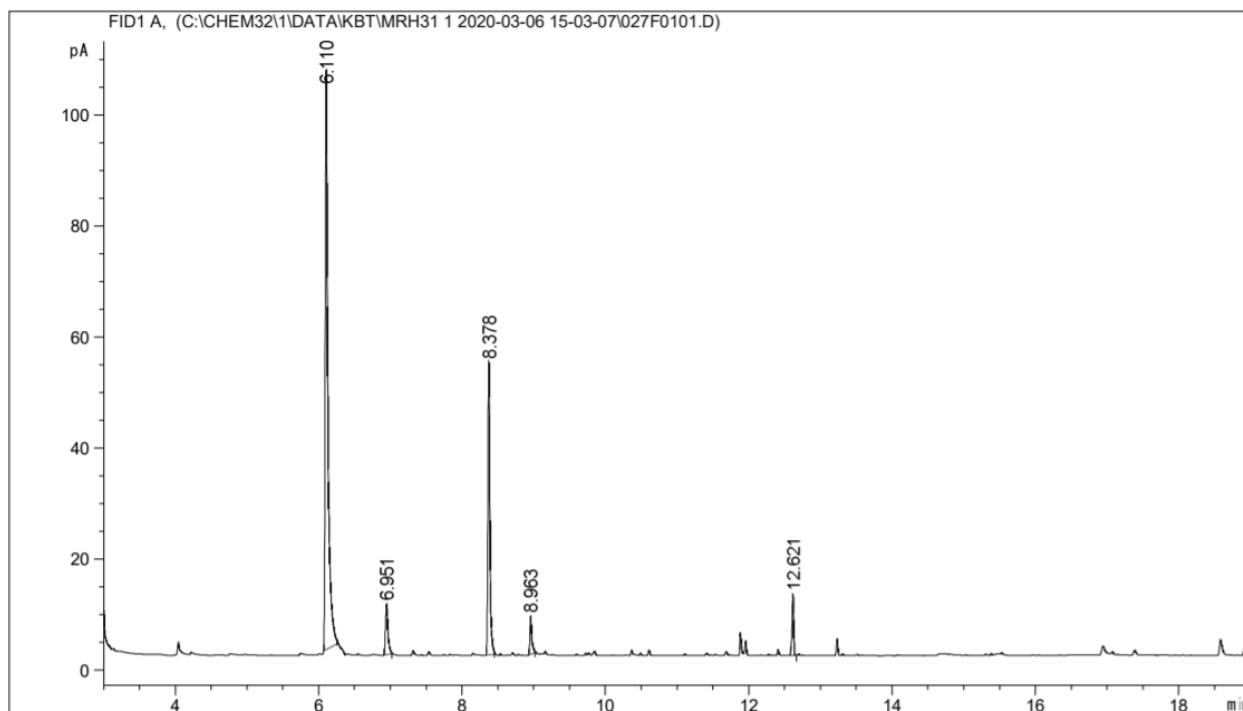


**Figure 39:** The GC-FID chromatogram for the 48 hour reaction aliquot.

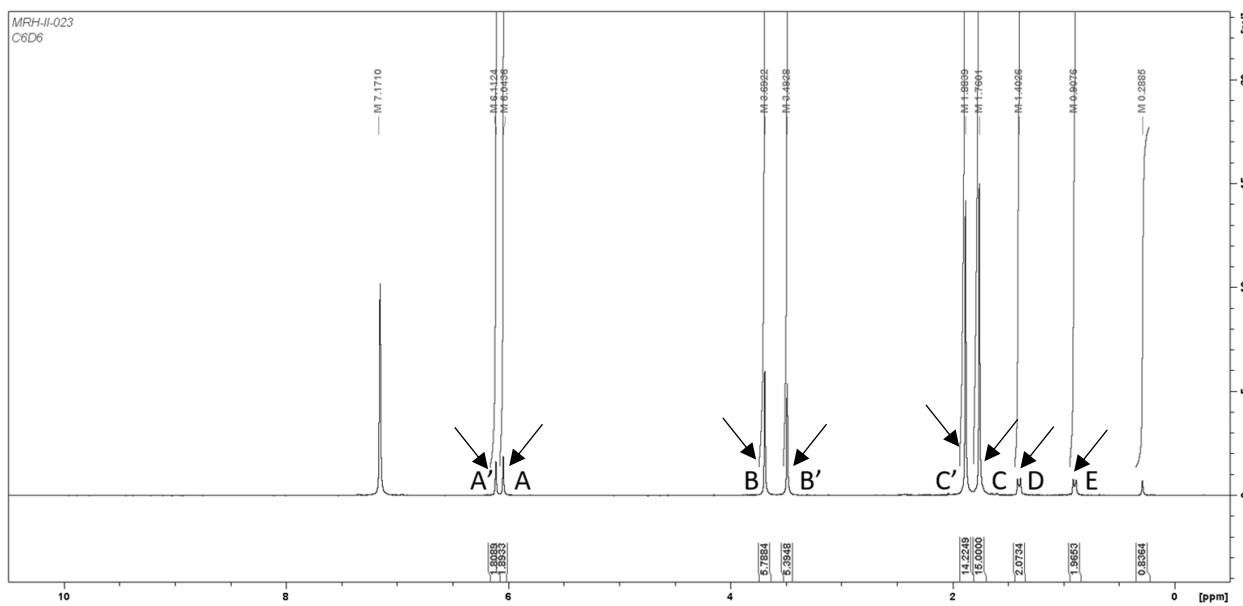


**Figure 40:** The NMR spectra of the synthesis of  $[\text{Cp}^*\text{Co}(\text{Me}_2\text{Im})]_2$  Trial 1 in  $\text{C}_6\text{D}_6$  ( $\delta=7.16$ ). It can be seen that the major and minor peaks are at equal proportions

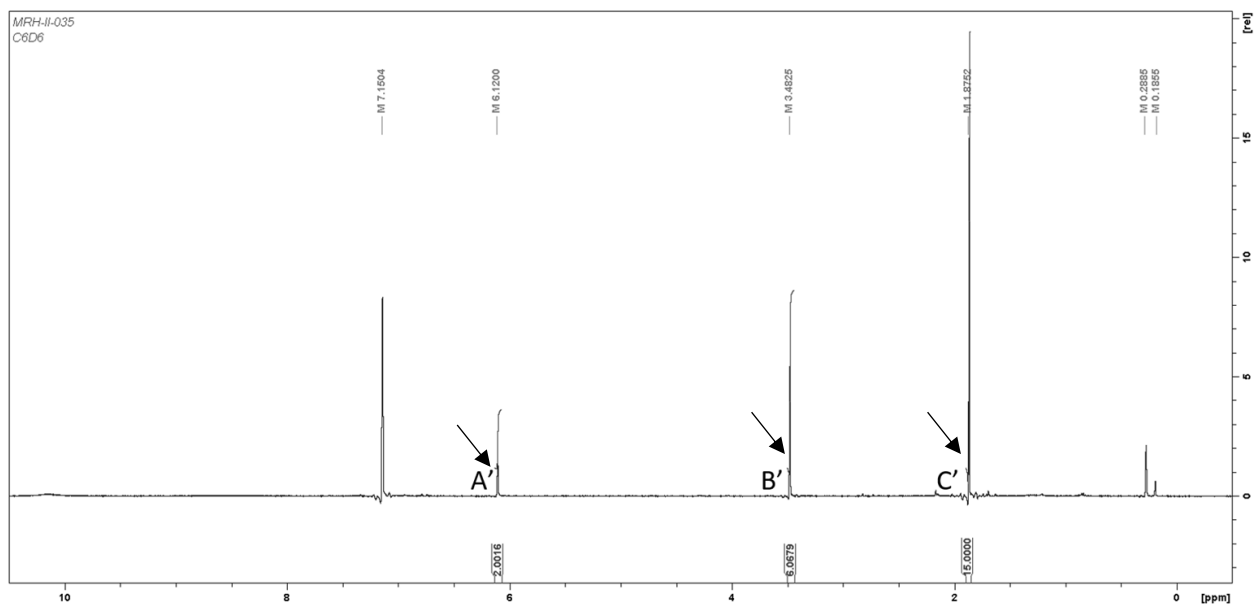


**Figure 41:** The NMR spectra of the synthesis of  $[\text{Cp}^*\text{Co}(\text{Me}_2\text{Im})_2]$  Trial 2 in  $\text{C}_6\text{D}_6$  ( $\delta=7.16$ ). It can be seen that the monomeric material has been driven off, leaving only the dimer product.

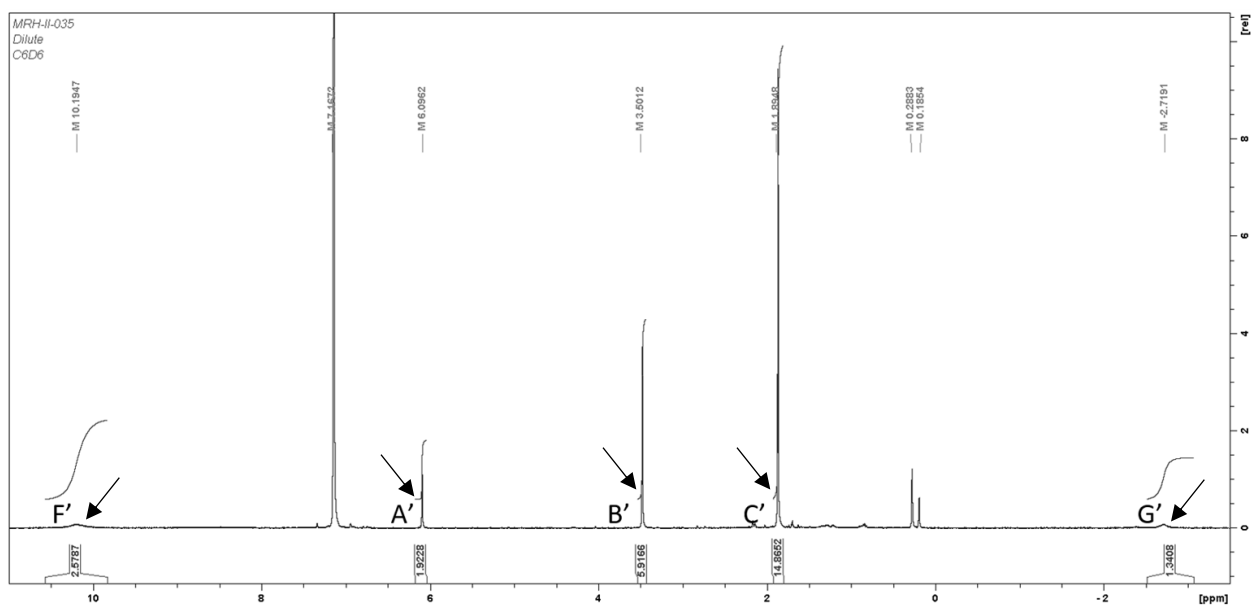


**Figure 42:** The NMR spectra of the synthesis of  $[\text{Cp}^*\text{Co}(\text{Me}_2\text{Im})_2]$  Trial 2 in  $\text{C}_6\text{D}_6$  ( $\delta=7.16$ ) after one week. Peaks F' and G' are new, and are labeled as so to not imply their identity is ethene.

## List of Figures

- Figure 1:** A distribution of the common industrial uses of linear  $\alpha$ -olefins from 2016, and a projection for 2024. As seen, a vast majority are used for copolymer modification of LDPE. Figure adapted from Ahuja & Singh.<sup>3</sup> ..... 1
- Figure 2:** The catalytic cycle of the Shell Higher Olefin Process, complex A) undergoes repeated insertions of ethene to yield a distribution of alkyl complexes. These alkyl complexes then undergo  $\beta$ -elimination to give the desired olefin products. Figure adapted from Keim.<sup>4</sup> ..... 2
- Figure 3:** A measured distribution of linear  $\alpha$ -olefin production using three prevalent full range processes. As seen, a significant quantity is produced outside of the desired range (12-18 carbon number). Figure adapted from Lappin & Sauer.<sup>2</sup> ..... 3
- Figure 4:** A reported pathway to recover some waste from linear  $\alpha$ -olefin production. 1 eq. 1-octene and 1 eq. 1-eicosene is isomerized and metathesized to form 2 eq. of 4-tetradecene, then isomerized again to form the linear olefin product, 2-tetradecene. .... 3
- Figure 5:** A) A trimerization catalytic cycle of ethene to 1-hexene showing metallacyclic addition of ethene and B) the products of Bollman et al. experiments on a tetramerization catalyst. The metallacyclic mechanism is suggested, but not confirmed due to doubt about the stability of a 9-membered ring. .... 4
- Figure 6:** The catalytic cycle of the Broene-Brookhart catalyst, showing activation to a cationic species,  $\alpha$ -olefin insertion to form an internal species, isomerization to move the agostic interaction to a terminal  $\beta$ -hydrogen, and  $\beta$ -elimination to reform the olefin, coupled with charge transfer to a different cobalt species. As shown, only olefin dimers are created; the type of dimer is elaborated in detail in Fig. 7. .... 5
- Figure 7:** The insertion equilibrium of the  $\alpha$ -olefin to the cobalt catalyst, where it can be seen that the geometry of insertion is determined by the steric bulk of supporting ligands. Compounds A) and B) are in equilibrium, where insertion direction determines which isomer is created. .... 6
- Figure 8:** The design of a targeted catalyst with a bidentate ligand. The chelating effect of this ligand was believed to prevent bond rotation, thus freeing space to allow for better ratios of linear to branched product. .... 7
- Figure 9:** The complex synthetic scheme used by prior members of the Broene lab to attempt to synthesize the precatalyst ( $\eta^5$ -ethene)(1-(8-quinoyl)-2,3,4,5-tetramethylcyclopentadiene)cobalt. Complexes A and B are easily made, whereas methods of forming C have been unsuccessful to date. Figure adapted from Keefe.<sup>12</sup> ..... 8
- Figure 10:** Examples of N-heterocyclic carbenes A) N,N'-dimethyl B) N,N'-di(2,6-diisopropyl) and C) N,N'-di(2,4,6-trimethylbenzene)-imidazolium-2-ylidene. Carbenes B and C are more commonplace due to ease of synthesis, whereas carbene A is kinetically unfavored to form. .... 9
- Figure 11:** The structure of N,N'-dimethylimidazolium iodide. .... 10
- Figure 12:** The structure of N,N'-dimethylimidazolium-2-carboxylate. .... 10
- Figure 13:** The structure of [Cp\*Co(ethene)(N,N'-dimethylimidazolium-2-ylidene)], the target molecule of this project. .... 10
- Figure 14:** The synthetic scheme detailing formation of [Cp\*Co(ethene)<sub>2</sub>] from [Co<sub>2</sub>(CO)<sub>8</sub>]. .... 22



<b>Figure 15:</b> The NMR spectra of Cp*Co(CO) <sub>2</sub> ( <b>1</b> ) in C <sub>6</sub> D <sub>6</sub> (δ=7.16). As shown, two components are present, the desired cobalt complex and excess Cp*. Paramagnetic material is also present, as seen by the line broadening of the resonances. ....	23
<b>Figure 16:</b> The NMR spectra of Cp*Co(CO)(I) <sub>2</sub> ( <b>2</b> ) in CDCl <sub>3</sub> (δ=7.26). It can be seen that the material is pure, with the minor peak at δ=1.6 being water.....	24
<b>Figure 17:</b> The NMR spectra of [Cp*Co(I) <sub>2</sub> ] <sub>2</sub> ( <b>3</b> ) in CDCl <sub>3</sub> (δ=7.26). As shown, the material is pure, the minor peak at δ=1.6 is determined to be water.....	24
<b>Figure 18:</b> The NMR spectra of Cp*Co(ethene) <sub>2</sub> ( <b>4</b> ) in C <sub>6</sub> D <sub>6</sub> (δ=7.16). Three narrow resonances are assigned structurally, and indicate high purity of the compound. ....	25
<b>Figure 19:</b> The synthetic scheme of N,N'-dimethylimidazolium iodide.....	25
<b>Figure 20:</b> The NMR spectrum of the unsuccessful synthesis of N,N'-dimethylimidazolium iodide Trial 1 in MeOD (δ=3.31). The structure of the compound is provided for reference, though the material is unidentified. ....	26
<b>Figure 21:</b> The synthesis of N,N'-dimethylimidazolium iodide ( <b>5</b> ) Trial 2 in D <sub>2</sub> O (δ=4.79). ....	26
<b>Figure 22:</b> The synthetic scheme for the synthesis of N,N'-dimethylimidazolium-2-carboxylate Trial 1. Though only <b>6</b> is desired, <b>7</b> was formed as an unwanted byproduct. ....	27
<b>Figure 23:</b> The NMR spectra of the synthesis of N,N'-dimethylimidazolium-2-carboxylate ( <b>6</b> ) Trial 1 in D <sub>2</sub> O (δ=4.79). Here the mixture of products can be seen, with their peaks assigned to their respective structures. ....	28
<b>Figure 24:</b> A proposed literature mechanism for the formation of N,N'-dimethylimidazolium-2-carboxylate from 1-methylimidazole and dimethylcarbonate. Mechanism adapted from Voutchkova. <sup>29</sup> .....	28
<b>Figure 25:</b> The NMR spectra of N,N'-dimethylimidazole-2-carboxylate Trial 2 in D <sub>2</sub> O (δ=4.79). Impurities consist of methanol; δ=0 indicates TMS.....	29
<b>Figure 26:</b> The initial reaction conditions for the coordination of N,N'-dimethylimidazolium-2-carboxylate to Cp*Co(ethene) <sub>2</sub> . Here the free NHC <b>6A</b> is formed by thermal dissociation of CO <sub>2</sub> from <b>6</b> , this carbene species readily coordinates to cobalt, forming Cp*Co(ethene)(N,N'-dimethylimidazolium-2-ylidene). ....	29
<b>Figure 27:</b> The NMR spectra of the coordination of N,N'-dimethylimidazolium-2-carboxylate to Cp*Co(ethene) <sub>2</sub> Trial 1 in C <sub>6</sub> D <sub>6</sub> (δ=7.16). As shown, a large quantity of paramagnetic material is present, preventing accurate analysis.....	30
<b>Figure 28:</b> The NMR spectra of the coordination of N,N'-dimethylimidazolium-2-carboxylate to Cp*Co(ethene) <sub>2</sub> Trial 1 in C <sub>6</sub> D <sub>6</sub> (δ=7.16) after filtration. The structure of the desired complex is shown, and the relevant peaks are labeled. C' and C'' refer to minor peaks in the vicinity of C that may represent Cp* in a minor product.....	31
<b>Figure 29:</b> An updated reaction scheme of the coordination of N,N'-dimethylimidazolium-2-carboxylate to Cp*Co(ethene) <sub>2</sub> showing the possible formation of a bis-NHC complex.....	31
<b>Figure 30:</b> The NMR spectra of the coordination of N,N'-dimethylimidazolium-2-carboxylate to Cp*Co(ethene) <sub>2</sub> Trial 2 in C <sub>6</sub> D <sub>6</sub> (δ=7.16). The structure is provided for the desired product, and peaks are labeled. The use of ' refers to peaks from the same ligands on a different product, i.e. A and A' refer to the alkene hydrogens on the NHC, where A' is in the minor product .....	32

<b>Figure 31:</b> The NMR spectra of the stepwise decarboxylation of N,N'-dimethylimidazolium-2-carboxylate and coordination to Cp*Co(ethene) <sub>2</sub> Trial 3 in C <sub>6</sub> D <sub>6</sub> (δ=7.16). The separation of the paramagnetic material formed was not possible, and thus characterization of the reaction products was not possible. ....	33
<b>Figure 32:</b> The NMR spectra of the coordination of N,N'-dimethylimidazolium-2-carboxylate to Cp*Co(ethene) <sub>2</sub> Trial 4 in C <sub>6</sub> D <sub>6</sub> (δ=7.16). The desired complex is shown, and peaks were assigned as shown. ....	33
<b>Figure 33:</b> The COSY NMR spectra of the coordination of N,N'-dimethylimidazolium-2-carboxylate to Cp*Co(ethene) <sub>2</sub> Trial 4 in C <sub>6</sub> D <sub>6</sub> . As can be seen, no cross peaks are present for the minor peaks A', B', and C'.....	35
<b>Figure 34:</b> The NMR spectra of the coordination of N,N'-dimethylimidazole-2-carboxylate to Cp*Co(ethene) <sub>2</sub> Trial 5 in C <sub>6</sub> D <sub>6</sub> (δ=7.16).....	35
<b>Figure 35:</b> The NMR spectra of the coordination of N,N'-dimethylimidazolium-2-carboxylate to Cp*Co(ethene) <sub>2</sub> Trial 6 in C <sub>6</sub> D <sub>6</sub> (δ=7.16).....	36
<b>Figure 36:</b> A scheme showing the activation of the desired precatalyst Cp*Co(ethene)(Me <sub>2</sub> Im) by Brookhart's Acid. This forms the agostic hydrogen complex <b>8</b> .....	37
<b>Figure 37:</b> The proposed catalytic cycle of complex <b>7</b> , showing activation to complex <b>8</b> , and catalysis as described by Broene et al. <sup>11</sup> .....	37
<b>Figure 38:</b> The GC-FID chromatogram for the 24 hour reaction aliquot. ....	38
<b>Figure 39:</b> The GC-FID chromatogram for the 48 hour reaction aliquot. ....	38
<b>Figure 40:</b> The NMR spectra of the synthesis of [Cp*Co(Me <sub>2</sub> Im)] <sub>2</sub> Trial 1 in C <sub>6</sub> D <sub>6</sub> (δ=7.16). It can be seen that the major and minor peaks are at equal proportions.....	39
<b>Figure 41:</b> The NMR spectra of the synthesis of [Cp*Co(Me <sub>2</sub> Im)] <sub>2</sub> Trial 2 in C <sub>6</sub> D <sub>6</sub> (δ=7.16). It can be seen that the monomeric material has been driven off, leaving only the dimer product... ..	40
<b>Figure 42:</b> The NMR spectra of the synthesis of [Cp*Co(Me <sub>2</sub> Im)] <sub>2</sub> Trial 2 in C <sub>6</sub> D <sub>6</sub> (δ=7.16) after one week. Peaks F' and G' are new, and are labeled as so to not imply their identity is ethene.. ..	40

## List of Tables

<b>Table 1:</b> A relationship between cone angle, electron donation, and the branched:linear product ratio. It can be seen that smaller cone angles corresponded to more favorable product ratios. Data from Broene. <sup>11</sup> .....	7
<b>Table 2:</b> The correlation of reaction temperature to the ratio of products formed. It can be seen that lower reaction temperatures give significantly improved purity of the desired coordination complex.....	36